

Department of Civil Engineerig  
University of Washington  
Seattle, Washington 98195

EFFECTS OF STREAMFLOW REGULATION  
AND LAND COVER CHANGE ON  
THE HYDROLOGY OF THE MEKONG RIVER BASIN

by

Gopalakrishna Goteti  
Dennis P. Lettenmaier

Water Resources Series  
Technical Report No. 169

December 2001

## ABSTRACT

The Variable Infiltration Capacity (VIC) hydrologic model was used to simulate rainfall-runoff processes as they are affected by land cover in the Mekong River Basin. The VIC model was implemented at a ¼ degree resolution, for the period January 1979 through December 2000, and was calibrated so that observed streamflow was reproduced to a reasonable extent at selected discharge measurement stations on the main-stem of the Mekong and its tributaries. Model calibration included scaling the precipitation data in parts of the Lower Mekong Basin where scarce meteorological station densities otherwise lead to significant underprediction of observed flows. A water management model (MWMM) was developed to simulate the effects of streamflow regulation by existing and planned major dams and reservoirs in the basin. The MWMM, which is driven by VIC simulated streamflow and assumed operating procedures, produces simulations of annual hydropower that are in approximate accord with observed (or designed) values for most of the dams. The overall effects of the dams in the MWMM on the monthly streamflow of the main-stem Mekong were found to be quite small (less than 3.5% of observed monthly streamflow). The VIC model and the MWMM were then used to evaluate the hydrologic effects of changes in monthly streamflow resulting from changes in land cover in different parts of the basin. The maximum predicted streamflow change for current relative to historic land cover conditions was an increase of 53 percent in mean annual streamflow for the Chi-Mun River, a tributary to the Lower Mekong Basin in which major conversions of forest to cropland have occurred over the last 50 years.

## TABLE OF CONTENTS

TABLE OF CONTENTS.....	iv
LIST OF FIGURES .....	vi
LIST OF TABLES.....	viii
Chapter 1: Introduction.....	1
1.0 Overview.....	1
1.1 Motivation.....	5
1.2 Objectives .....	6
1.3 Overview of Approach.....	7
Chapter 2: Background .....	8
2.0 Overview.....	8
2.1 Physical Characteristics and Climate of the Mekong Basin .....	8
2.1.1 Upper Mekong .....	10
2.1.2 Lower Mekong.....	11
2.2 Hydroelectric Power Development and Flow Regulation .....	14
2.3 Agriculture and Land Use.....	17
2.3.1 Yunnan.....	18
2.3.2 Laos.....	18
2.3.3 Thailand .....	19
2.3.4 Cambodia.....	19
2.3.5 Vietnam.....	20
2.4 Fisheries .....	20
2.5 Competing Interests and the Role of Mekong River Commission .....	21
Chapter 3: Modeling Approach .....	23
3.0 Overview.....	23
3.1 Hydrology Model.....	23
3.1.1 Routing Model .....	26
3.2 Water Management Model .....	26
3.3 Approach.....	27
Chapter 4: Model Implementation .....	29
4.0 Overview.....	29
4.1 Land Surface Characteristics .....	29
4.1.1 Topography.....	29
a) Digital Elevation Model.....	29
b) River Routing Network .....	30
c) Elevation Bands .....	31
4.1.2 Soils.....	31
4.1.3 Vegetation .....	32
4.2 Meteorological Data.....	36
4.3 Streamflow Data .....	37
4.4 VIC Model .....	40

4.4.1 Parameter Estimation .....	40
Upstream of Vientiane .....	41
Northeastern Thailand .....	42
Central and Southern Laos .....	42
4.4.2 VIC Model Output .....	47
4.5 Water Management Model .....	52
4.5.1 Manwan Dam .....	54
4.5.2 Dachaoshan Dam .....	54
4.5.3 Nam Ngum Dam .....	54
4.5.4 Ubol Ratana or Nam Pong Dam .....	55
4.5.5 Pak Mun Dam .....	56
4.5.6 Proposed Dams .....	56
4.6 Effects of flow regulation on streamflow .....	65
Chapter 5: Vegetation Scenarios .....	66
5.0 Overview .....	66
5.1 Historical Land Cover .....	67
5.1.1 Region I .....	68
5.1.2 Region II .....	68
5.1.3 Region III .....	69
5.2 Future Land Cover .....	69
5.3 Effects of Land-use Change on Streamflow .....	71
5.3.1 100-year flood .....	73
5.4 Effects of Land-use Change on Hydropower Production and Irrigation .....	74
Chapter 6: Results and Conclusions .....	76
LIST OF REFERENCES .....	77

## LIST OF FIGURES

Figure 1.1 Mekong River Basin.....	1
Figure 1.2 Trends in total and urban population of Cambodia, Laos, Thailand and Vietnam (FAOSTAT, 2001).....	2
Figure 1.3 Trends in percentage growth of agricultural and forested areas in Cambodia, Laos, Thailand and Vietnam (FAOSTAT, 2001) .....	2
Figure 1.4 Trends in demand for water in Southeast Asia (Shiklomanov, 2000).....	3
Figure 1.5 Some of the existing and proposed dams in the Mekong River Basin (From many sources, see Chapter 2).....	4
Figure 2.1 Topography and significant political and physical features of the Mekong Basin .....	9
Figure 2.2 Upper Mekong.....	10
Figure 2.3 Laotian and Thai portion of the Mekong basin .....	12
Figure 2.4 Cambodian and Vietnamese portion of the Mekong basin .....	13
Figure 2.5 Existing (black triangles) and proposed (green triangles) dams in Yunnan and Burma.....	15
Figure 2.6 Existing (black triangles) and proposed (green triangles) dams in the Laotian and Thai portion of the Mekong basin.....	16
Figure 2.7 Existing (black triangles) and proposed (green triangles) dams in Cambodian and Vietnamese portion of the Mekong basin .....	17
Figure 3.1 Schematic showing the VIC model .....	25
Figure 4.1 ¼ DEM and ¼ degree river routing network.....	30
Figure 4.2 Fractional coverage of vegetation classes .....	34
Figure 4.3 Monthly LAI.....	36
Figure 4.4 Meteorological data stations used in interpolation .....	37
Figure 4.5 GRDC and MRC discharge measurement stations .....	38
Figure 4.6 Final 16 stations selected from GRDC and MRC stations .....	39
Figure 4.7 Comparison of GRDC and MRC data.....	40
Figure 4.8 Ratio of simulated mean annual evaporation and mean annual model precipitation for different soil depths in Northeastern Thailand.....	43
Figure 4.9 Comparison of observed runoff and accumulated precipitation for regions B, D and E .....	44
Figure 4.10 Effect of scaling precipitation data on precipitation and runoff.....	45
Figure 4.11 Comparison of VIC simulated monthly streamflow [solid line] and observed streamflow [broken line] at stations 1, 2, 3 and 4 of Figure 4.6 .....	48
Figure 4.12 Comparison of VIC simulated monthly streamflow [solid line] and observed streamflow [broken line] at stations 5, 6, 7 and 8 of Figure 4.6 .....	49
Figure 4.13 Comparison of VIC simulated monthly streamflow [solid line] and observed streamflow [broken line] at stations 9, 10,11 and 12 of Figure 4.6 .....	50
Figure 4.14 Comparison of VIC simulated monthly streamflow [solid line] and observed streamflow [broken line] at stations 13, 14, 15 and 16 of Figure 4.6 .....	51

Figure 4.15 Dams considered in the MWMM .....	52
Figure 4.16 MWMM output for Manwan Dam [Dam 1 in Figure 4.15] .....	58
Figure 4.17 MWMM output for Dachaoshan Dam [Dam 2 in Figure 4.15] .....	59
Figure 4.18 MWMM output for Nam Ngum Dam [Dam 3 in Figure 4.15] .....	60
Figure 4.19 MWMM output for Ubol Ratana Dam [Dam 4 in Figure 4.15] .....	61
Figure 4.20 MWMM output for Pak Mun Dam [Dam 5 in Figure 4.15] .....	62
Figure 4.21 MWMM output for proposed Jinghong Dam [Dam 6 in Figure 4.15] .....	63
Figure 4.22 MWMM output for proposed Xiaowan Dam [Dam 7 in Figure 4.15] .....	64
Figure 5.1 Three regions selected for the investigation of impacts due to land cover change .....	66
Figure 5.2 Constructed historical land cover .....	70
Figure 5.3 Mean monthly streamflow generated using HLC and FLC for all the three regions .....	72

## LIST OF TABLES

Table 2.1 Hydropower potential of the Mekong basin (Bakker, 1999).....	14
Table 4.1 Properties of different vegetation classes shown in Figure 4.2 .....	33
Table 4.2 Rooting depths and fraction of roots in each rooting zone .....	33
Table 4.3 Calibration parameters and their values for different regions .....	46
Table 4.4 Results of transfer of calibration parameters .....	46
Table 4.5 Performance of VIC model at different discharge measurement stations .....	47
Table 4.6 Attributes of the dams used in MWMM.....	54
Table 4.7 Summary of MWMM output.....	54
Table 5.1 Mean monthly streamflow ( $\text{m}^3/\text{s}$ ) using the current land cover and percentage change in streamflow relative to current land cover conditions .....	71
Table 5.2 Mean annual streamflow ( $\text{m}^3/\text{s}$ ) using the current land cover and percentage change in streamflow relative to current land cover conditions .....	73
Table 5.3 Magnitude of the 100-year flood ( $\text{m}^3/\text{s}$ ) and percentage change relative to current land cover conditions.....	73
Table 5.4 Mean annual power output (GWh) and percentage change relative to current land cover conditions .....	74

## ACKNOWLEDGEMENTS

Thanks to Dennis Lettenmaier for providing me with this opportunity to work with the Surface Water Modeling Group. Thanks to Jeff Richey, Rick Palmer and Bart Nijssen for serving on my thesis committee. Special thanks to Bart Nijssen for helping with the initial VIC model setup, special thanks to Alan Halmet for helping with the setup of the water management model and special thanks to Sarah Rodda for providing DEMs and the initial help with ARC/INFO. Thanks to all the members of the Surface Water Modeling Group at the University of Washington for their assistance. Thanks to Mr. Dirk Vanderstighelen and Mr. Sok of the Mekong River Commission, Phnom Penh for providing streamflow data. Thanks to Global Runoff Data Centre, Koblenz, Germany for providing streamflow data. Thanks to National Center for Atmospheric Research, Boulder, Colorado for the meteorological data. Some of the references quoted in this thesis are documents from the World Wide Web and the Uniform Resource Locators of these documents have been mentioned whenever such a reference was made. Thanks to Generic Mapping Tools (GMT™) software that was used to create most of the figures in this thesis.

## Chapter 1: Introduction

### *1.0 Overview*

The Mekong River is the largest river in Southeast Asia and the many wetlands, streams and small rivers in the Mekong Basin (Figure 1.1) are centers of agriculture and fisheries industry, which are major sources of employment for the people of this basin. The

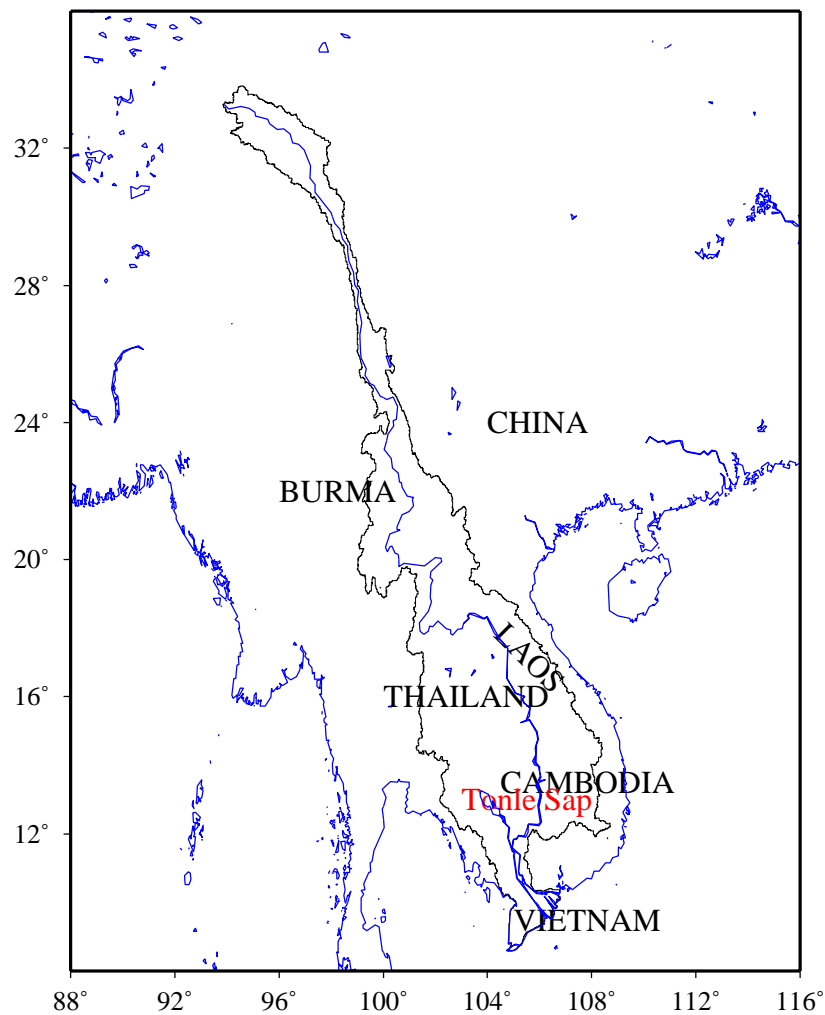


Figure 1.1 Mekong River Basin

anthropogenic changes taking place in the Mekong Basin have significant implications on

the resources of the Mekong River. Population growth in the Mekong Basin (Figure 1.2) has resulted in widespread conversion of forests into agricultural uses (Figure 1.3) to

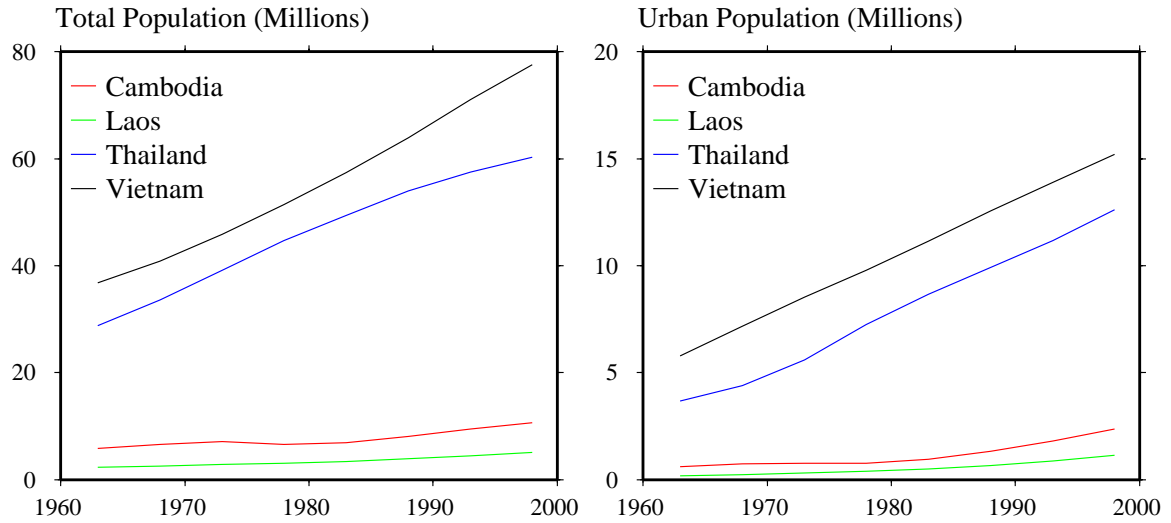


Figure 1.2 Trends in total and urban population of Cambodia, Laos, Thailand and Vietnam (FAOSTAT, 2001)

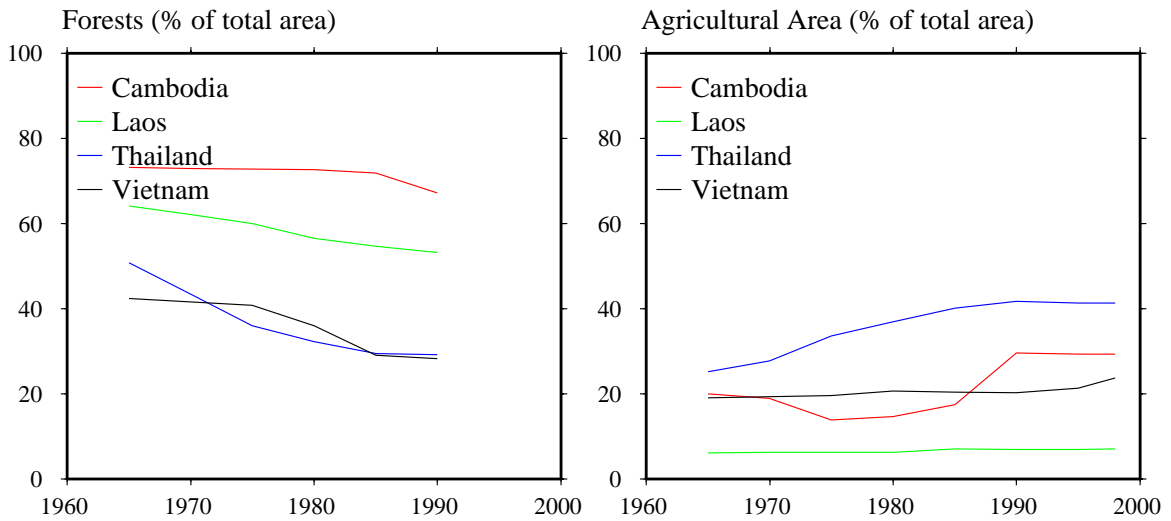


Figure 1.3 Trends in percentage growth of agricultural and forested areas in Cambodia, Laos, Thailand and Vietnam (FAOSTAT, 2001)

meet increased demand for food. The increase in agricultural areas, along with urbanization and industrialization, led to an overall increase in demand for water (Figure 1.4).

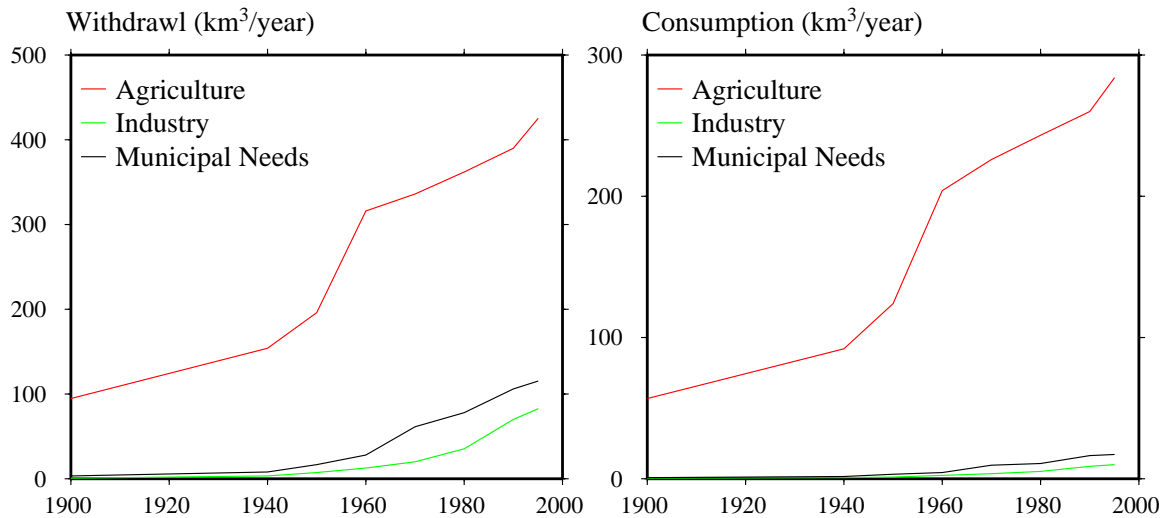


Figure 1.4 Trends in demand for water in Southeast Asia (Shiklomanov, 2000)

To meet the water demands of the growing population - for hydroelectric power, irrigation, domestic and industrial use - the riparian countries of the Mekong Basin have built, and are planning to build, dams and reservoirs, some of them shown in Figure 1.5, on the Mekong and its tributaries. Decreasing forest cover, changing land use practices and increasing flow regulation are changing the physical characteristics of the Basin and leading to adverse effects. The flood from August through October 2000 was a combined effect of large-scale changes in land use and vegetation cover, early onset of monsoons, prolonged rains, flow regulation, and spring tides in the Mekong River due to prolonged typhoons in the South China Sea (MRC annual report, 2000). This flood caused damage of more than US \$450 million, left 795 people dead, and thousands homeless in Thailand, Cambodia, Laos and Vietnam (MRC Annual Report, 2000). The monetary loss is a significant portion of the Annual Gross Domestic Product of these countries (the total market value of all goods and services produced within one year). Furthermore, the 795 lives lost in this flood compares with a total of 676 lives lost in the U.S. due to floods in the period 1990 through 1997 (National Weather Service online information, <http://www.essc.psu.edu/hazards/flood4.htm>).

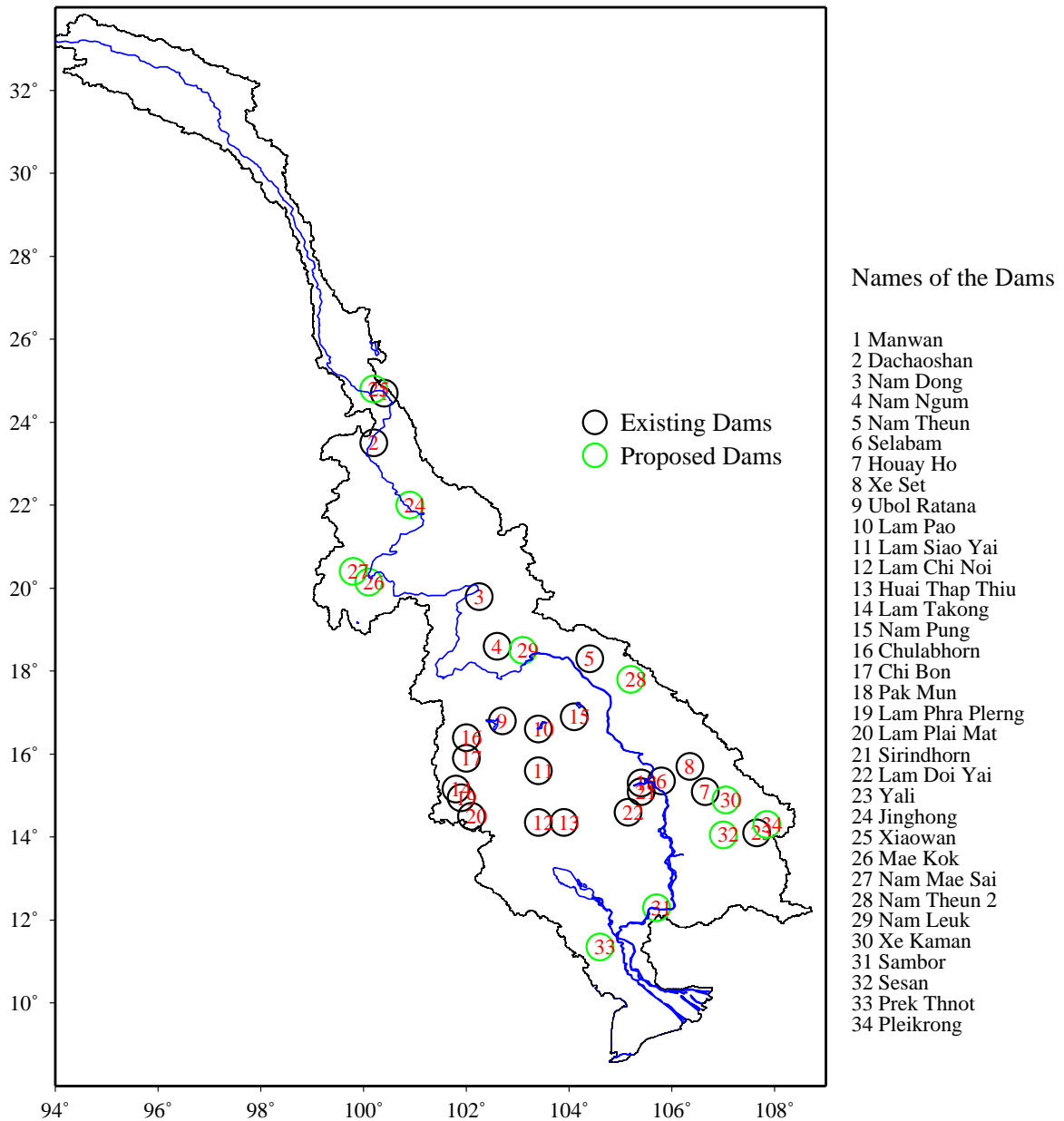


Figure 1.5 Some of the existing and proposed dams in the Mekong River Basin (From many sources, see Chapter 2)

Flooding in the Mekong Basin is crucial to the survival of ecosystems like the Tonle Sap Lake (see Figure 1.1) in Cambodia. A large portion of Cambodia's population lives in the plains surrounding this lake and is dependent on the resources of the lake for its

livelihood. Seasonal flooding in the lower reaches of the Mekong Basin brings an abundance of fish and plant life to the flood plains. These floods recede leaving deposits of fertile soil, which are used extensively for agriculture. Although floods have been a normal part of life in the plains of the Lower Mekong Basin and probably will continue to be, the human and economic losses they cause must be significantly reduced for the overall well being of the region.

### ***1.1 Motivation***

Human-induced changes in the Mekong Basin along with various environmental factors can have disastrous effects like devastating floods. An integrated approach to water resources planning and management is necessary to model the environmental and man-made changes affecting the hydrologic cycle of the Basin. Hydrologic models that predict runoff over the entire basin and accommodate spatial and temporal changes in land use and climate are required for such an integrated water management study.

Macro-scale hydrology models explicitly represent hydrologic processes occurring at the land surface (Wood, 1991). These models can predict the sensitivity of runoff to land use and climate change and thus can be used to simulate the changes in streamflow patterns with changes in the physical characteristics of the Basin. Also, these models are compatible with atmospheric general circulation models and can be used in streamflow forecasting (Wood et al., 2000; Hamlet and Lettenmaier, 1999).

As used for water resources planning and operations, macro-scale hydrology models are driven by land surface characteristics (soils, topography, vegetation) and meteorological data. The scarcity of data derivable from in situ sources can be overcome to some extent with satellite remote sensing data. Remote sensing data can provide timely and detailed

information about the features of the Earth and its atmosphere and can be used to estimate meteorological variables such as precipitation (Huffman et al., 1997; 1995).

The application of macro-scale hydrology models and remote sensing data to water resources planning and management is the motivation behind this study. The work reported here was conducted cooperatively with the Southeast Asia START (SysTem for Analysis, Research and Training) Regional Centre in Chulalongkorn University, Bangkok, Thailand. This cooperation is part of a larger project, known as Southeast Asia River Basins Model (SEA-BASINS), which is aimed at developing a scientific model to evaluate changes in water resources as a function of changes in land use, land cover and regional climatology over the Mekong River Basin and other river basins in Southeast Asia.

## ***1.2 Objectives***

The objectives of this study are:

1. To implement a model that simulates the hydrology of the Mekong River Basin, including the effects of land use change and water management on flows of the Mekong River and its major tributaries.
2. To develop a water management model which simulates the effects of flow regulation by existing and planned major dams and reservoirs in the basin, and to evaluate the reliability of the planned reservoir system.
3. To analyze the hydrologic impacts of large-scale deforestation in different parts of the basin using the hydrology model and the water management model.

### ***1.3 Overview of Approach***

The Variable Infiltration Capacity (VIC) macro-scale hydrologic model (see Section 3.1) was used to simulate rainfall-runoff processes of the Mekong Basin. Observed streamflow data from the Mekong River Commission (MRC) and the Global Runoff Data Centre (GRDC) were used to assess the model's performance at various discharge measurement locations in the basin. From the initial model runs it was evident that precipitation was inadequately represented in parts of the Lower Mekong Basin, due to the poor meteorological station density. In these parts of the basin, the precipitation data was scaled to give a reasonable agreement between the simulated and observed runoff (see Section 4.4).

A water management model, which represents all the existing and planned significant dams and reservoirs in the Mekong Basin, was developed. Although the existing dams are generally not large enough to significantly affect the discharge on the main stem of the Mekong, several large dams are under consideration, and flow regulation scenarios which included the effects of these proposed dams, were evaluated. Different scenarios of deforestation at varying spatial scales were also analyzed with the help of the hydrology and the water management models. Possible effects of various combinations of water management and deforestation scenarios are considered in Chapter 5.

## Chapter 2: Background

### ***2.0 Overview***

The water resources of the Mekong River are of immense economic and political significance to the riparian countries of the Mekong Basin. An understanding of the water resources problems in the region is necessary for efficient water resources management. This chapter addresses the principal environmental and water resources-related issues in the Mekong Basin.

### ***2.1 Physical Characteristics and Climate of the Mekong Basin***

The headwaters of the Mekong River are in China. It then flows through Burma, Thailand, Laos and Cambodia, and then into the South China Sea via Vietnam's Mekong delta. The topography of the Mekong River Basin and the significant geographical and political features of the region are shown in Figure 2.1. The source of the Mekong lies 5000 m above sea level, in the Tibetan highlands. The main stem of the river is more than 4800 km long, with a drainage area of 795,000 km<sup>2</sup>, and a mean annual flow of 470 billion m<sup>3</sup> (equivalent to a depth of 570 mm over the basin area) at its mouth (MRC Annual Report, 1988). The Mekong is the eighth largest river in the world in terms of discharge, twelfth largest river in terms of length and twenty-first largest in terms of drainage area (MRC Annual Report, 1998).

The Mekong is broadly divided into two political regions – the Upper and the Lower Basins. The portion of the Mekong that drains China and Myanmar is treated as the Upper Mekong Basin, while that portion of the drainage in Laos, Thailand, Cambodia and Vietnam is considered to be the Lower Mekong Basin.

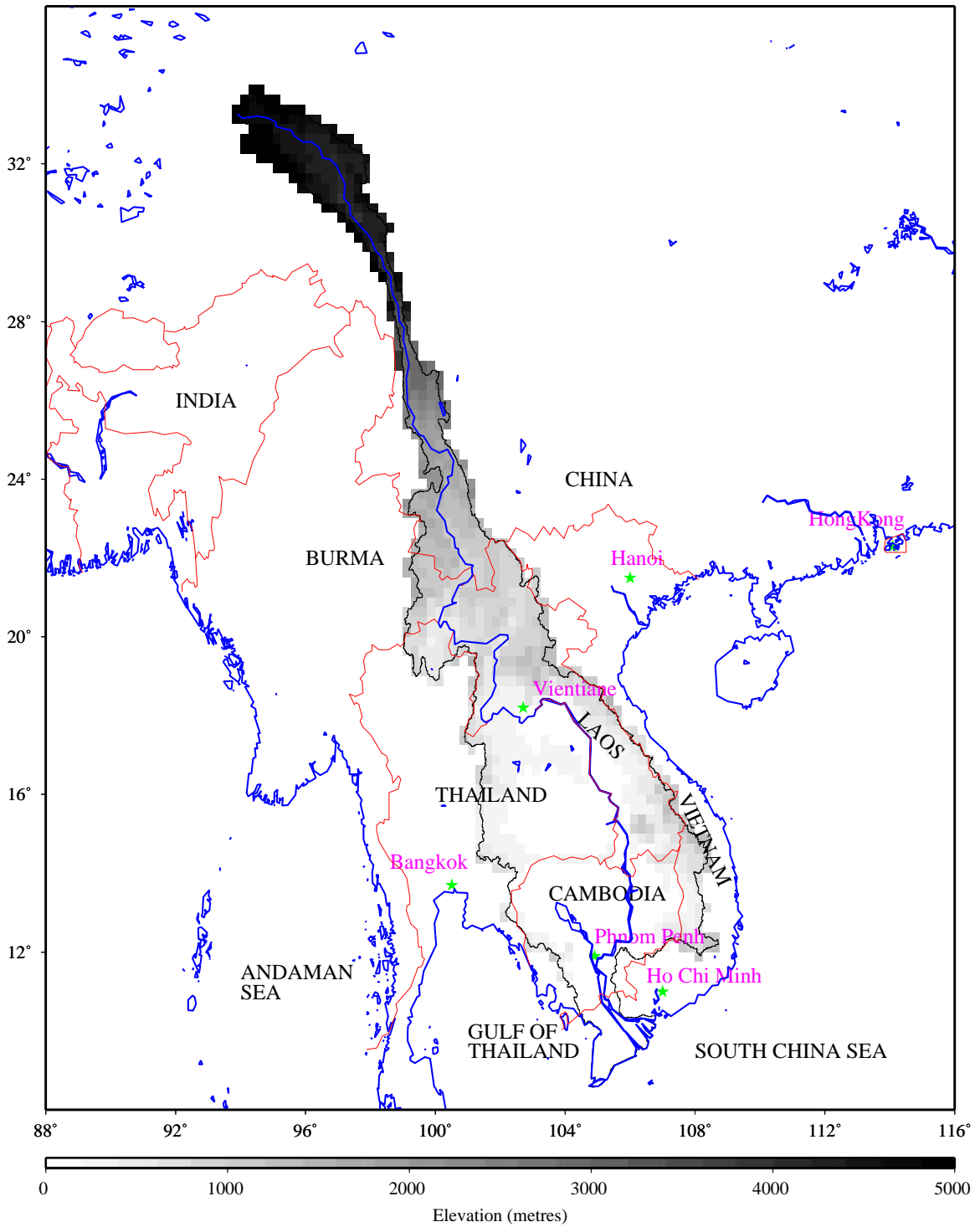


Figure 2.1 Topography and significant political and physical features of the Mekong Basin

### 2.1.1 Upper Mekong

The Mekong, known as Lancang Jiang in China, originates in eastern Tibet or Qinghai (Berman, 1998), and flows through the provinces of Qinghai, Sichuan and Yunnan before leaving China (Figure 2.2). This part of the basin is characterized by steep topography, and the river is confined by narrow gorges for most of its length. This region accounts for about one-sixth of the total basin area, and its flow is about one-fifth of the total. Due to the nature of the topography, this region has considerable potential for hydroelectric power development.

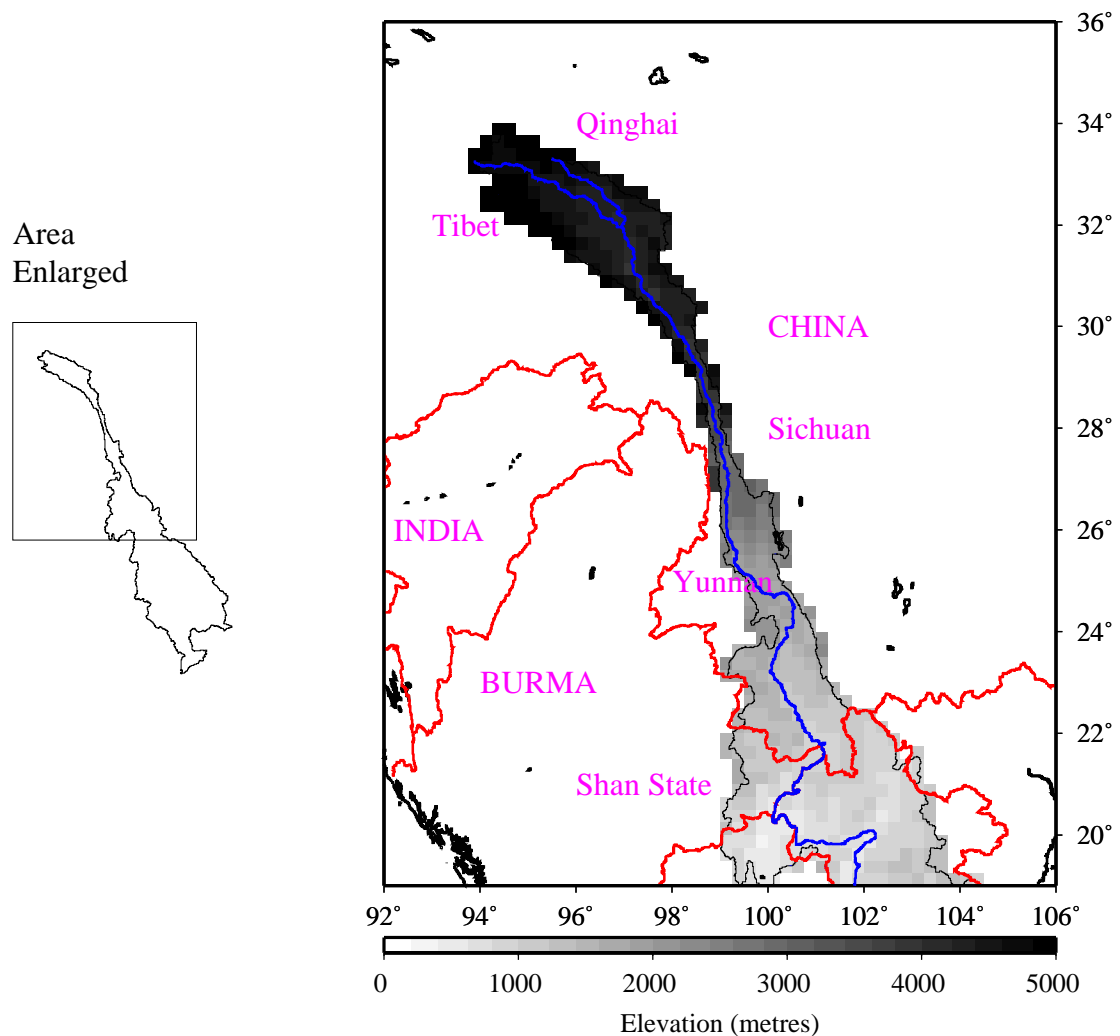


Figure 2.2 Upper Mekong

The section of the basin in Yunnan accounts for more than 50% of the Mekong's drainage area within China. Due to lack of information about the remainder of the basin lying within China, in all the future discussions of the Mekong basin in China, only the Yunnan portion will be considered.

Myanmar has only 2% of the total Basin area of the Mekong, most of which is in the Eastern Shan state (see Figure 2.2) (Bo and Win, 2000). The Nam Mae Kok tributary of the Mekong originates in this region, which is mostly hilly and forested.

#### 2.1.2 Lower Mekong

Large amounts of rainfall and steep topography make Northern Laos a good potential site for hydroelectric power generation. The northern and eastern parts of Laos are hilly or mountainous with elevations ranging from 200 to 2820 meters (Cheong, 1998). Several tributaries like Nam Ngum, Nam Ou, Nam Theun, Se Bang and Se Kong originate in Laos (Figure 2.3), which contribute about a third of the total flow of the river at its mouth. Laos has a tropical climate with the southwest monsoon from mid-April to mid-October creating more than 70% of the annual rainfall, which varies from 1000 mm in the provinces surrounding Vientiane, to more than 3000 mm in the hills of Central and Southern Laos (Cheong, 1998).

The northern tip of Thailand and Northeast portion of Thailand, also known as the Khorat Plateau, constitute the Thai portion of the Mekong basin (Figure 2.3). The Khorat Plateau is mainly drained by the Chi and Mun rivers and by smaller rivers that flow directly into the Mekong. The northern tip receives annual rainfall of 1250-1875 mm, whereas the Khorat Plateau is the driest part of the basin with annual rainfall of 1000-1250 mm (Pednekar, 1997).

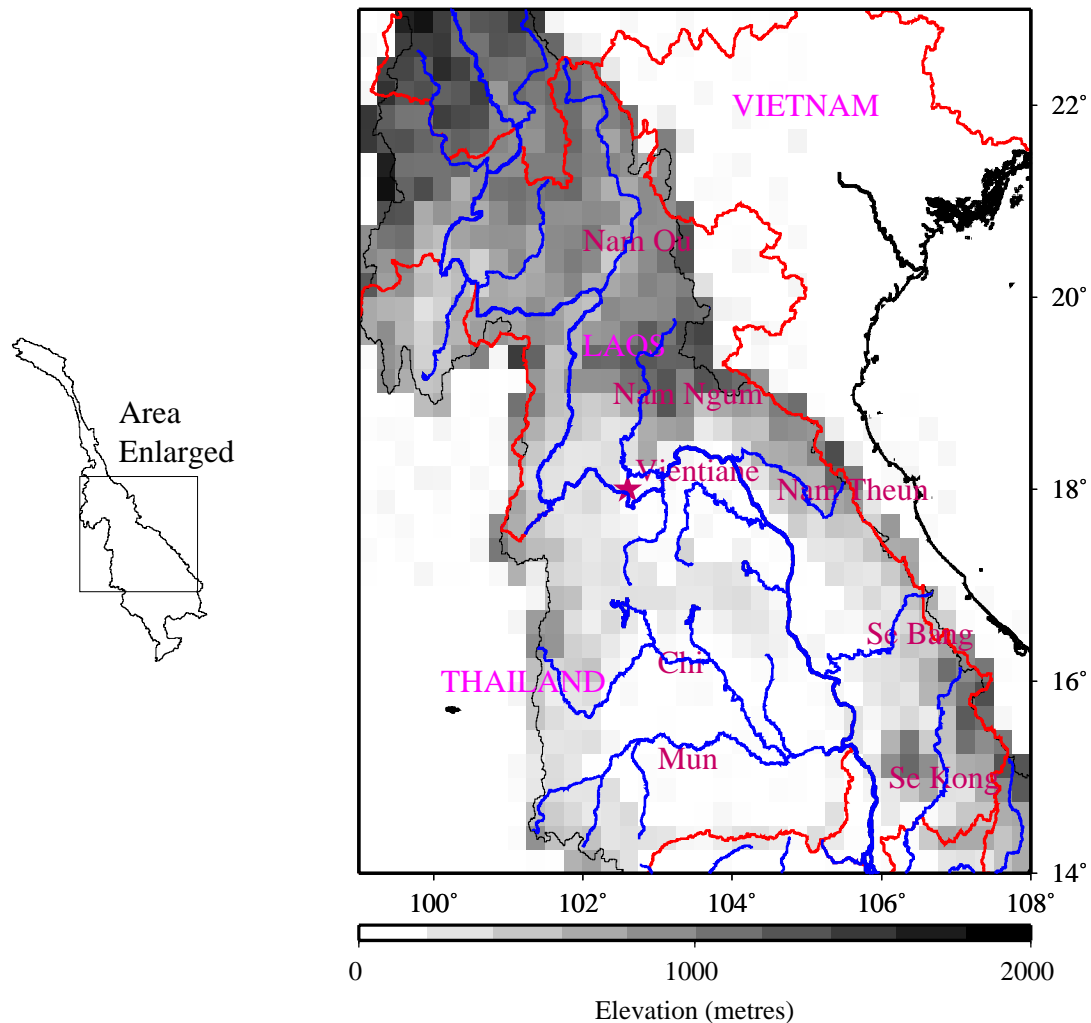


Figure 2.3 Laotian and Thai portion of the Mekong basin

The Mekong and the Tonle Sap Lake system are the main features of the Cambodian plains (Figure 2.4), whose average elevation is less than 10m. The Tonle Sap Lake regulates the flow of the main-stem of the Mekong by storing portions of peak flow from July to September and releasing it from October to April (MRC Annual Report, 1994). Thus the size of the Lake increases from about 2600 km<sup>2</sup> in the dry season to about 10,500 km<sup>2</sup> in the rainy season (Gartrell, 1997). The Tonle Sap Lake – Mekong system forms the backbone of Cambodia’s predominantly agricultural economy.

The Vietnamese portion of the Mekong basin (Figure 2.4) consists mainly of the Mekong Delta and the Central Highlands. The Mekong Delta, which is only 0.8 m above mean sea level, is a rich agricultural production zone contributing over 50% of the total paddy production of Vietnam (Miller et al., 1999). The network of rivers and canals in the

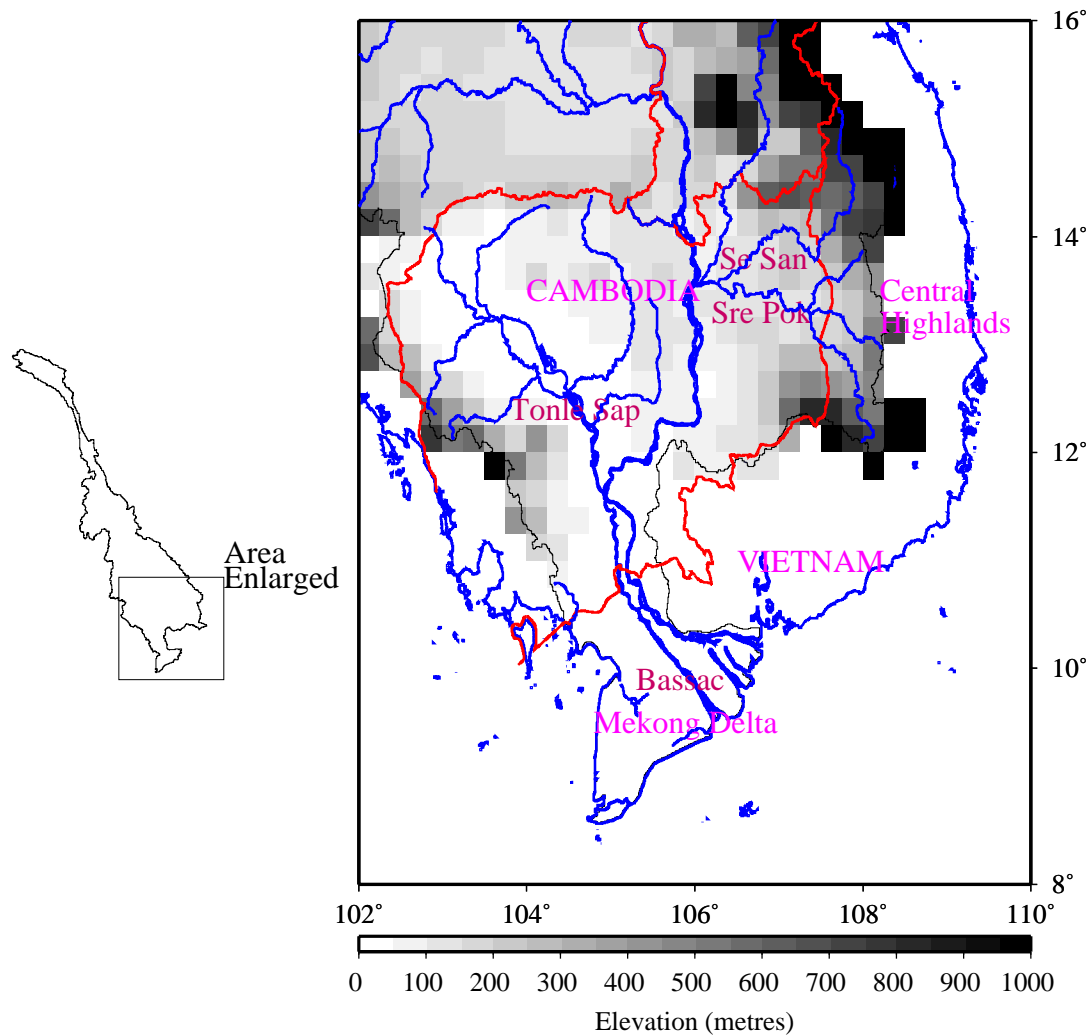


Figure 2.4 Cambodian and Vietnamese portion of the Mekong basin

Delta, which total to more than 10,000 km of waterways, is used extensively for irrigation and transportation purposes. This region is severely affected by salt water

intrusion during the dry season and by acute flooding during the wet season. Though the Central Highlands are not as agriculturally productive as the Delta, they are known for their coffee and rubber plantations. Se San and Sre Pok are the main tributaries of the Mekong that originate in these highlands.

## ***2.2 Hydroelectric Power Development and Flow Regulation***

Though hydropower development plans in the Mekong basin were created in the 1950s (Bakker, 1999), political conflict over three decades in most of the riparian countries prevented their implementation. Political stability since the ending of the Cambodian conflict in 1991 and increasing demands for electric power have motivated exploration of hydropower potential of the basin. The countries of this region view export of electricity, especially to relatively rich Thailand, as an attractive means to acquire foreign currency. Construction of dams and reservoirs in the basin could significantly alter the main-stem flow during the rainy and dry seasons. Wet season flow is critical to fish and rice production in the Mekong Delta and the Cambodian plains. Decrease in dry season flows could affect transport and commerce and could increase seawater intrusions in the Delta.

Table 2.1 Hydropower potential of the Mekong basin (Bakker, 1999)

Country	Hydropower Potential (MW)	Hydropower Potential (%)
China (Yunnan)	13000	42
Myanmar	-	-
Laos	13000	42
Thailand	1000	3
Cambodia	2200	7
Vietnam	2000	6
Total	31200	100

Most of the hydroelectric power development of the Upper Mekong is likely to be on the main-stem due to the narrow gorges and the incised nature of the topography.

Hydroelectric power dams have been planned at seven sites (Figure 2.5) in China's Yunnan province (Chapman and Daming, 2000). Of these seven sites, the Manwan dam was completed in 1993, near the city of Lincang in Yunnan. The damming of the upper portions of the Mekong has the potential to affect the downstream discharge patterns significantly, and concerns have been raised about possible environmental damage (Chapman and Daming, 2000; Hinton, 1998).

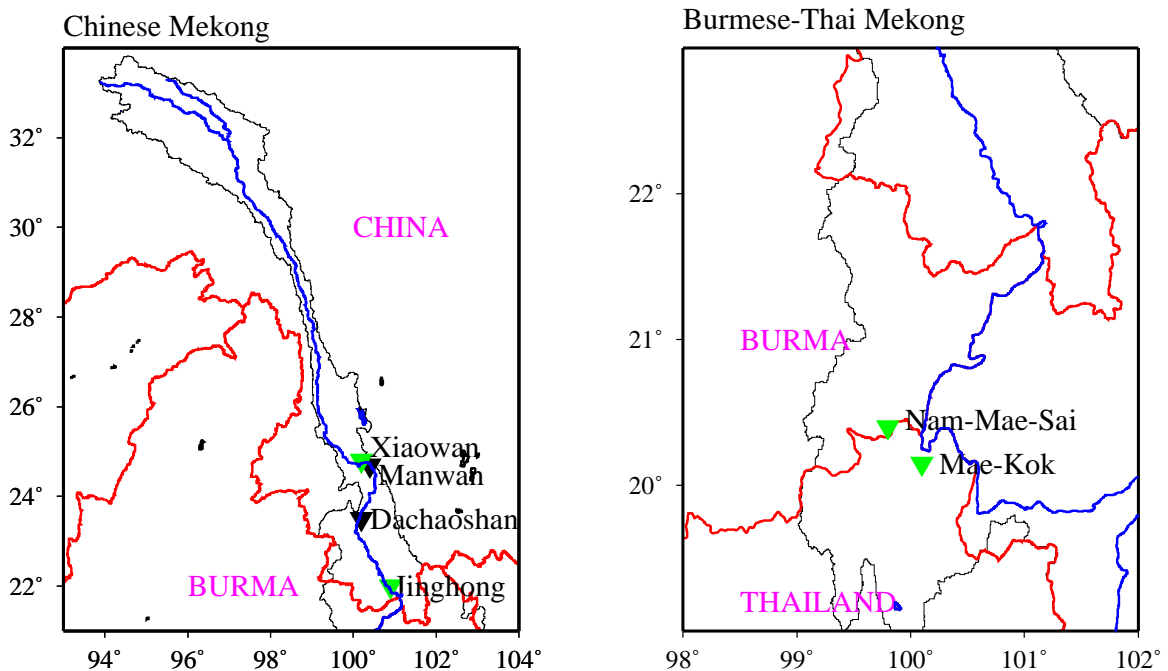


Figure 2.5 Existing (black triangles) and proposed (green triangles) dams in Yunnan and Burma

Dams at various locations (Figure 2.6) in the Laotian portion of the Mekong basin have been proposed by the government of Laos mainly to produce power for export to neighboring Thailand (Dansie, 1994 and IRN, 1999). The Nam Ngum dam, which was completed in 1985, and the Nam Theun Hinboun and the Houay Ho trans-basin diversion

schemes, which were completed in 1998, were designed to supply power to Thailand. Poor financial viability, problematic environmental impact assessments and inadequate resettlement practices are some of the causes for public protest against some of these projects (IRN, 1999).

In the Thailand part of the Mekong basin, which has relatively low hydropower potential (Table 2.1), most of the hydropower has already been exploited (Figure 2.6). Building of new dams is unlikely in this region because of environmental movements against the construction of large dams (Rigg, 1995). The Pak Mun Dam on the Mun River, which was completed in 1994, is one such example. Fish populations, which are an important

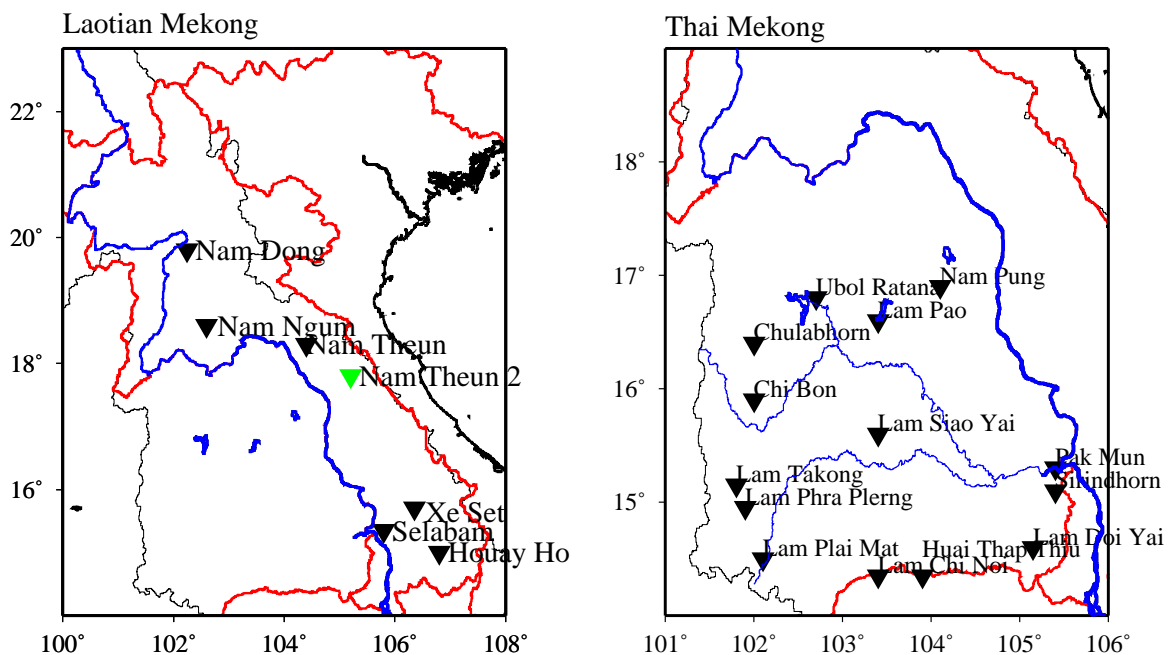


Figure 2.6 Existing (black triangles) and proposed (green triangles) dams in the Laotian and Thai portion of the Mekong basin

source of income for the local people, have decreased significantly following completion of the dam. Furthermore, the dam has not functioned at its designed capacity for various reasons (Amornsakchai et al., 2000). As result of public protest, the gates of the Pak Mun

Dam were opened temporarily in June 2001 to assess the impacts of the dam on fisheries of the Mun River.

Political and economic stability of Cambodia is a prerequisite for hydropower development in the Cambodian portion of the Mekong basin. Hydropower development projects have been proposed in several parts of Cambodia (FAO Cambodia, 1996), some of which are shown in Figure 2.7.

The existing Yali Falls dam on Se San River and the proposed Pleikrong dam (Figure 2.7) in Vietnam are designed to provide electricity for central and southern parts of Vietnam (Miller et al., 1996). The irregular water releases from the reservoir of the Yali falls dam have been of serious concern for the downstream people of Cambodia (NTFP, 2000).

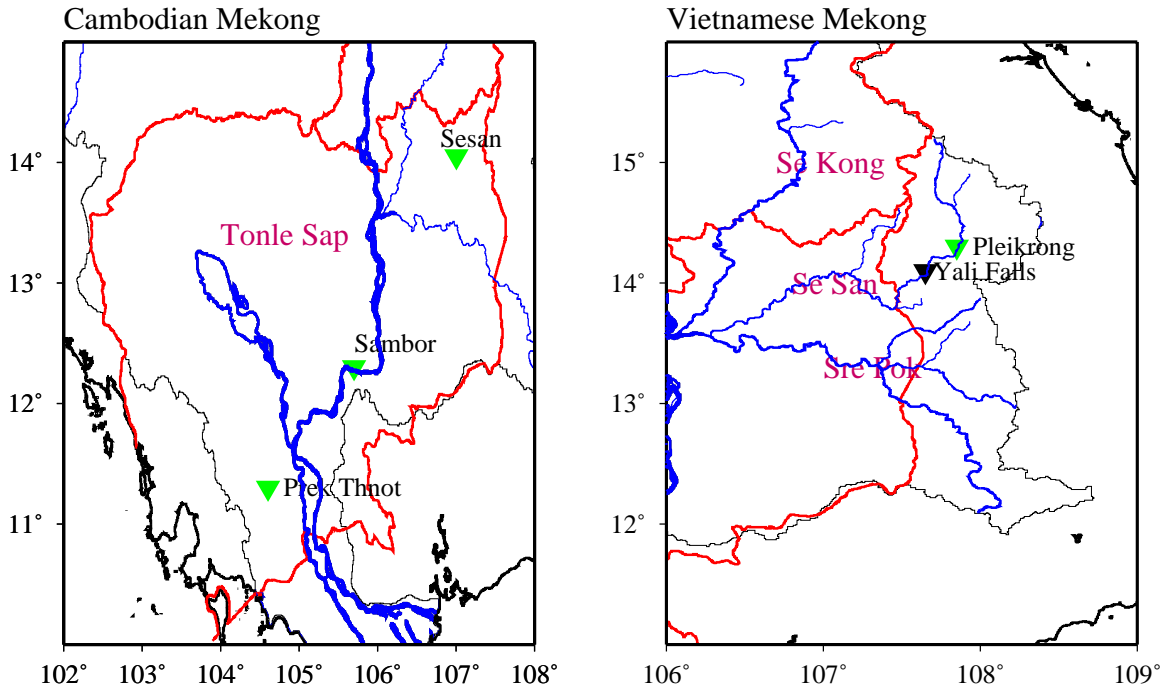


Figure 2.7 Existing (black triangles) and proposed (green triangles) dams in Cambodian and Vietnamese portion of the Mekong basin

### ***2.3 Agriculture and Land Use***

The main cause of deforestation in the Mekong basin is expansion of agricultural land or shifting cultivation. Agricultural lands are gradually replacing forests, as a result of increasing food demands associated with increased population of the region (see Chapter 1). The agricultural practices and the state of the forests in each region of the Mekong basin are discussed in this section.

#### **2.3.1 Yunnan**

Large-scale agricultural development of the Upper Mekong is not feasible due to the mountainous terrain and narrow gorges. Forest cover is 39.1% of the total land area in the Yunnan portion of the Mekong basin (Puustjarvi, 2000a). Deforestation due to mining, during the early periods of Mao era, and shifting cultivation practices, have lead to widespread soil erosion, which is a serious problem in this area. As of 1998, the erosion prone areas account for 28.1% of the total area of the basin in Yunnan (Puustjarvi, 2000a). To improve forestry and watershed management and soil erosion control, the government has planned reforestation measures and banned commercial logging.

#### **2.3.2 Laos**

In Laos, only 16% of the potentially cultivable land is used under both lowland terrace and upland shifting cultivation systems (Cheong, 1998). In shifting cultivation type farming, forests are burnt down to some extent and the land is cultivated. When there is no more forest to burn, and the productivity of the soil has declined, the farmers move to new areas. Under this practice, the soil recovers within 10 to 20 years, provided the fields are not burnt off excessively (Chazee, 1994). The amount of cultivable land and the type

of cultivated crop vary with the terrain, which is mostly hilly. In the uplands of Northern Laos, where shifting cultivation is predominant, the area under rice cultivation accounts for 27% of the national total (Lao Agricultural Census 1998-99, 2000). In the other parts, lowland terrace farming is predominant with rice as the primary crop.

The extent of forest cover in Laos has been steadily decreasing during the past few decades (Figure 1.2, Chapter 1). A study by Forest Cover Monitoring Project (Puustjarvi, 2000b) shows that during the period 1993-97, out of the total forestland cleared, 25% was replaced by wood and shrub-land, 63% by shifting cultivation, and the rest by permanent agriculture.

### 2.3.3 Thailand

Although Northeast Thailand has an annual rainfall of more than 1000 mm, high evaporation rates make it a semi-arid region. Sandy and saline soils occur throughout this region and make the land unsuitable for water intensive crops like wet-rice. In spite of poor soil fertility, agriculture is intensive in this region. Glutinous rice, maize and cassava are the main crops (Pednekar, 1997).

The Northern Thailand portion of the Mekong basin is the most forested part of Thailand. The change in forest cover in Thailand over the last fifty years is the highest among the countries of the Mekong basin (Figure 1.2, Chapter 1). In the Khorat Plateau, forest cover decreased from 42% in 1961 to 13% in 1993 (Pednekar, 1997). Logging and agricultural expansion are the main causes of deforestation in this region.

### 2.3.4 Cambodia

Rice is the predominant crop of Cambodia, where the agricultural sector accounts for half of the GDP and employs 80-85% of the country's labor force (Gartrell, 1997). Rice production in the flood plains surrounding the Tonle Sap, Mekong, and Bassac rivers is the main component of agriculture.

More than half of Cambodia is covered with evergreen, mixed or deciduous forests. Due to commercial logging, shifting cultivation, expansion of agricultural land, and various other reasons the forest cover in Cambodia has decreased from 73% in 1973 to 63% in 1993 (Ikunaga, 1999). The upstream and the downstream currents of the Tonle Sap Lake system are crucial to the livelihood of the people of the Cambodian plains and support 90% of Cambodia's population. A decrease in the forest cover of the region could affect this system by changing the patterns of erosion, flooding, and siltation.

### 2.3.5 Vietnam

Agriculture accounts for 63% of the land in the Mekong Delta of Vietnam and 10% of the land in the Central Highlands (Miller et al., 1999). Though extreme floods cause damage to the agricultural lands of the Delta, the fertile soil and acid flushing of the annual floods are beneficial to farming. Upstream flow regulation and other human activity can affect the seasonal flow patterns of the Mekong and might aggravate problems like saltwater intrusion and acute flooding.

There has been a decrease in forest cover: from 23% to 9% in the Mekong Delta, and from 93% to 60% in the Central Highlands during the period 1943-1991 (Puustjarvi, 2000c). Deforestation in these regions is mainly due to agricultural expansion or shifting cultivation (Miller et al., 1999). In the Mekong Delta forests are essential for soil conservation and also for coastal protection and maintenance of bio-diversity.

## ***2.4 Fisheries***

Fish production, which is mainly from capture fisheries and partly from aquaculture (ICCILMB, 1992), is a significant industry in the countries of the Lower Mekong basin. The main-stem of the Mekong and its major tributaries, the Tonle Sap Lake, the floodplains in southern Cambodia, the reservoirs of Thailand and Laos, and the brackish water zone of the Mekong delta are the main fisheries systems. The 1200 species found in the lower basin compare to the 3000 fish species found in the Amazon basin, whose drainage area is about ten times larger than that of the Mekong (Rainboth, 1996). The combined effect of development of water resources, logging, expansion of farmland, use of agricultural chemicals and sewage from the cities is a serious concern relative to the future health of the fisheries resources of the Mekong basin (Chapman and Daming, 2000).

## ***2.5 Competing Interests and the Role of Mekong River Commission***

The resources of the Mekong River basin are shared among six different countries, which have different resource-utilization priorities. Upstream China is interested in development of hydropower, whereas downstream Cambodia and Vietnam are concerned with flood control. As discussed in the earlier sections of this Chapter, flow regulation and other changes occurring in the upstream countries of the basin can have effects on the downstream countries. To achieve cooperation for the sustainable development of the resources of the basin, the Lower Mekong Basin countries of Laos, Thailand, Cambodia, and Vietnam formed the Mekong River Commission (MRC) in 1995. The member countries of the MRC agree to cooperate in all fields of sustainable development, utilization, management, and conservation of the water and related resources of the Mekong River basin, such as navigation, flood control, fisheries, agriculture, hydropower, and environmental protection (MRC Annual Report, 1998). Though China and Burma are not a part of the MRC, probably due to political reasons, the MRC

maintains regular dialogue with these countries. The MRC, since its inception in 1995, is cooperating with several developed countries and international organizations (MRC Annual Report, 2000) to achieve its goals.

## Chapter 3: Modeling Approach

### ***3.0 Overview***

In Chapter 2, streamflow regulation, deforestation, agricultural expansion and other man made changes taking place in the Mekong basin were discussed. These changes have the potential to affect the streamflow patterns of the Mekong and its tributaries and could have serious environmental, economic, and social impacts on the region. The response of the Mekong water resources system to these changes can be viewed as an interaction between the land surface hydrologic cycle, the physical infrastructure of the water resources system (dams and reservoirs), and water resources management practices (reservoir operating policies). Hydrologic and water management simulation tools can be used to explore the response of the water resources system to these interactions.

Macro-scale hydrology models can simulate rainfall-runoff processes of large river basins like the Mekong (Nijssen et al., 1997). These models are designed to represent the effects of vegetation on runoff, and thus can be used to simulate the effects of vegetation change (like deforestation and agricultural expansion) on surface hydrological processes. The effects of flow regulation can be simulated using water management models (Hamlet and Lettenmaier, 1999; Leung et al., 1999). Thus, a hydrology model when combined with a water management model (e.g. Hamlet and Lettenmaier, 1999) can be used to model the streamflow of the Mekong River and its tributaries. The hydrology and water management models used in this study are described briefly in this chapter.

### ***3.1 Hydrology Model***

The hydrology model used in this study is the Variable Infiltration Capacity (VIC) model, which has been applied to such large continental river basins as the Columbia (Nijssen et

al., 1997), the Arkansas-Red (Abdulla et al., 1996), and the Upper Mississippi (Cherkauer and Lettenmaier, 1999), among other rivers. A detailed description of the VIC model can be found in Liang et al. (1994, 1996 and 1998) and only an overview is presented here. The implementation of the VIC model for the Mekong basin is described in detail in Chapter 4.

The VIC model can be operated in two different modes: an energy balance mode and a water balance mode. In the energy balance mode, all the water and energy fluxes near the land surface are calculated, and the surface energy budget is closed by iterating over an effective surface temperature. In the water balance mode, the effective surface temperature is assumed to equal the air temperature and only the surface water balance fluxes are calculated. In this study, the VIC model is operated in the water balance mode, which is equivalent to the manner in which most operational hydrological models function. Precipitation, maximum and minimum temperature, and wind speed are the meteorological variables that drive the model in the water balance mode.

Some of the distinguishing characteristics of the VIC model are (Figure 3.1):

- the representation of subgrid variability in soil moisture storage capacity as a spatial probability distribution;
- the representation of drainage from the lowest soil moisture zone as a nonlinear recession;
- the representation of subgrid variability in land surface cover;
- the representation of subgrid variability in topography through the use of multiple elevation bands.

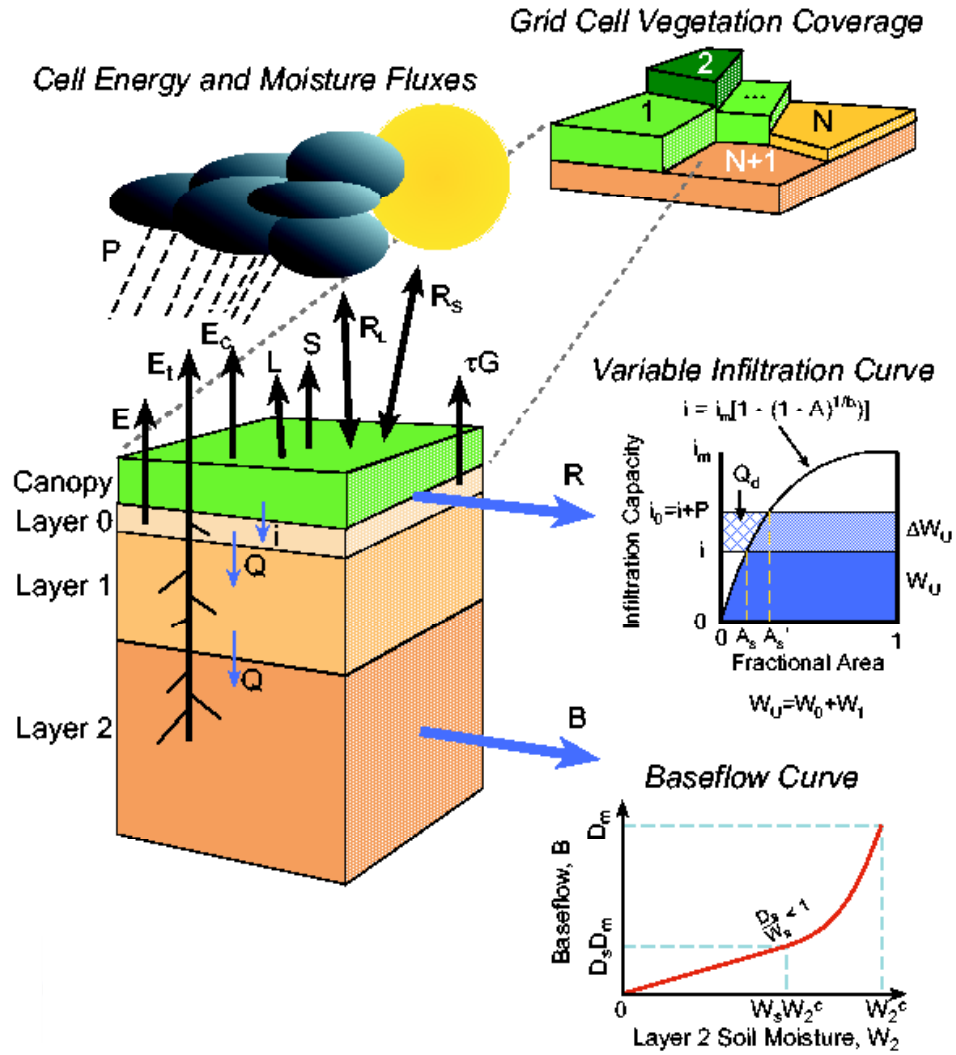


Figure 3.1 Schematic showing the VIC model

The subsurface is characterized in the vertical direction by an arbitrary number of soil layers with moisture and energy fluxes exchanged between the layers. In this study three soil layers were used. The top soil layer contributes runoff via fast response mechanisms whereas the deepest soil layer produces base flow according to the ARNO base flow

formulation (Todini, 1996), thus separating subsurface flow from quick storm response. Drainage between the soil layers is modeled as gravity driven.

Variability in land surface cover within each grid cell is represented using a given number of vegetation classes and specifying the fraction of the grid cell covered by each class. For each vegetation class, the leaf area index (LAI), canopy resistance, and relative fraction of roots in each of the soil layers are specified. Evapotranspiration from each vegetation type is calculated using a Penman-Monteith formulation (Liang et al., 1994).

Subgrid variations in temperature and precipitation, due to variations in elevation, are represented by subdividing each grid cell into a number of elevation bands. In this study, precipitation was assumed constant with elevation within a grid cell, but air temperature was lapsed from the mean grid cell elevation to the mean elevation of each elevation band using a lapse rate of  $-6.5^{\circ}\text{C}/\text{km}$ .

Precipitation is partitioned into rain and snow as a function of air temperature. The fraction of precipitation falling as rain or snow varies linearly between a rain and a snow threshold. All the precipitation above the snow threshold is treated as rain, and all the precipitation below the rain threshold is treated as snow. In this study the rain threshold was set to  $-0.5^{\circ}\text{C}$ , and the snow threshold was set to  $+0.5^{\circ}\text{C}$ . The effects of snow accumulation and melt are represented using an internal coupled snow model and is described in Storck and Lettenmaier (1999).

### 3.1.1 Routing Model

The VIC model is coupled to a linear streamflow routing scheme that transports the runoff generated within each grid cell through a specified channel network. The routing model is described in detail in Lohmann et al. (1996; 1998). The single runoff time-series

produced for each grid cell is routed to the grid cell outlet using a triangular unit hydrograph. Flow from each grid cell can exit into any one its eight neighbors, but all flow must exit in the same direction. The flow from each grid cell is weighted by the fraction of the grid cell that lies within the basin. The hydrographs for the individual grid cells are routed to the basin outlet through the channel network using linearized St. Venant's equations (Lohmann et al. 1996; 1998). The routing model does not account for channel losses, extractions, diversions and reservoir operations.

### ***3.2 Water Management Model***

A water management model represents the interaction between the physical infrastructure of the water resources system (dams and reservoirs) and water management practices reflected in reservoir operating policies. The Mekong water management model (henceforth referred to as MWMM) operates on a monthly time scale and is driven by streamflow data simulated by the VIC model. The dams considered in the MWMM (see Table 4.6, Chapter 4) are all designed for hydroelectric power generation and/or irrigation.

Hydroelectric power dams considered in the MWMM include many run-of-the-river dams, which use the volume of flowing water to generate electricity without causing an appreciable change in the flow of the river. Dams other than the run-of-the-river dams are assumed to be operating in two major planning periods for each water year. In the wet season, when dams have more than sufficient flows to meet their particular demands, part of the inflow is used to fill the storage reservoir. In the dry season, when inflow into the dam is inadequate to meet the demand, water from the storage reservoir along with the inflow is used to fulfill the demand. The operation of these dams is according to assumed rule curves, since information about the operating policies was not available.

The cross-sections of the reservoirs associated with the dams represented in the MWMM are assumed to be rectangular, with the storage level varying linearly between a specified minimum level and the maximum possible storage level. This specified minimum level corresponds to the minimum head required for operation of the dam. The power generated by each dam is a function of the amount of flow that passes through the reservoir's turbines and the head associated with this flow, and is given by

$$power = \rho \times flow \times g \times h \times \eta \quad (3-1)$$

where,  $\rho$  = density of water,

$g$  = acceleration due to gravity,

$h$  = hydrostatic pressure head associated with of the inflow

$\eta$  = efficiency of the power generating system

The only operational target to be met by hydropower dams in the MWMM was the observed (or designed) power output. The operational targets to be met by multipurpose (irrigation and hydropower) dams were the observed (or designed) irrigation release and the observed (or designed) power output. The implementation of the MWMM is discussed in Section 4.5.

### ***3.3 Approach***

The overall approach taken in this study was:

1. Implement the VIC model for the Mekong basin and calibrate it to give reasonable agreement between the simulated flows and recent observed discharge at various locations on the main-stem and tributaries of the Mekong.

2. Implement the water management model taking into account the existing and planned major dams and reservoirs in the basin and evaluate the reliability of the planned reservoir system.
3. Analyze the impacts of large-scale deforestation in different parts of the basin using the hydrology model and the water management model.

## Chapter 4: Model Implementation

### *4.0 Overview*

As described in Chapter 3, the VIC model is a grid-based model. The choice of grid-resolution depends primarily on the availability of meteorological data. In this study, the VIC model was implemented in daily water balance mode (see Section 4.4) at  $\frac{1}{4}$  degree spatial resolution. The grid size represents a compromise between the availability of data and the need to resolve tributaries on which major reservoirs are located. The data required for the implementation of the VIC model for the Mekong River basin and the results of this implementation are discussed in this chapter, as is the implementation of the water management model (see Section 4.5).

### *4.1 Land Surface Characteristics*

Topographical data, soil data, and vegetation cover data are the three kinds of surface characteristics data needed for the implementation of the VIC model. This section describes the sources from which these data have been obtained and the processing of these data.

#### 4.1.1 Topography

##### a) Digital Elevation Model

A Digital Elevation Model (DEM) of the Mekong River basin, at a resolution finer than the model resolution, is required for the simulation of the river network (see sub-section b) and for the determination of snow elevation bands (see sub-section c). A 30-arcsecond DEM of the Mekong basin, obtained from GTOPO30 online database

(<http://edcdaac.usgs.gov/gtopo30/gtopo30.html>) and processed by Sarah Rodda of the School of Oceanography, University of Washington, was used in this study. This DEM was aggregated to  $\frac{1}{4}$  degree (see Figure 4.1), the pixels of which formed the grid cells of the VIC model. For the grid cells lying on the boundary of the basin, the fraction of the grid cell lying inside the basin was specified. Only those grid cells for which a minimum of one percent of their area lay within the basin were considered, thus resulting in a total of 1280  $\frac{1}{4}$  latitude x  $\frac{1}{4}$  longitude grid cells.

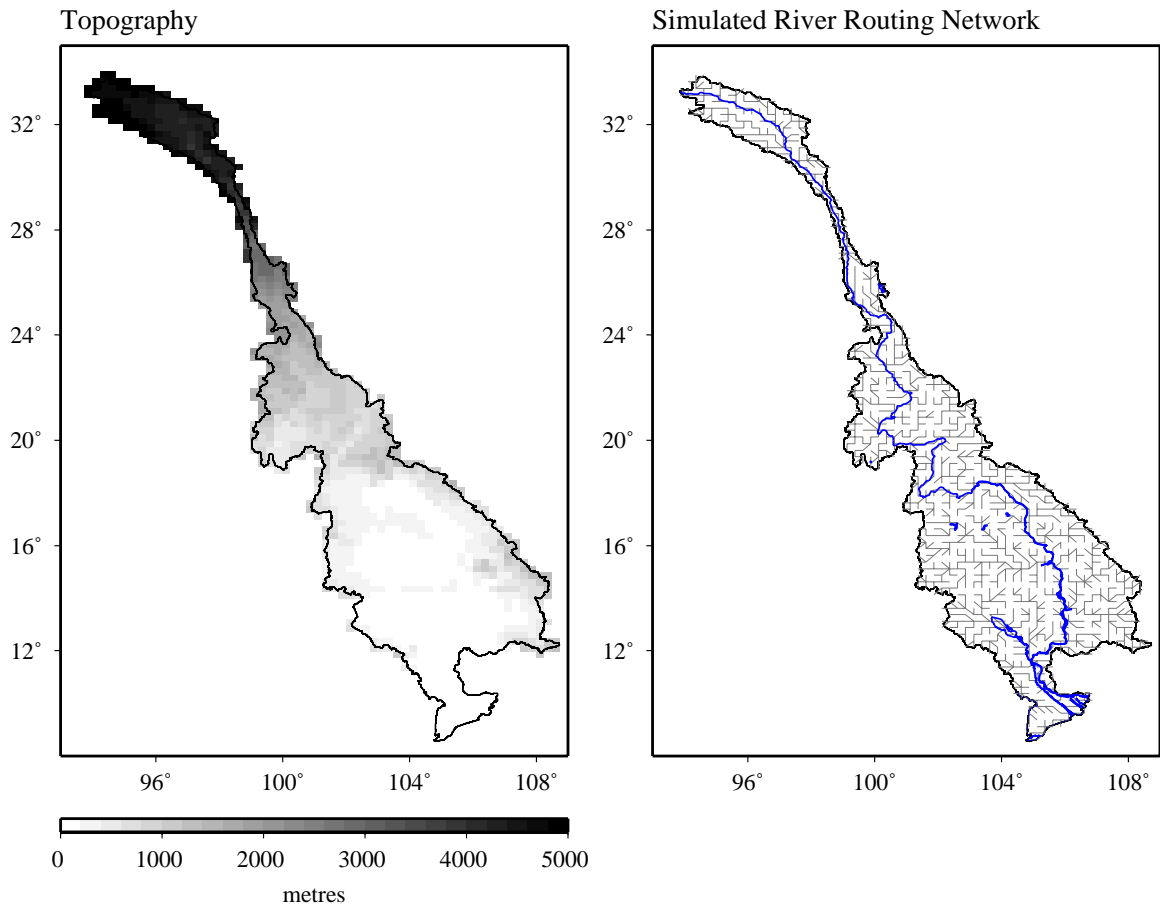


Figure 4.1  $\frac{1}{4}$  DEM and  $\frac{1}{4}$  degree river routing network

## b) River Routing Network

The routing model (see Chapter 3) represents the internal movement of runoff produced by the VIC model and subsequently between grid cells through the river system. The 30-arcsecond DEM was used to produce a 30-arcsecond flow accumulation matrix, calculated by assigning each cell a value equal to the number of cells flowing into it, in Arc-Info. This flow accumulation matrix was then used to derive the river routing network at  $\frac{1}{4}$  degree resolution using the algorithm of O'Donnell et al. (1999). The  $\frac{1}{4}$  degree river network thus generated (see Figure 4.1) was manually corrected to produce a model river network similar to the one from MRC (MRC Annual Report, 1998). Thus the flow paths of Nam Ou, Nam Theun, Se Bang Fai rivers (all in Laos) and Nam Songhkram River (in Thailand) were changed in the  $\frac{1}{4}$  degree routing network to match the flow paths of these rivers in the above reference.

#### c) Elevation Bands

In the VIC model, sub-grid variability in temperature, precipitation and snow accumulation is represented using elevation bands. Elevation band centers were assigned arbitrarily to be roughly greater than 250 m and less than 500 m, dependent on the elevation range of the grid cell (the difference between the maximum and minimum elevation of the 30-arcsecond pixels within the  $\frac{1}{4}$  degree grid cell). For example, if the range was 1200 m, three bands were created with nominal mid-band elevations of 200, 600 and 1000 m. The maximum number of elevation bands per grid cell was specified to be eight, and this maximum was realized for some grid cells in the northern portions of the basin.

#### 4.1.2 Soils

The soil data and its processing followed methods reported by Nijssen et al. (2001a), and this section largely follows Section 3.b.2 of that reference. Soil textural information and bulk densities were obtained by application of the SOILPROGRAM of Carter and

Scholes (1999) which combines the 5-minute FAO/UNESCO digital soil map of the world (FAO, 1995) with the World Inventory of Soil Emission Potentials (WISE) pedon database (Batjes, 1995). The FAO digital soil map records the dominant soil type for each 5-minute (roughly 10 km) grid cell, while the WISE database contains attributes for a large number of soil profiles around the globe. The SOILPROGRAM assigns attributes for each soil type by sampling the WISE database. The program allows specification of the depth of each soil horizon for which attributes are to be determined. The combined depth of the three soil layers was initially chosen as 1.5 m. The upper layer was taken as 0.1 m and the second layer as 1.0 m. The depth of the third layer was equivalent to 100 mm of water storage, which corresponds to a depth of about 0.25 m, depending upon the porosity. The depth of the second soil layer is a calibration parameter and it was changed during the process of calibration (see Section 4.4.1). Once the processing was completed at 5-minute resolution, soil attributes were aggregated to  $\frac{1}{4}$  degree by taking an arithmetic average over all 5-minute pixels in the VIC grid cell.

The remaining soil characteristics, such as porosity and saturated hydraulic conductivity, were based on Cosby et al. (1984). The moisture contents at field capacity and wilting point were determined by calculating the moisture retention at a metric pressure of -33 kPa and -1500 kPa, respectively. The program TRIANGLE, from Gerakis (1999), was used to convert soil textural information to the United States Department of Agriculture (USDA) soil textural classes used by Cosby et al. (1984). The ARNO parameters at  $\frac{1}{4}$  degree spatial resolution were obtained by interpolating the  $2^0 \times 2^0$  parameters from Nijssen et al. (2001a) to the  $\frac{1}{4}$  degree model grid cells.

#### 4.1.3 Vegetation

Vegetation data for the Mekong basin were taken from the Advanced Very High Resolution Radiometer (AVHRR) – based, 1-km, global land classification from Hansen

et al. (2000) which uses 13 land cover classes plus a water class. In this study, only 11 of these 13 land cover classes have been used. The water class was not considered a part of the land area and the fractional coverage of urban builtup class and bare ground class was not specified in the vegetation data. In the VIC model, the fraction of a grid cell not belonging to any of the 11 vegetation classes is treated as bare soil. The 11 different vegetation classes and their fractional coverage are shown in Figure 4.2. The properties of the 11 different vegetation classes are described in Table 4.1.

The monthly LAI values (see Figure 4.3) were taken from the 15-minute global LAI dataset processed by Nijssen et al. (2001a). The fraction of roots was assigned in such a way that trees and plants would predominantly take moisture from the top two soil layers. The rooting depths were so specified that only a nominal fraction of the roots extended beyond a depth of 1.0 m (see Table 4.2). The specification of other vegetation parameters such as height, minimum stomatal resistance, architectural resistance, roughness length, and displacement height was based on Nijssen et al. (2001a).

Table 4.1 Properties of different vegetation classes shown in Figure 4.2

<b>Vegetation Class</b>	<b>Properties</b>
Evergreen Needle-Leaf Forests	Canopy cover > 60%, Height > 5m All trees remain green all year, Canopy is never without green foliage
Evergreen Broad-leaf Forests	Canopy cover > 60%, Height > 5m All trees remain green all year, Canopy is never without green foliage
Deciduous Needle-leaf Forests	Canopy cover > 60%, Height > 5m Trees shed leaves simultaneously in response to cold seasons
Deciduous Broad-leaf Forests	Canopy cover > 60%, Height > 5m Trees shed leaves simultaneously in response to cold seasons
Mixed Forests	Canopy cover > 60%, Height > 5m Mixture of Needle-leaf and Broad-leaf forests
Woodlands	Canopy cover > 40% and < 60%, Height > 5m Herbaceous or woody understories, Evergreen or deciduous
Wooded Grasslands	Canopy cover > 10% and < 40%, Height > 5m Herbaceous or woody understories, Evergreen or deciduous
Closed Bushlands or Shrublands	Bush or shrub > 40%, Bush height < 5m, Trees < 10% Remaining cover is barren or herbaceous
Open Shrublands	Shrub > 10% and < 40%, shrub height < 2m Remaining cover is barren or herbaceous
Grasslands	Tree or shrub < 10% Continuous Herbaceous Cover
Croplands	Crop land > 80%

Table 4.2 Rooting depths and fraction of roots in each rooting zone

<b>Vegetation Type</b>	<b>Depth 1 (m)</b>	<b>Fraction in 1</b>	<b>Depth 2 (m)</b>	<b>Fraction in 2</b>	<b>Depth 3 (m)</b>	<b>Fraction in 3</b>
Evergreen Needle-Leaf Forests	0.10	5%	1.00	90%	5.00	5%
Evergreen Broad-leaf Forests	0.10	5%	1.00	90%	5.00	5%
Deciduous Needle-leaf Forests	0.10	5%	1.00	90%	5.00	5%
Deciduous Broad-leaf Forests	0.10	5%	1.00	90%	5.00	5%
Mixed Forests	0.10	5%	1.00	90%	5.00	5%
Woodlands	0.10	10%	1.00	85%	1.00	5%
Wooded Grasslands	0.10	10%	1.00	85%	1.00	5%
Closed Bushlands or Shrublands	0.10	10%	1.00	85%	0.50	5%
Open Shrublands	0.10	10%	1.00	85%	0.50	5%
Grasslands	0.10	10%	1.00	85%	0.50	5%
Croplands	0.10	10%	1.00	85%	0.50	5%

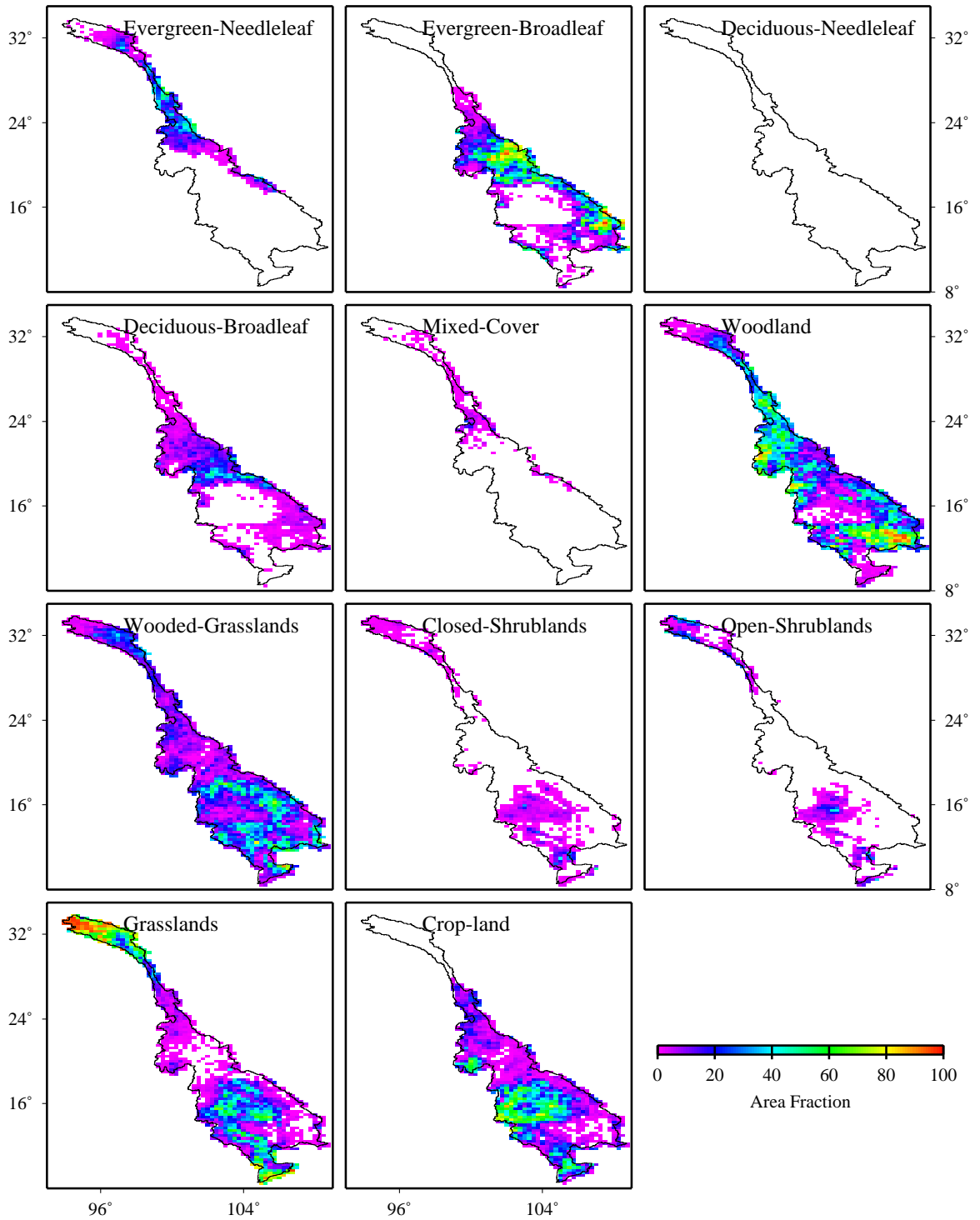


Figure 4.2 Fractional coverage of vegetation classes

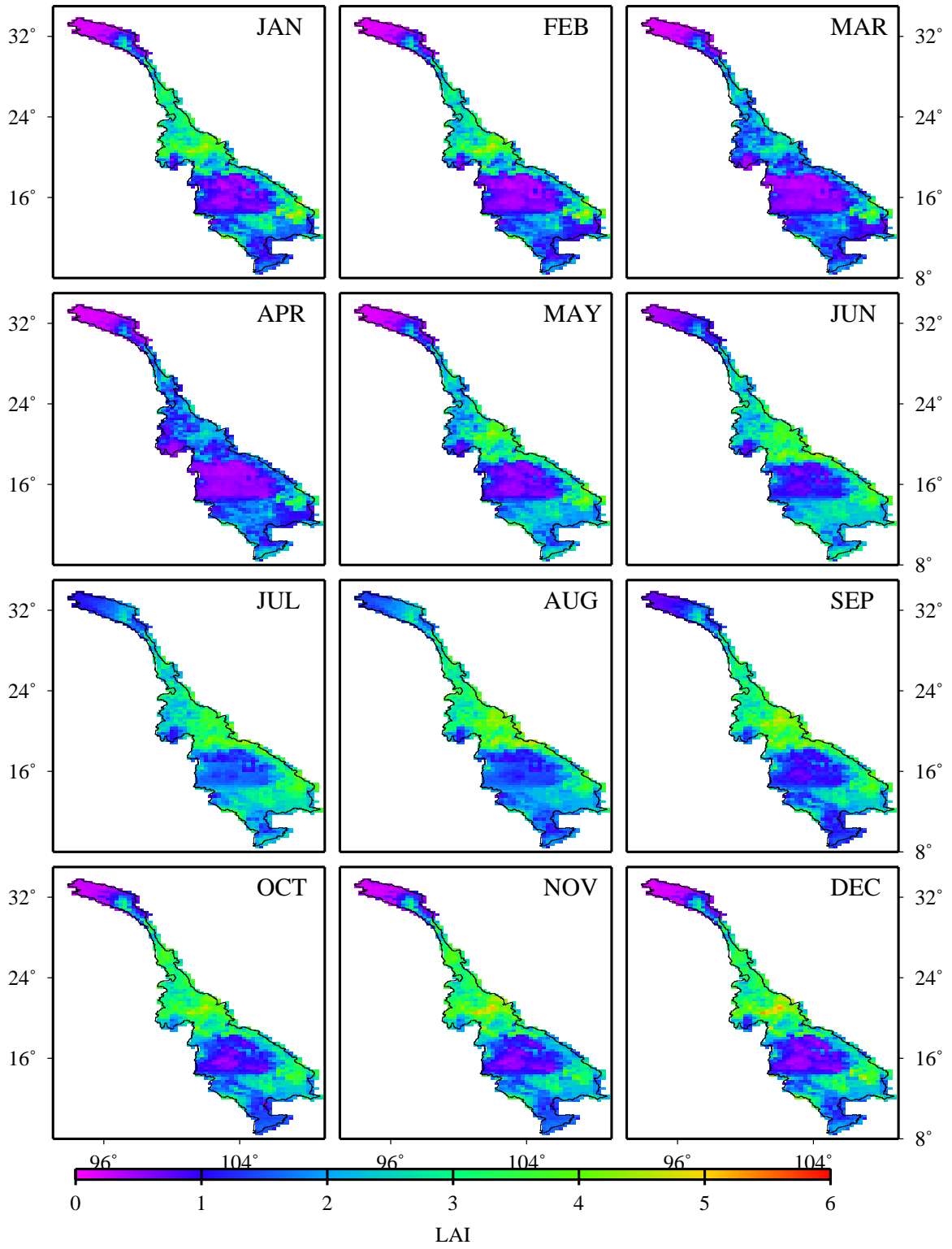


Figure 4.3 Monthly LAI

#### ***4.2 Meteorological Data***

The meteorological data used to drive the VIC model includes daily values of precipitation, maximum and minimum temperatures, and wind velocity. Station observations of daily precipitation and temperature were obtained from the NOAA Climate Prediction Center Summary of the Day data archived at the National Center for Atmospheric Research for the period January 1979 through December 2000. Data from 279 stations (Figure 4.4) were interpolated to the model grid cells using the SYMAP algorithm (Shepard, 1984) to obtain daily time series of precipitation and maximum and minimum temperature for each grid cell. Temperature data were interpolated using a lapse rate of  $-6.5^{\circ}\text{C}/\text{km}$  to adjust temperature from the station to the grid cell elevations. Wind speed data at  $\frac{1}{4}$  degree were obtained by interpolating  $2.5^{\circ} \times 2.5^{\circ}$  daily data from NCEP-NCAR Reanalysis (Kalnay et al., 1996) to the  $\frac{1}{4}$  degree model grid cells.

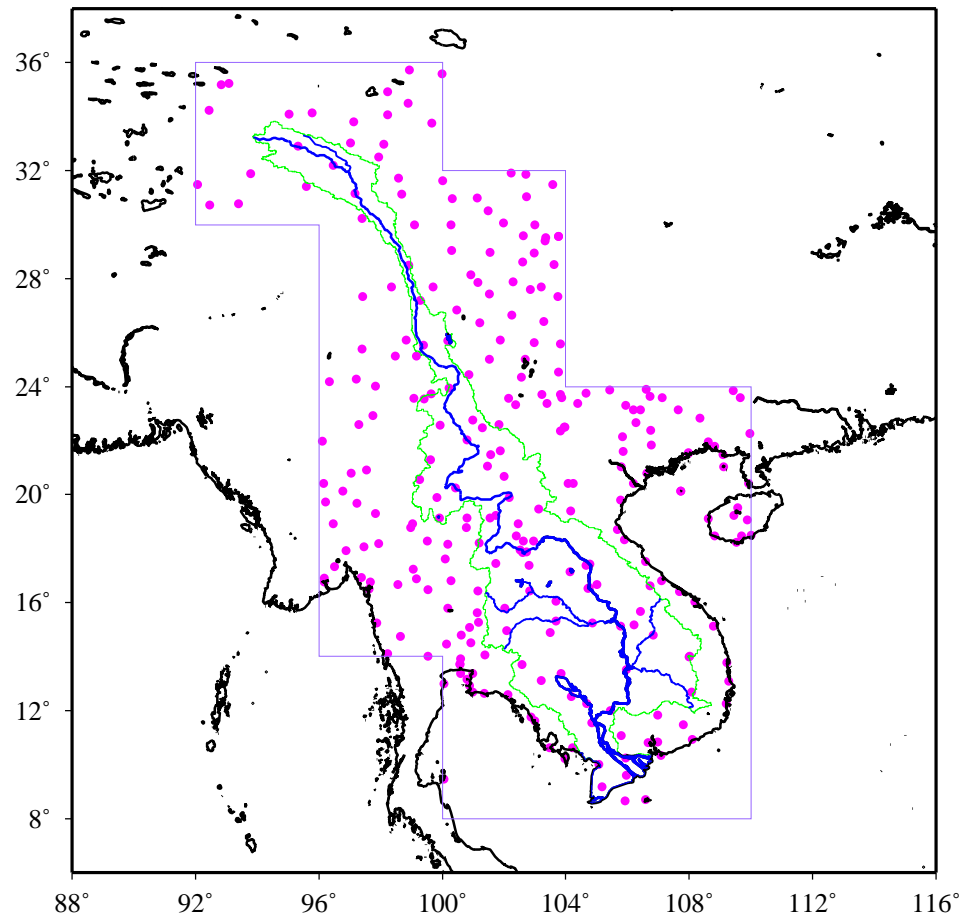


Figure 4.4 Meteorological data stations used in interpolation

### ***4.3 Streamflow Data***

Daily and monthly discharge observations were obtained from the Global Runoff Data Centre (GRDC, Koblenz, Germany) and the Mekong River Commission (MRC, Phnom Penh, Cambodia). The data from GRDC were discontinuous. The data records for the 51 GRDC stations (Figure 4.5) all began in January 1979 or later and ended in December 1993 or earlier. The data for the 13 MRC stations (Figure 4.5) were typically for the period January 1980 through December 1999.

All the stations obtained from GRDC and MRC are located in the Lower Mekong basin countries of Thailand, Laos, Cambodia, and Vietnam. Data from MRC and GRDC were merged, whenever possible, to give a more complete time series of streamflow measurements. Only those stations having a minimum drainage area of ten VIC grid cells (equivalent to approximately 1% of the total basin drainage area) and a minimum record length of five continuous years were used in this study. Because no station on any of the Mekong's tributaries in Laos satisfied the latter criterion, one station on each major tributary in Laos was selected. The final 16 stations so selected are shown in Figure 4.6. Data obtained from GRDC and MRC at four stations are compared in Figure 4.7, which confirms that in most cases the reported observations are identical, as was expected.

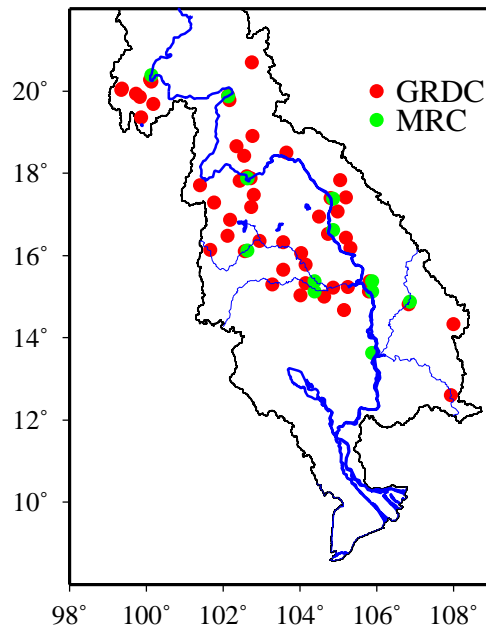


Figure 4.5 GRDC and MRC discharge measurement stations

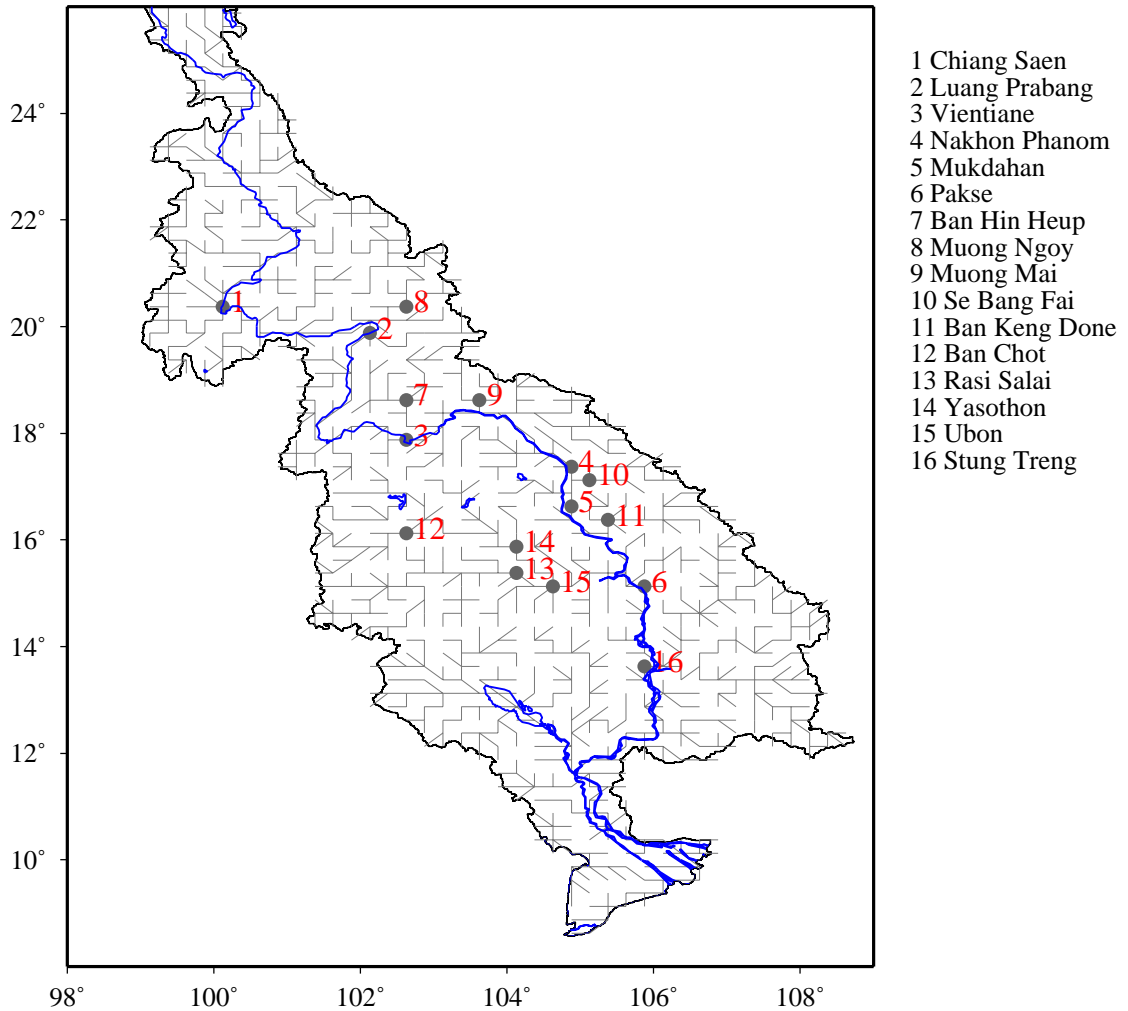


Figure 4.6 Final 16 stations selected from GRDC and MRC stations

The data from the 16 selected stations were used to evaluate VIC model output on the main-stem of the Mekong and its major tributaries. The observations reflect, in some cases, the effects of upstream regulation, whereas the VIC model simulates streamflow under natural flow conditions. However, the current reservoir system in the Mekong basin has a negligible effect on discharge at a monthly time step (see VIC model output in Section 4.4.2), so the comparison of VIC simulated streamflow data with monthly observations is justified. For all model calibration and validation purposes in this study, only observed monthly data were used.

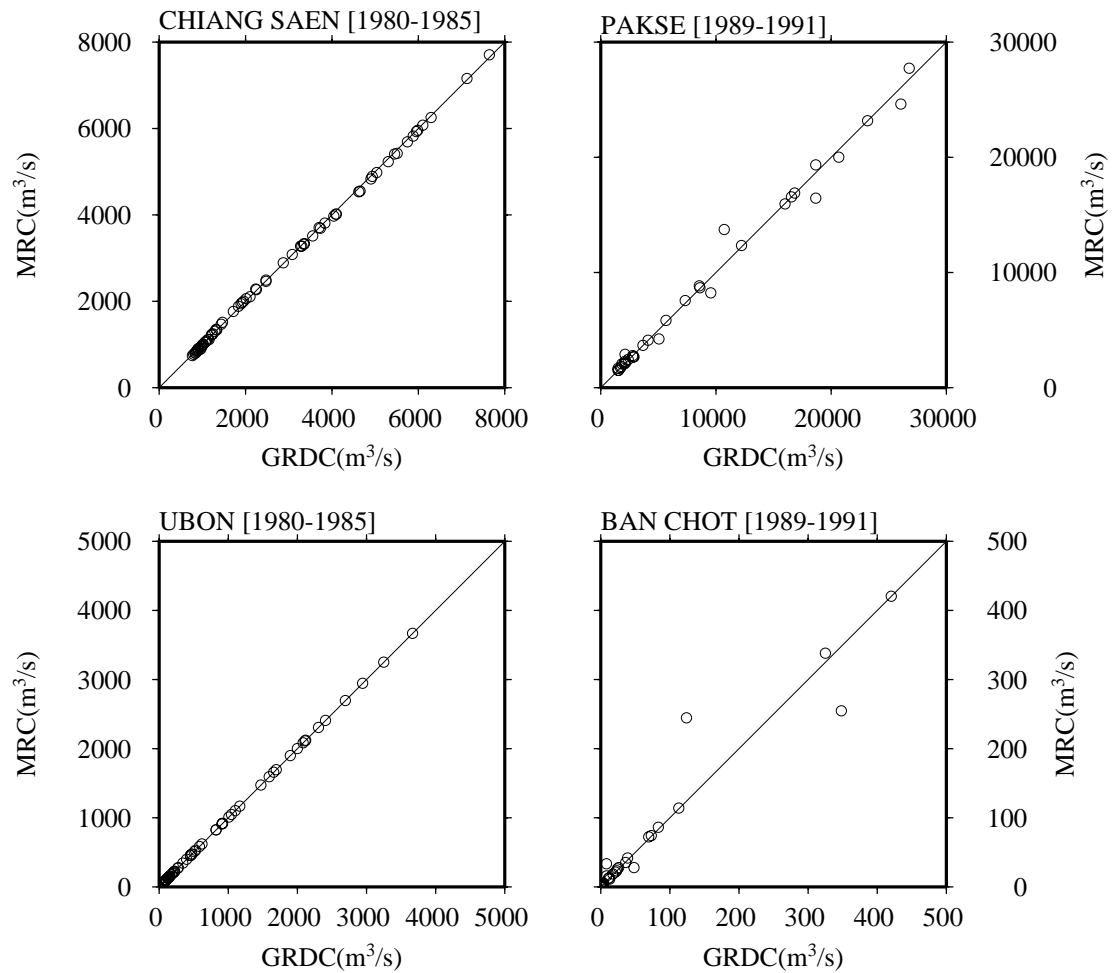


Figure 4.7 Comparison of GRDC and MRC data

## 4.4 VIC Model

### 4.4.1 Parameter Estimation

Runoff is parameterized in the VIC model due to the large spatial extent of each model grid cell. Calibration of some model parameters is necessary to give a good agreement between simulated and observed runoff. The identification of the calibration parameters

was based on Nijssen et al. (2001b). The variable infiltration parameter ( $b_i$ ), the depth of the second soil layer ( $D_2$ ), the saturated hydraulic conductivity of the second layer ( $k_{s2}$ ), and the exponent for the unsaturated hydraulic conductivity in the second layer ( $n_2$ ) were the calibration parameters. The sensitivity of the VIC model to changes in each of the above parameters is discussed in detail in Nijssen et al. (2001b). An increase in  $b_i$  or  $k_{s2}$  usually leads to an increase in total runoff. An increase in usually  $n_2$  results in a net decrease of total runoff and an increase in  $D_2$  leads to an increase in evaporation and thus to a decrease in total runoff.

For model calibration, streamflow gauging stations were divided into three groups: (1) stations upstream of Vientiane (stations 1, 2, 3, 7 and 8 in Figure 4.6), (2) stations in Northeastern Thailand (stations 12 through 15 in Figure 4.6), and (3) stations in Central and Southern Laos (stations 9 through 11 in Figure 4.6) and the main-stem stations of 4, 5, 6 and 16. The regions contributing runoff to each of these groups of stations were calibrated separately.

#### Upstream of Vientiane

The VIC model slightly underestimated runoff for stations upstream of Vientiane - stations 1, 2, 3, 7 and 8 (Figure 4.6). The calibration parameters mentioned above were adjusted to obtain better simulation of observed runoff. For the region upstream of Chiang Saen (station 1 in Figure 4.6), in addition to the calibration parameters mentioned above, wilting point ( $wp_2$ ) values of the second soil layer were also changed whenever increased dry season flow was required. Field capacity must always be greater than wilting point. Therefore the field capacity ( $fc_2$ ) values of the second soil layer were also increased whenever wilting point was increased. An increase in field capacity and wilting point decreases the amount of water available for evapotranspiration, which leads to an increase in the amount of water available for runoff and hence leads to an increase in total runoff.

### Northeastern Thailand

The initial model runs overestimate observed streamflow at stations 12, 13, 14 and 15 (Figure 4.6). Observations of mean annual precipitation and mean annual Class-A pan evaporation at several locations in Northeastern Thailand (obtained from the website of Department of Energy Development and Promotion, Thailand, <http://www.dedp.go.th>) indicate high rates of evaporation in this region. Higher evaporation rates were achieved through the use of thicker second soil layer depths and higher values of  $n_2$  and lower values of  $k_{s2}$ . The increase in net evaporation, after calibration of model parameters, can be seen in Figure 4.8.

### Central and Southern Laos

In the initial model runs streamflow was highly underestimated at station 4, 5, 6 and 16 (Figure 4.6). Except parts of Northeastern Thailand and Central Laos (Region B in Figure 4.9), Southern Laos (Region D in Figure 4.9), parts of Cambodia and Vietnam (Region E in Figure 4.9), all the regions contributing drainage to stations 4, 5, 6 and 16 were calibrated and reproduced observed flows reasonably well, indicating that the VIC model underestimated runoff in Regions B, D and E.

Precipitation, accumulated over the contributing drainage area is multiplied by the grid cell area to get accumulated precipitation in  $m^3/s$ , and is compared with observed streamflow for these three regions in Figure 4.9. The high monthly runoff values, which for many years exceed the precipitation, indicate that precipitation is misrepresented, which can be attributed to hilly terrain and scarce meteorological station density in these regions. Therefore, the daily precipitation data were scaled up by suitable factors to obtain reasonable agreement between simulated and observed streamflow. Data for Region B were scaled up by 35%, data for Region D were scaled up by 40% and data for

Region E were scaled up by 85%. The mean annual precipitation, before and after scaling the precipitation data, and the ratio of mean annual runoff to mean annual precipitation, before and after scaling the precipitation data, are shown in Figure 4.10. The ratio of mean annual runoff to mean annual scaled precipitation for regions B, D and E was compared with the same ratio for region A (see bottom portion of Figure 4.10), which has similar topography (see Section 4.1.1) and vegetation (see Figure 4.2).

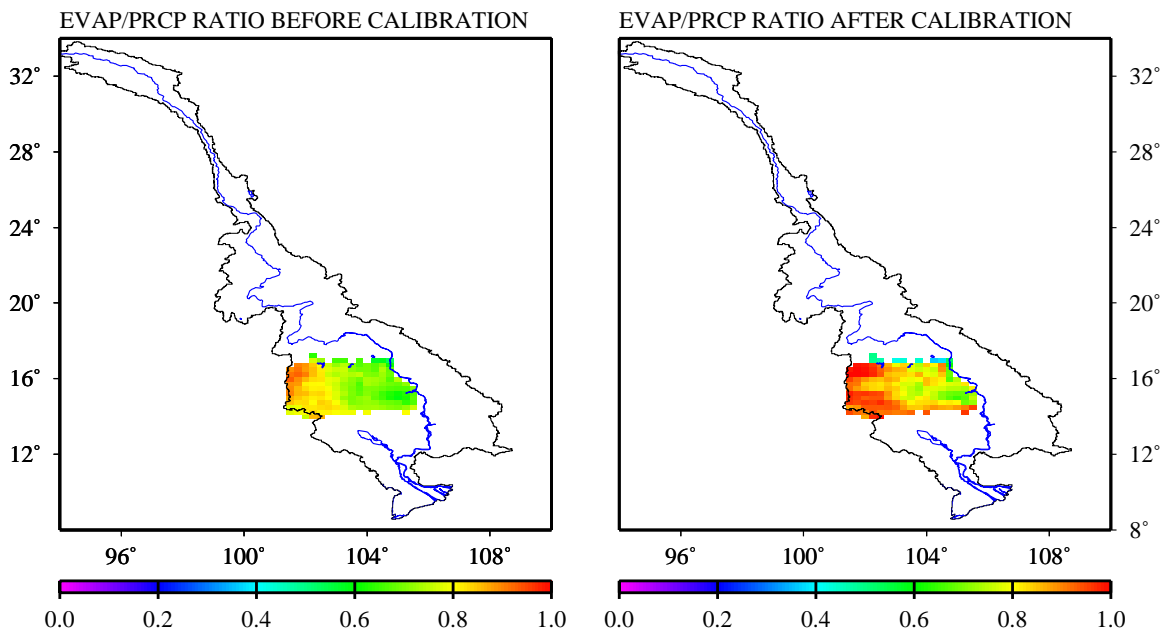


Figure 4.8 Ratio of simulated mean annual evaporation and mean annual model precipitation for different soil depths in Northeastern Thailand

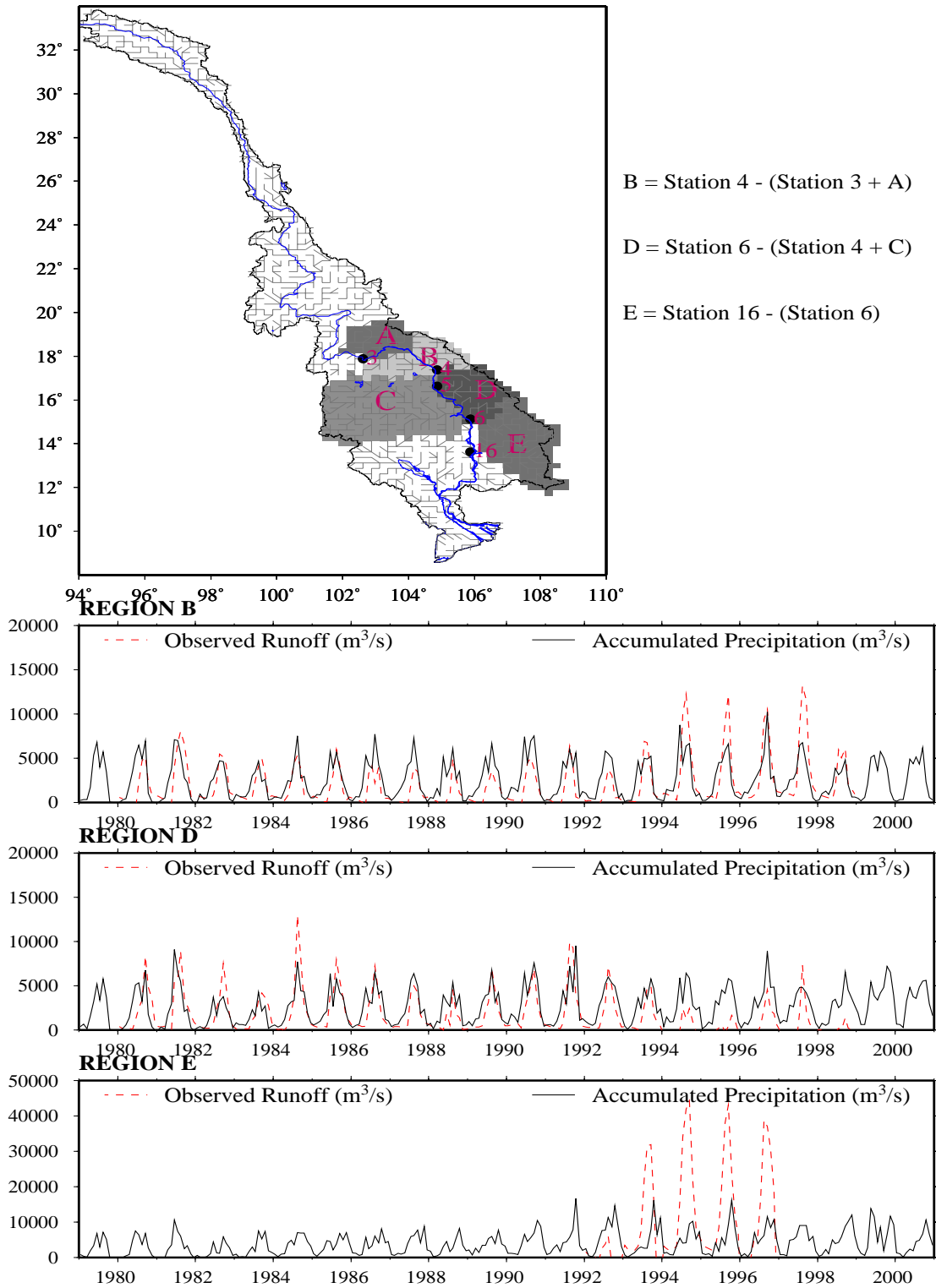


Figure 4.9 Comparison of observed runoff and accumulated precipitation for regions B, D and E

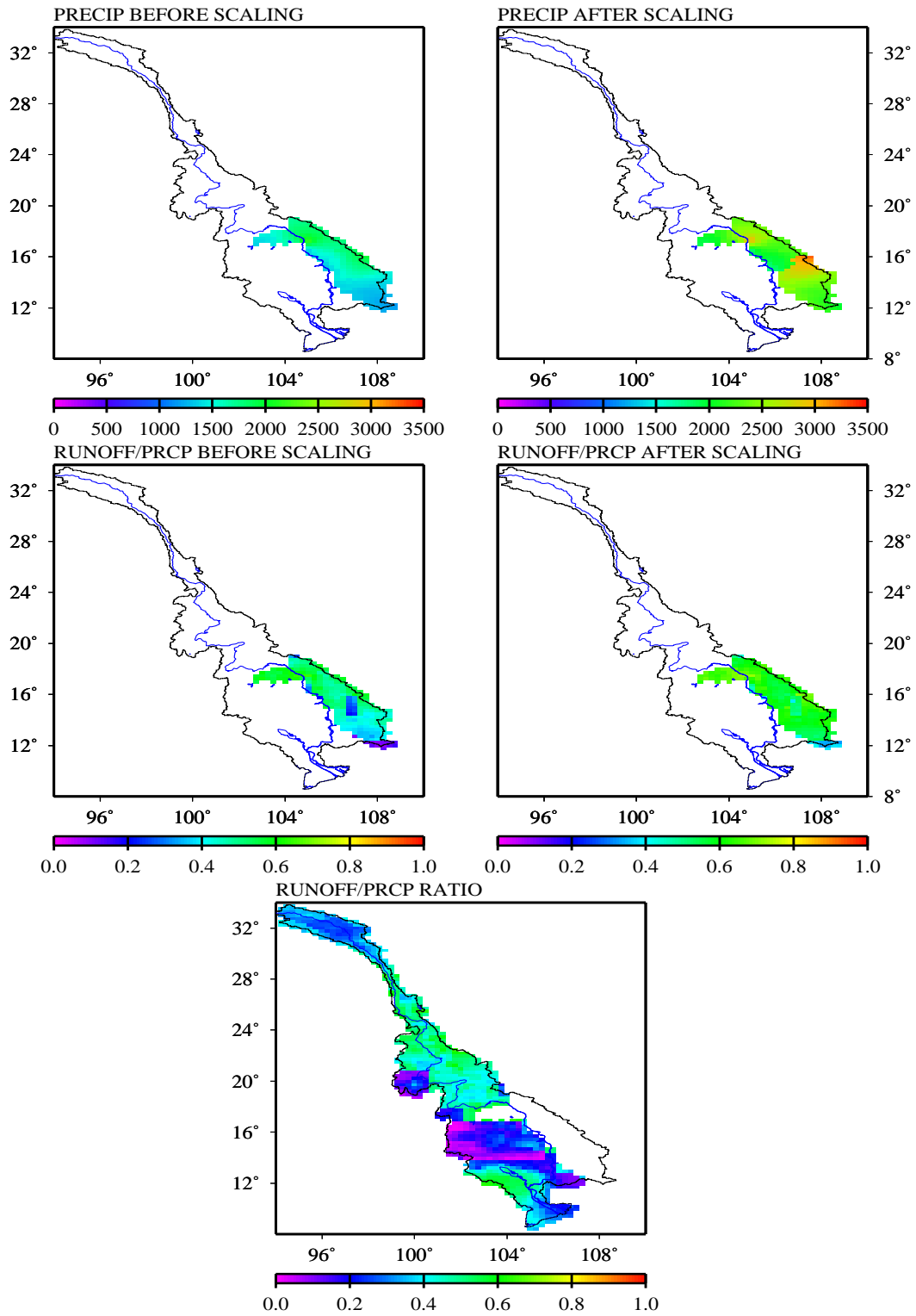


Figure 4.10 Effect of scaling precipitation data on precipitation and runoff

The values of the estimated parameters for the different calibration regions are shown in Table 4.3. Calibration involved splitting the period of simulation into two periods: 1979-1988 and 1989-2000. The model was calibrated for the first ten years of simulation (1979-1988), and the calibration parameters were transferred for the remaining period of simulation (1989-2000). Table 4.4 shows that model performance in the calibration and verification periods was quite similar with a slight degradation during the verification (transfer) period. Table 4.5 shows model performance summaries for parameter estimates using the entire period of record, which are generally somewhat superior to those based on the shorter calibration or verification periods. The Table 4.5 parameters were used in all subsequent model runs.

Table 4.3 Calibration parameters and their values for different regions

Region	$b_i$	$D_2$	$fc_2$ & $wp_2$	$n_2$	$k_{s2}$
		meters	% change from original values		
Upstream of Vientiane	0.25-0.65	0.25-1.00	+60%	-40%	0%
Northern & Northeastern Thailand	0.01-0.15	1.15 - 4.75	0%	+50% - +85%	-15% - -60%
Laos	0.65	0.30	0%	-40%	+60%
Rest of the Basin	0.25	1.00	0%	0%	0%

Table 4.4 Results of transfer of calibration parameters

Station	Location in Figure 4.5		Period	Simulated Mean Annual Streamflow (m <sup>3</sup> /s)	Observed Mean Annual Streamflow (m <sup>3</sup> /s)	(Simulated - Observed) as a % of Observed
<b>Mainstem Stations</b>						
Chaing Saen	1	Calibration	1979-1988	2611.2	2557.2	2%
		Transfer	1989-1998	2545.4	2596.5	-2%
Nakhon Phanom	4	Calibration	1979-1988	6621.3	6538.6	1%
		Transfer	1989-1998	6756.4	6978.4	-3%
Pakse	6	Calibration	1980-1988	9244.8	9475.1	-2%
		Transfer	1989-1999	9310.8	9254.2	1%
<b>Tributaries in Laos</b>						
Ban Hin Heup	7	Calibration	1988	310.6	210.9	47%
		Transfer	1989-1990	320.5	209.7	53%
<b>Tributaries in Thailand</b>						
Ubon	15	Calibration	1979-1988	645.4	636.1	1%
		Transfer	1989-1991	675.4	621.5	9%

Table 4.5 Performance of VIC model at different discharge measurement stations

Station	Location in Figure 4.5	Period	Simulated Mean Annual Streamflow (m <sup>3</sup> /s)	Observed Mean Annual Streamflow (m <sup>3</sup> /s)	(Simulated - Observed) as a % of Observed
<b>Mainstem Stations</b>					
Chaing Saen	1	1979-1998	2586	2577	0%
Luang Prabang	2	1980-1999	3781	3781	0%
Vientiane	3	1980-1999	4231	4176	1%
Nakhon Phanom	4	1979-1998	6781	6759	0%
Mukdahan	5	1979-1998	7358	7224	2%
Pakse	6	1980-1999	9504	9354	2%
Stung Treng	16	1992-1996	14062	14097	0%
<b>Tributaries in Laos</b>					
Ban Hin Heup	7	1987-1990	291	236	23%
Muong Ngoy	8	1987 & 1990-1991	514	381	35%
Muong Mai	9	1987 & 1989	154	146	5%
Se Bang Fai	10	1980 & 1982-1984	317	286	11%
Ban Keng Done	11	1989 & 1991	757	429	77%
<b>Tributaries in Thailand</b>					
Ban Chot	12	1980-1998	50	50	-1%
Rasi Salai	13	1980-1998	205	163	25%
Yasothon	14	1979-1998	329	224	47%
Ubon	15	1979-1991	635	633	0%

#### 4.4.2 VIC Model Output

The VIC model was run in water balance mode at a daily time step for the period January 1979 through December 2000. Initial soil moistures for each model grid cell were set to 80% of the field capacity as in Nijssen et al. (2001a). The effect of initial conditions on model simulation was assumed to be insignificant and no model spin-up period was considered. The surface runoff and baseflow generated at each grid cell, at each time step, were used as input to the routing model. The routing model transports this surface

runoff and baseflow from the center of each grid cell to the basin outlet through the river channel network as described in section 3.1.1. The simulated daily streamflow was averaged over a month and was compared with the observed monthly streamflow at each of the 16 stations in Figure 4.6. The results of these comparisons are shown in Figures: 4.11 – 4.14.

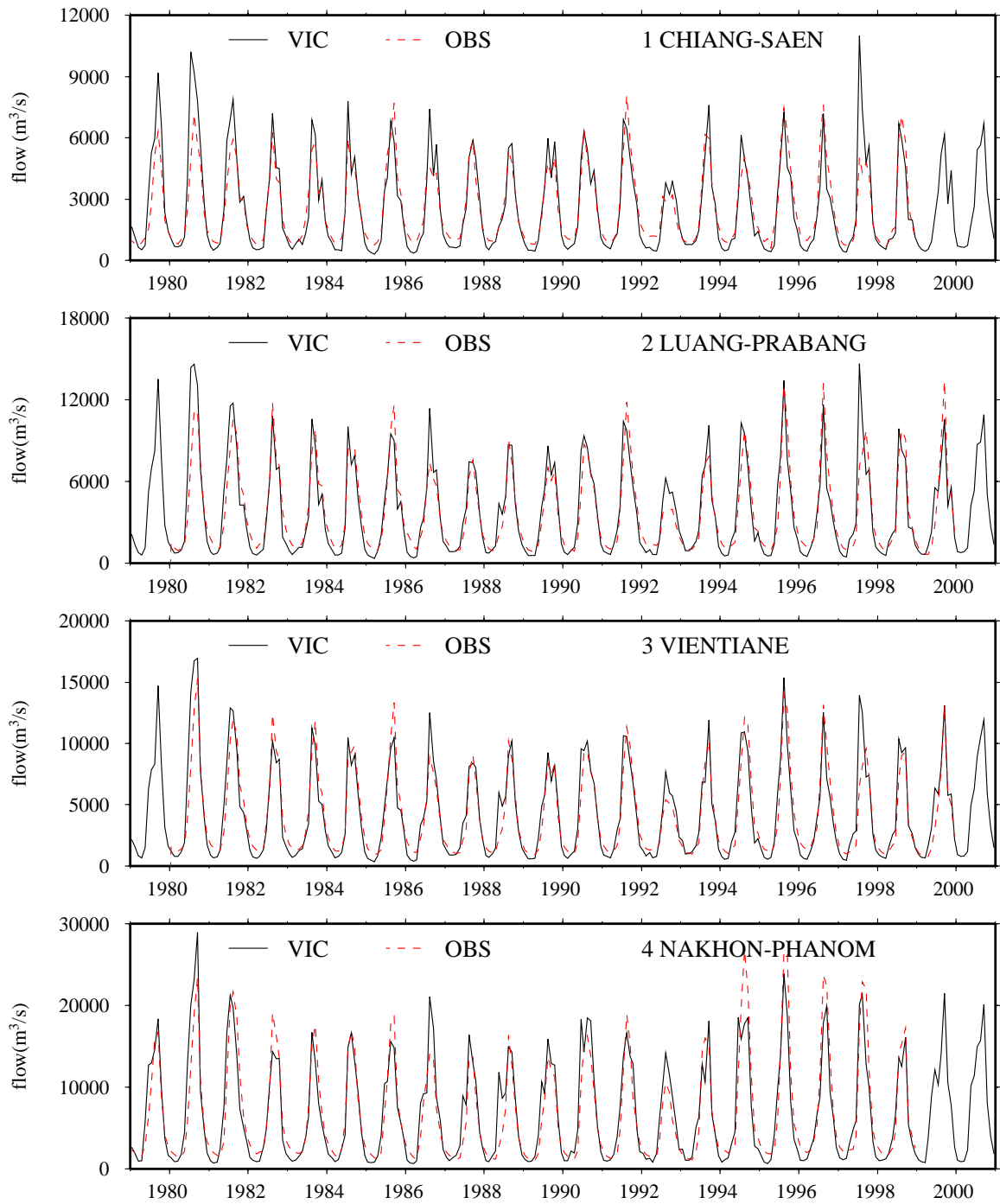


Figure 4.11 Comparison of VIC simulated monthly streamflow [solid line] and observed streamflow [broken line] at stations 1, 2, 3 and 4 of Figure 4.6

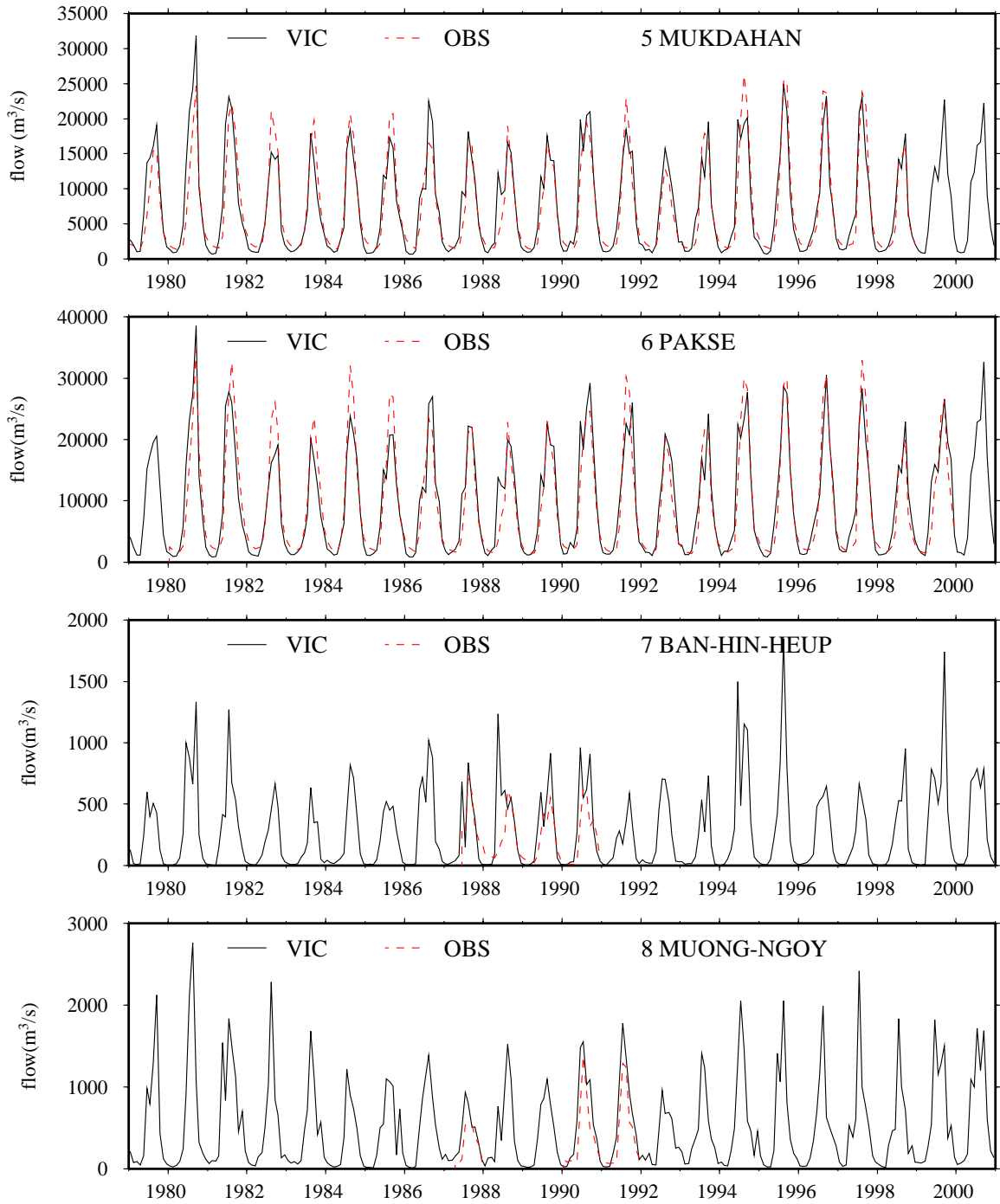


Figure 4.12 Comparison of VIC simulated monthly streamflow [solid line] and observed streamflow [broken line] at stations 5, 6, 7 and 8 of Figure 4.6

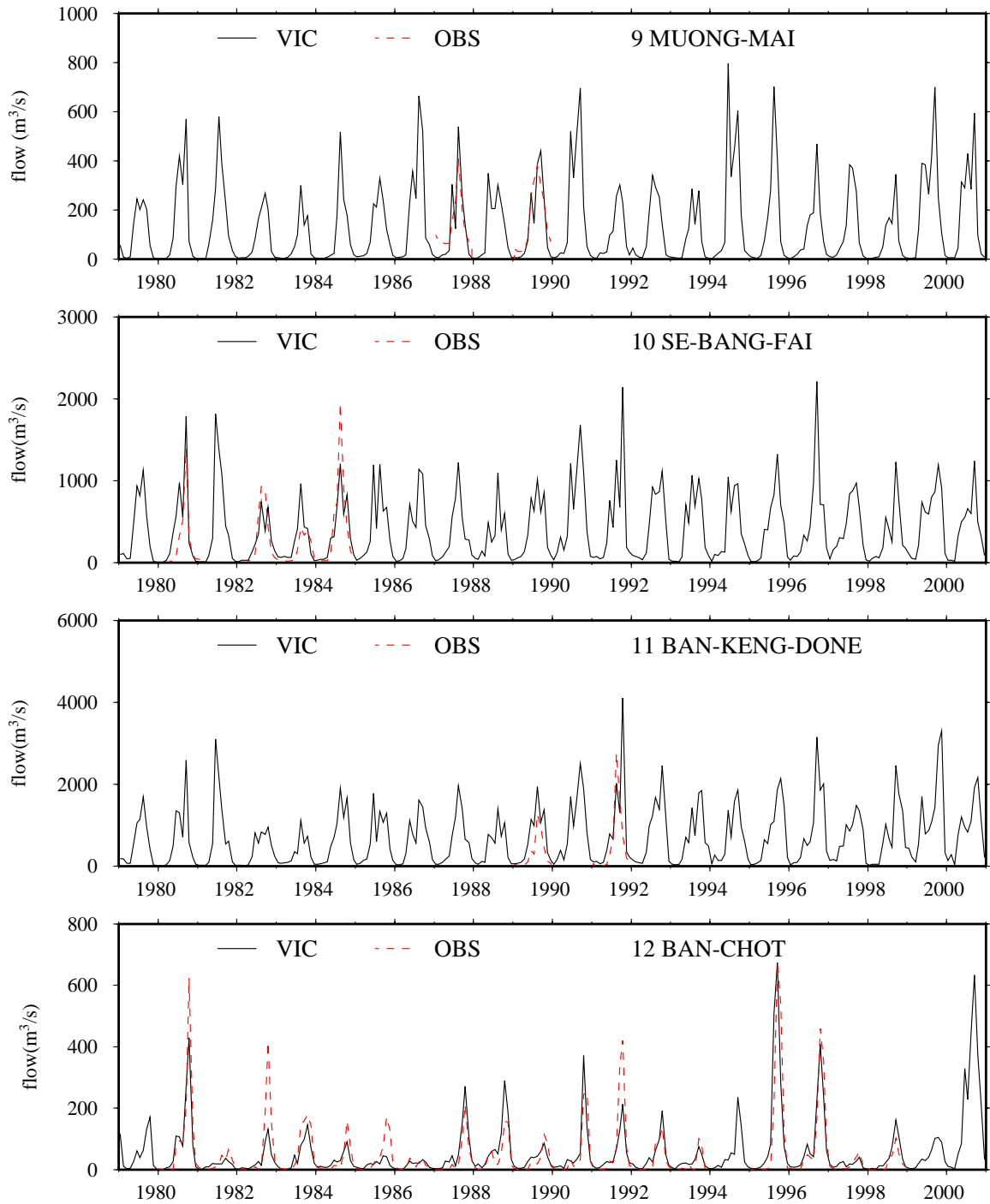


Figure 4.13 Comparison of VIC simulated monthly streamflow [solid line] and observed streamflow [broken line] at stations 9, 10, 11 and 12 of Figure 4.6

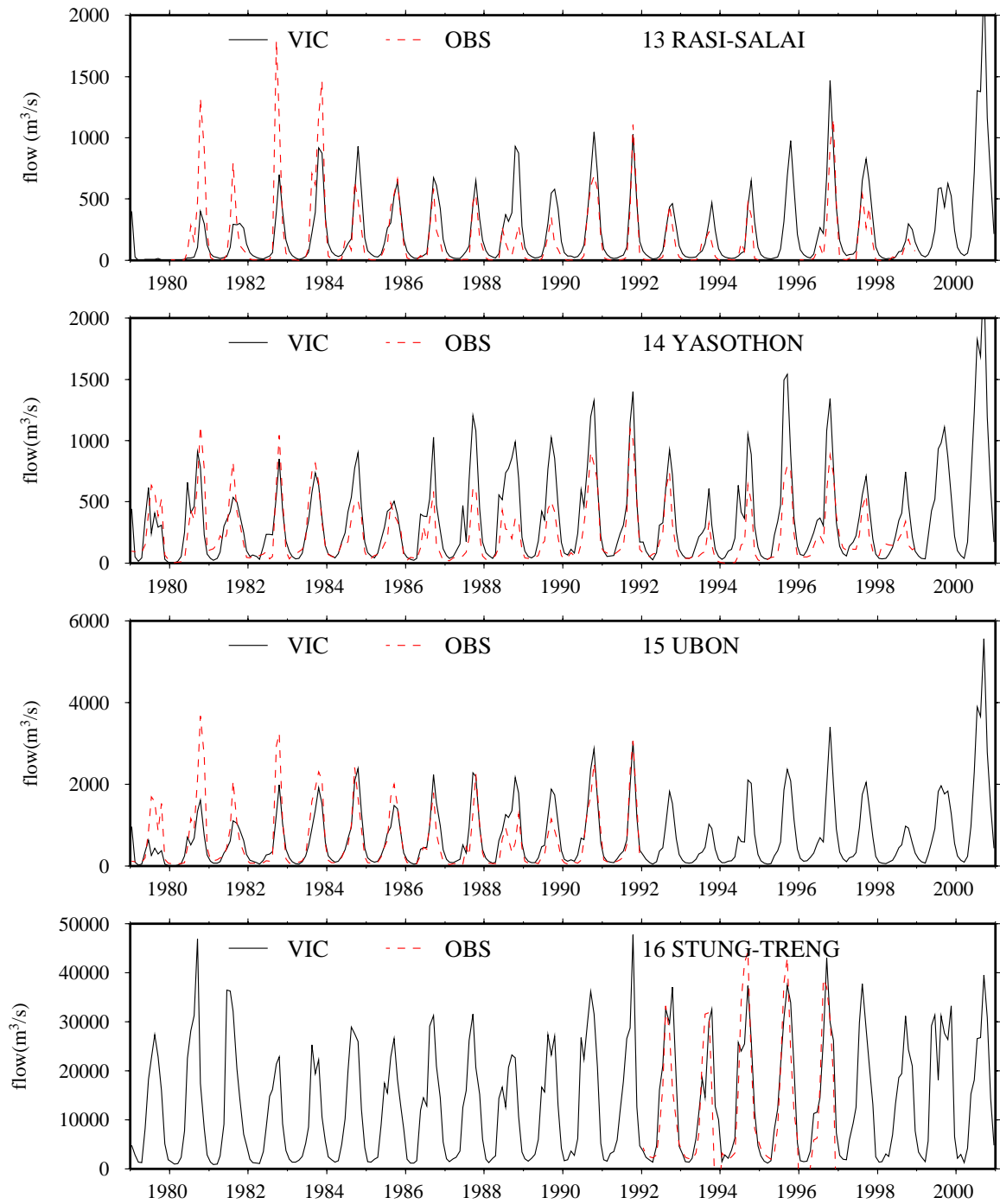


Figure 4.14 Comparison of VIC simulated monthly streamflow [solid line] and observed streamflow [broken line] at stations 13, 14, 15 and 16 of Figure 4.6

#### 4.5 Water Management Model

The Mekong water management model (MWMM, see Chapter 3) considers only those existing and proposed dams that have runoff contribution from a minimum of 10 VIC grid cells (approximately equal to 1% of total basin drainage area). Figure 4.15 shows the dams that are represented in the MWMM. Table 4.6 gives the attributes of these dams such as type and purpose of the dam, maximum head, active reservoir storage, and installed power generation capacity. The sources from which these attributes were obtained are given at the bottom of Table 4.6.

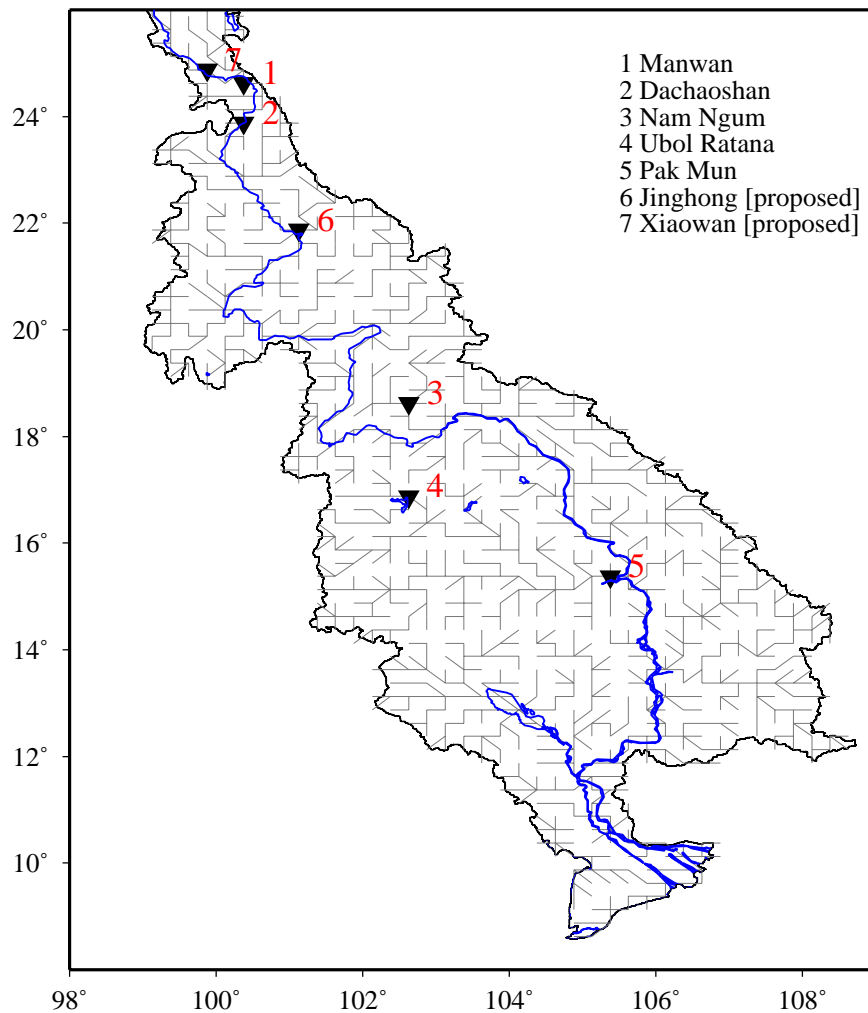


Figure 4.15 Dams considered in the MWMM

The cross-section of the reservoir associated with each dam in the MWMM is assumed to be rectangular, with the dead pool level as the minimum water head and the total storage level as the maximum water head. As described in Section 3.2, the water head used for power generation varies linearly with storage, with the minimum water head as the lower bound and the maximum water head as the upper bound. Because information on the time taken to fill the dead pool storage of each reservoir in the MWMM is not available, this time was assumed to be zero. Thus, all the dams in the MWMM were assumed to have reached a steady state of operation by the end of the first month of their operation. For the dams built prior to 1991, the simulation period in the MWMM is from January of the year of completion through December 2000. For the dams built after 1991 and also for the proposed dams, the simulation period is from January 1991 through December 2000.

The only operational target to be met by a hydropower dam in the MWMM was the observed (or designed) power output. The operational target to be met by a multipurpose (irrigation and hydropower) dam was the observed (or designed) irrigation release and the observed (or designed) power output. The implementation of the MWMM for each dam in Figure 4.15 is described in the following sub-sections. The MWMM output for each dam is presented in the form of plots in the following sub-sections where monthly and annual power generated by each dam is compared with observed (or designed) power output, whenever such data were available. In all of these plots (Figures 4.16-4.22), black lines (solid, broken or dotted) represent VIC model generated flows or attributes of the dams described in Table 4.6, red lines represent MWMM output, blue lines represent the assumed operating rule curves, and green lines represent any observed data. In Table 4.7, the performance of the MWMM is summarized.

Table 4.6 Attributes of the dams used in MWMM

Name of the Dam	Manwan	Dachao shan	Nam Ngum	Ubol Ratana	Pak Mun	Jingho ng	Xiaow an
Location in Figure 4.15	[1]	[2]	[3]	[4]	[5]	[6]	[7]
Purpose - Type	P - R	P - R	P - S	I,P - S	P - R	P - R	P - R
First Year of Operation	1995	2003	1985	1966	1994	2013	2012
Simulation Period	1991- 2000	1991- 2000	1985- 2000	1979- 2000	1991- 2000	1991 - 2000	1991- 2000
Height of the Dam (m)	126	111	75	35	17	-	292
Width of the Dam (m)	421	460	468	880	324	-	920
Reservoir Area at Max. Water Level (km <sup>2</sup> )	24	-	370	410	60	-	-
Reservoir Surface Elevation (m - Mean Sea Level)	994	899	212	182	108/10 6	602	1240
Dead Pool Surface Elevation (m - Mean Sea Level)	-	-	196	174	-	-	-
Total Reservoir Storage (MCM)	920	940	7000	2263	225	1233	15132
Active Reservoir Storage (MCM)	257	367	4700	1762	150	250	990
Design/Observed Annual Inflow (m <sup>3</sup> /s)	1230	1330	315	-	690	-	-
Dammed Water Head (m)	100	80	45.5	16	11.6	67	248
Minimum Water Head for Power Generation (m)	-	-	29.5	8	-	-	-
Installed Capacity (MW)	1250	1350	150	25	136	1500	4200
Designed Firm Capacity (MW)	384.2	363.1	-	-	-	-	-
Designed /Observed Annual Energy Output (GWh)	6200	5931	811	50	290	8059	18890
Efficiency of Power Generation System	0.85	0.85	0.85	0.85	0.85	0.85	0.85

**Legend -**

P - Power, I - Irrigation, S - Storage, R - Run-of-the-River

Assumed Values When Required Data Unavailable

- Data Not Available

**References -**

[1] Xuemin, 1991; ICOLD Online; McCormack, 2001, [2] ICOLD Online; McCormack, 2001,[3] Pluss, 1986; North and Demaine, 2000, [4] Bogardi and Duckstein, 1992  
 [5] Amornsakchai et al., 2000, [6] Chapman and Daming, 2000; McCormack, 2001 [7] Chapman and Daming, 2000; Chuhan et al., 2000; McCormack, 2001

Table 4.7 Summary of MWMM output

Name of the Dam	Manwan	Dachashan	Nam Ngum	Ubol Ratana	Pak Mun	Jinghong	Xiaowan
Location in Figure 4.15	[1]	[2]	[3]	[4]	[5]	[6]	[7]
Simulation Period	1991-2000	1991-2000	1985-2000	1979-2000	1991-2000	1991-2000	1991-2000
Ratio of Max Active Storage and Simulated Mean Annual Inflow into Dam	1.0%	1.2%	52.8%	100.3%	0.5%	0.4%	4.9%
Simulated Mean Annual Inflow into Dam as % of Simulated Mean Annual flow at most downstream discharge measurement station (Stung Treng)	6.0%	6.7%	2.0%	0.5%	5.7%	12.7%	4.5%
Observed or Designed Mean Annual Inflow into Dam (m <sup>3</sup> /s)	1230	1330	315	-	690	-	-
Simulated Mean Annual Inflow into Dam (m <sup>3</sup> /s)	869.7	973.6	286.3	66.4	818.8	1838.2	648.8
Ratio of Simulated and Observed (or designed) Inflow into Dam	70.7%	73.2%	90.9%	-	118.7%	-	-
Observed or Designed Annual Power Output (GWh)	6200	5931	811	50	290	8059	18890
Simulated Mean Annual Power Output (GWh)	5683	5351.4	908.37	56.509	473.77	7190.7	11600
Ratio of Simulated and Observed (or designed) Power Output	91.7%	90.2%	112.0%	113.0%	163.4%	89.2%	61.4%

#### 4.5.1 Manwan Dam

The Manwan dam is located in the upper reaches of the Mekong in the Yunnan province of China. This dam, which is operated as a run-of-the-river dam, is the first major dam to be built on the main-stem of the Mekong. Power generation began in 1995 when the first phase of construction of this dam was completed (ICOLD Online, 2000). Though the simulated annual inflow into the dam is consistently less than the designed mean annual inflow, the annual power produced by the MWMM (Figure 4.16) is 91.7% (see Table

4.7) of the designed mean annual power output. The lack of observed streamflow data in the Yunnan region restricts further analysis of the MWMM output.

#### 4.5.2 Dachaoshan Dam

The Dachaoshan dam, which is downstream of the existing Manwan Dam, is expected to be complete by 2003 (McCormack, 2001). The MWMM model output for this dam, which will be operated as a run-of-the-river dam, is shown in Figure 4.17. The trend in annual and monthly power generated by the MWMM for the Dachaoshan dam is similar to the trend in the power generated by the MWMM for the Manwan dam.

#### 4.5.3 Nam Ngum Dam

The construction of the third phase of the Nam Ngum hydropower dam, which is on the Nam Ngum River in Laos, was completed in 1985 (Pluss, 1986). The power generated by the MWMM depends on the seasonal power demand and minimum storage requirement criteria. The Nam Ngum dam is a good source of foreign exchange for Laos since most of the power generated is supplied to Thailand (Pluss, 1986). Thus to maximize revenue generation, the seasonal power demand was assumed to be a constant value of 150MW, which is the installed power generation capacity of this dam. Storage release for power generation was based on a specified rating curve, which ensures partial storage of wet season flow and release of this storage during the dry season. Thus the reservoir is filled during the wet season and drawn down during the dry season, always maintaining a specified minimum operating level.

The simulated annual inflow into the dam is 90% of the designed annual inflow into the Nam Ngum dam (Figure 4.18), and the annual power generated by the MWMM is 110% of the observed annual power output (from North and Demaine, 2000) and 112% of the

design mean annual output (Table 4.7). Lack of information on observed inflow into the dam and insufficient information on observed power output restrict further analysis of the MWMM output.

#### 4.5.4 Ubol Ratana or Nam Pong Dam

The Ubol Ratana or Nam Pong multipurpose dam, which was built in 1965 on the Pong River in Northeast Thailand, is used for irrigation and power generation. In this region where dry season irrigation is extensive (see Section 2.3.3), irrigation releases are given priority over power generation releases (Bogardi and Duckstein, 1992). Water released for irrigation depends on a specified irrigation demand curve and also depends on a specified power release curve. Data on seasonal irrigation demand were not available and hence a constant irrigation demand of 150 MCM was assumed for the dry season (November through April) and no irrigation demand was assumed for the wet season (June through October). The constant value of 150 MCM was chosen to match the mean annual irrigation release of the model of Bogardi and Duckstein (1992). Water is released for power production only during the wet season and only if the reservoir storage is above a specified minimum storage level. This minimum storage level is set to 95% of the maximum active storage.

The annual irrigation releases simulated by MWMM and the annual power output are shown in Figure 4.19. The irrigation release from the MWMM is about 200% of the mean annual irrigation release of Bogardi and Duckstein (1992), and the annual power output is 113% of the observed mean annual power output for the period of 1966-1988.

#### 4.5.5 Pak Mun Dam

The Pak Mun Dam on the Mun River, located about 5 km upstream from the confluence of Mun River with the Mekong, is operated as a run-of-the-river dam. The maximum head during the rainy season (June through December) is 11.6 m and during the dry season (January through May) it is 9.6 m (Amornsakchai et al, 2000a). The head available for power production is also dependent on the backwater effects of the Mekong and also on the need to preserve rapids upstream of the Pak Mun dam which are good sources of fisheries (Amornsakchai et al., 2000b). The MWMM does not account for these factors and hence produces 60% more power than the observed annual power output (Figure 4.20).

#### 4.5.6 Proposed Dams

The Jinghong dam and Xiaowan Dam are part of the Lancang Cascade project, which aims to create a cascade of eight dams in the middle and lower portions of the Upper Mekong basin. The Jinghong dam, expected to be complete by 2012 (McCormack, 2001), will be operated as a run-of-the-river dam. The MWMM simulates 89.2% of the designed mean annual power output (Figure 4.21).

The proposed Xiaowan dam, which is upstream of the existing Manwan dam, is a hydropower dam with a total storage capacity of 15132 MCM (McCormack, 2001). Since the maximum active storage of Xiaowan's reservoir is typically less than the monthly inflow into the dam (see Figure 4.22), this dam was treated as a run-of-the-river dam in the MWMM. The MWMM produces only 61.4% of the designed annual power output. Lack of additional information on inflow into the dam and the operational policies of the dam, restricts further analysis of the MWMM output for this dam.

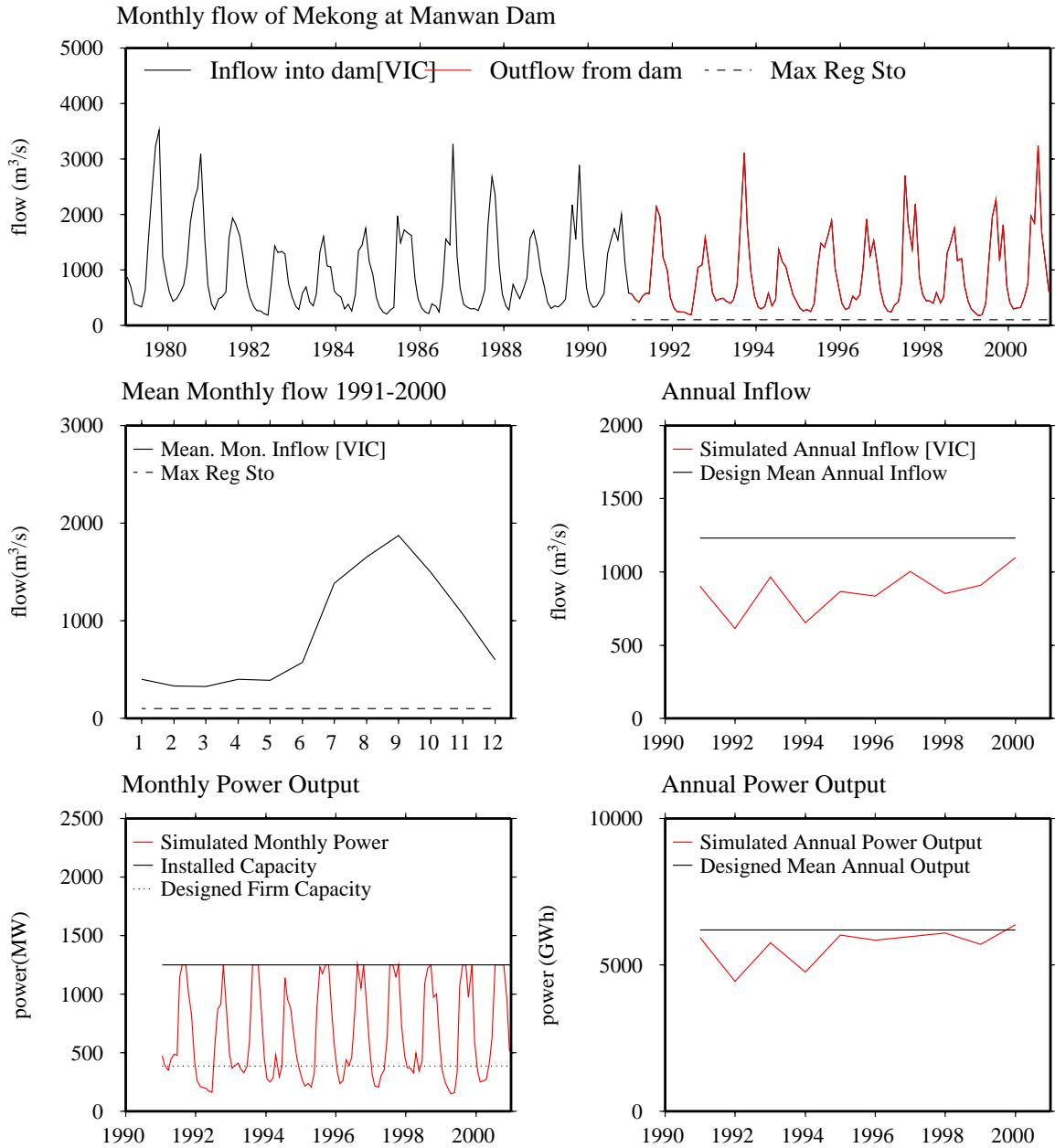


Figure 4.16 MWMM output for Manwan Dam [Dam 1 in Figure 4.15]

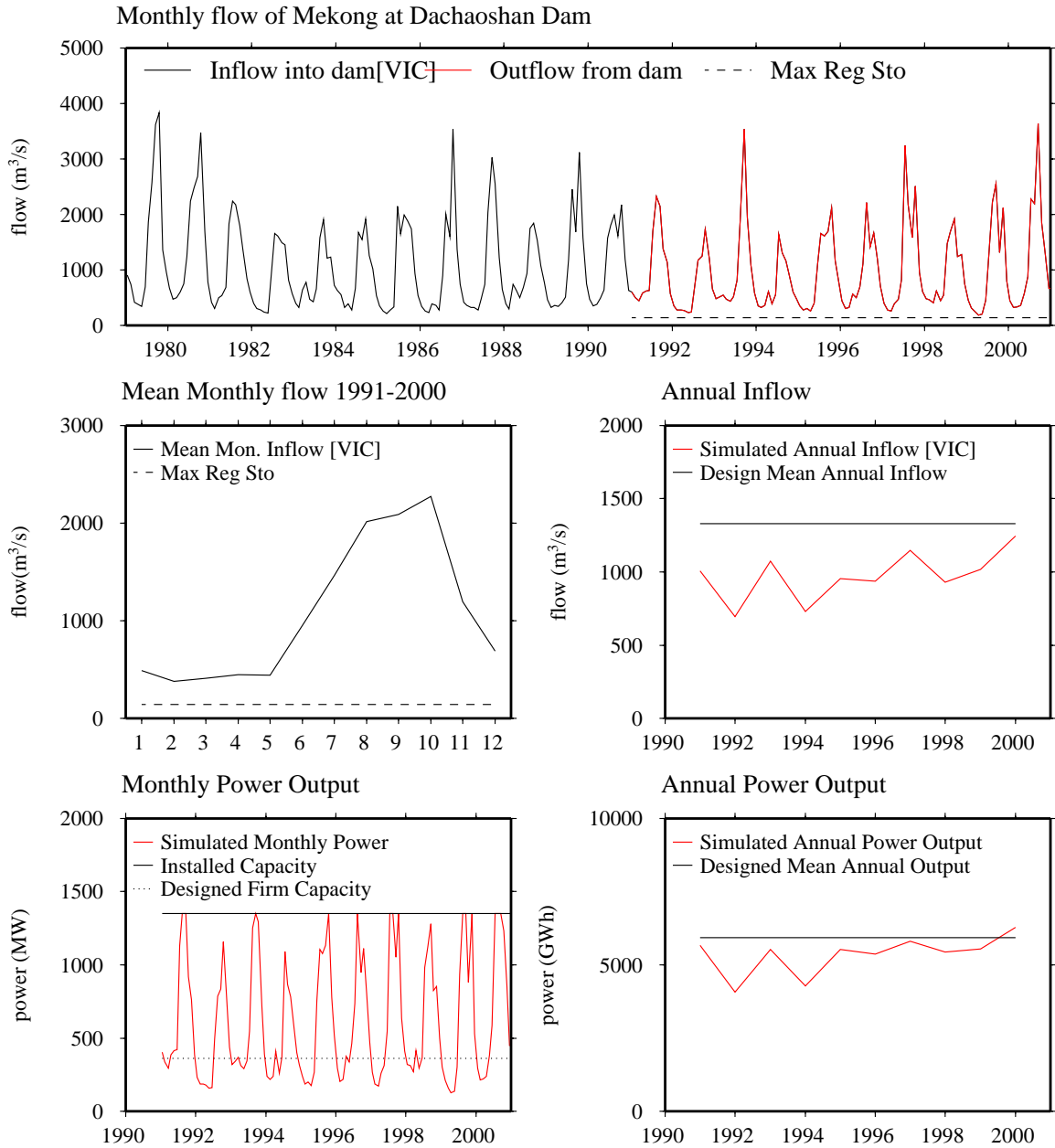


Figure 4.17 MWMM output for Dachaoshan Dam [Dam 2 in Figure 4.15]

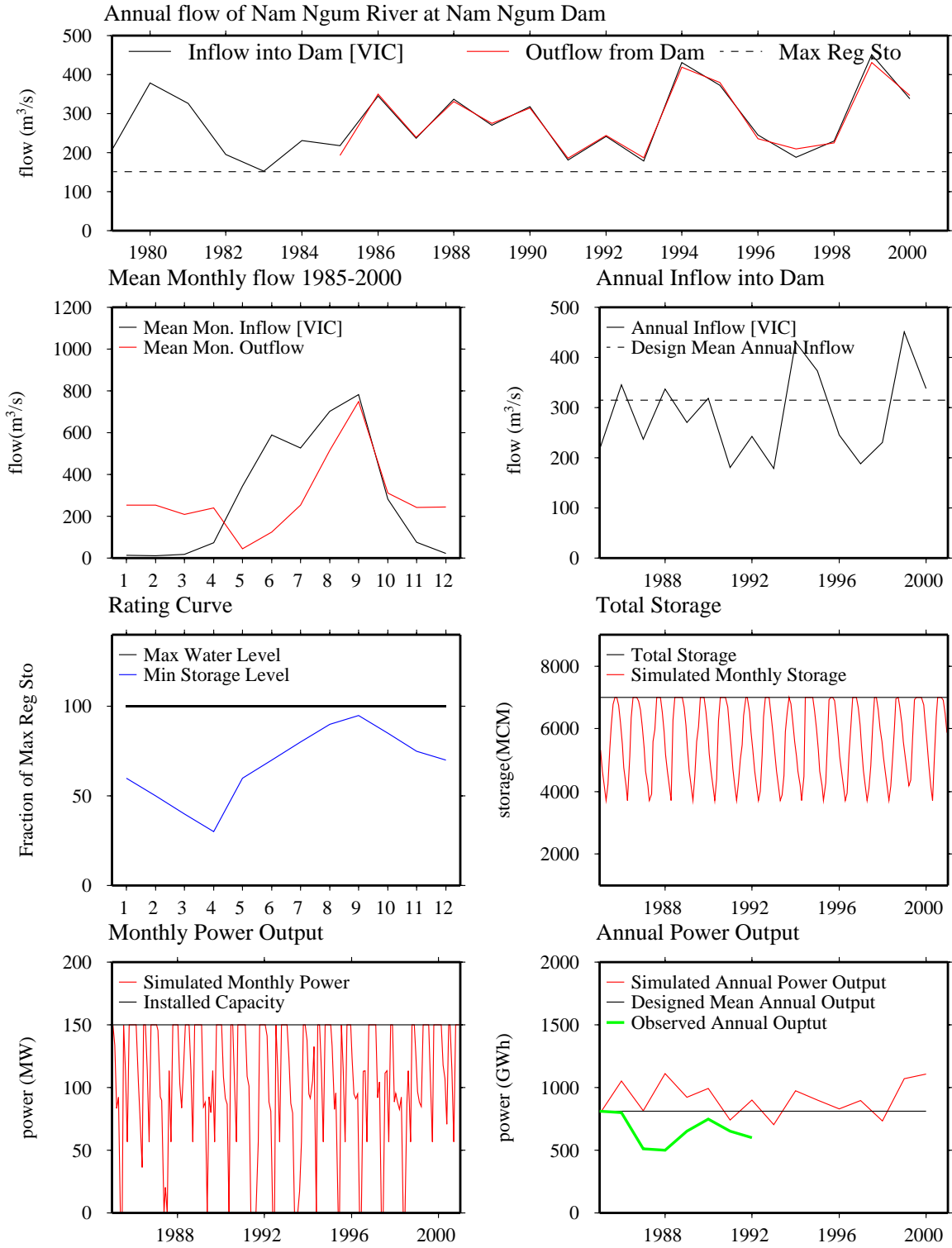


Figure 4.18 MWMM output for Nam Ngum Dam [Dam 3 in Figure 4.15]

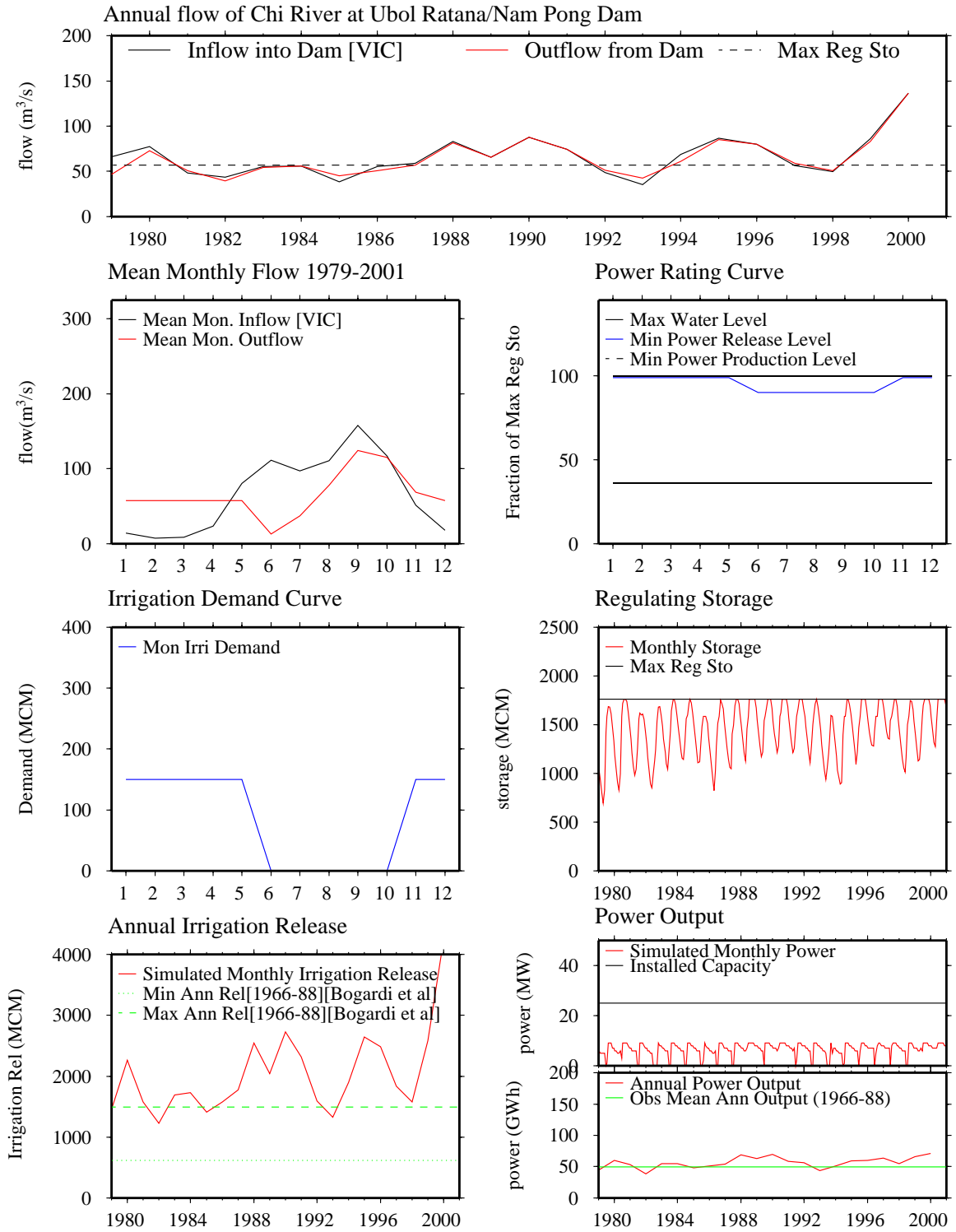


Figure 4.19 MWMM output for Ubol Ratana Dam [Dam 4 in Figure 4.15]

Monthly flow of Mekong at Pakmun Dam

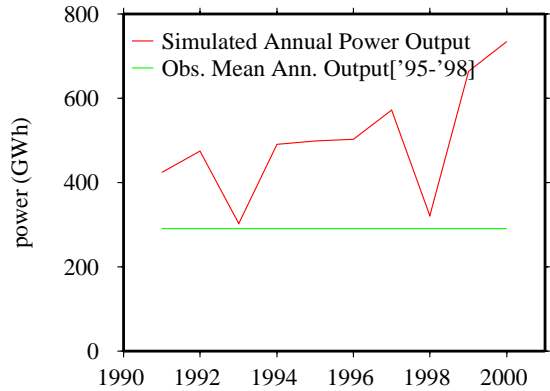
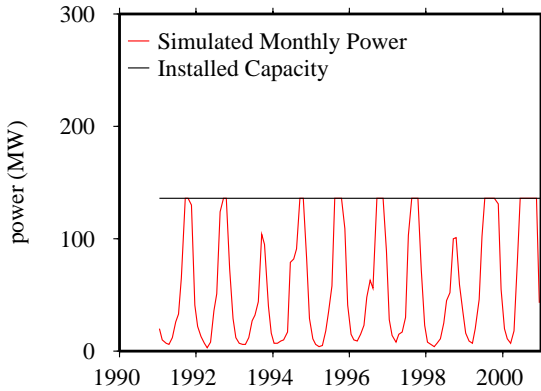
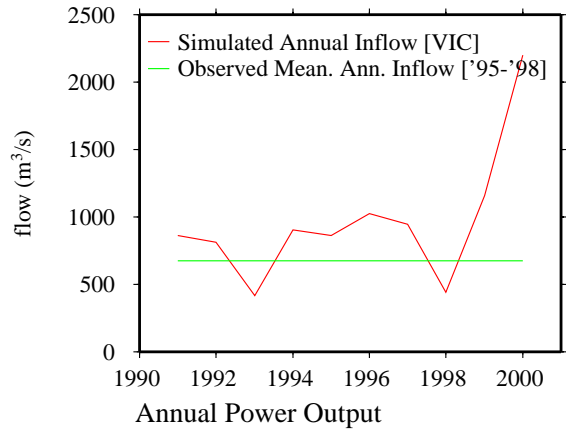
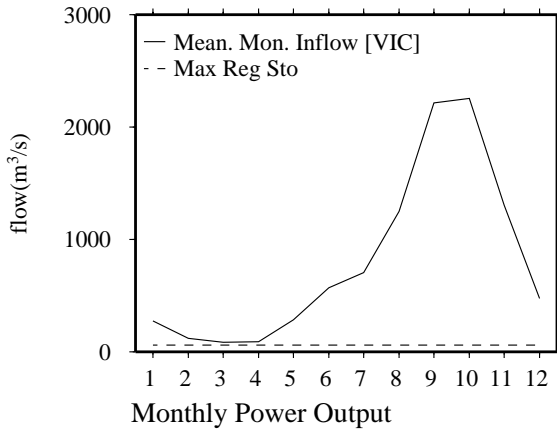
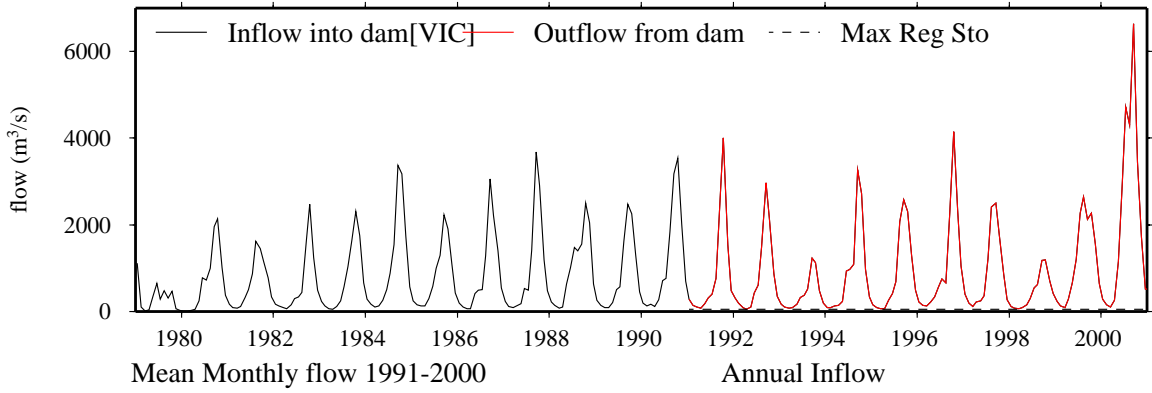


Figure 4.20 MWMM output for Pak Mun Dam [Dam 5 in Figure 4.15]

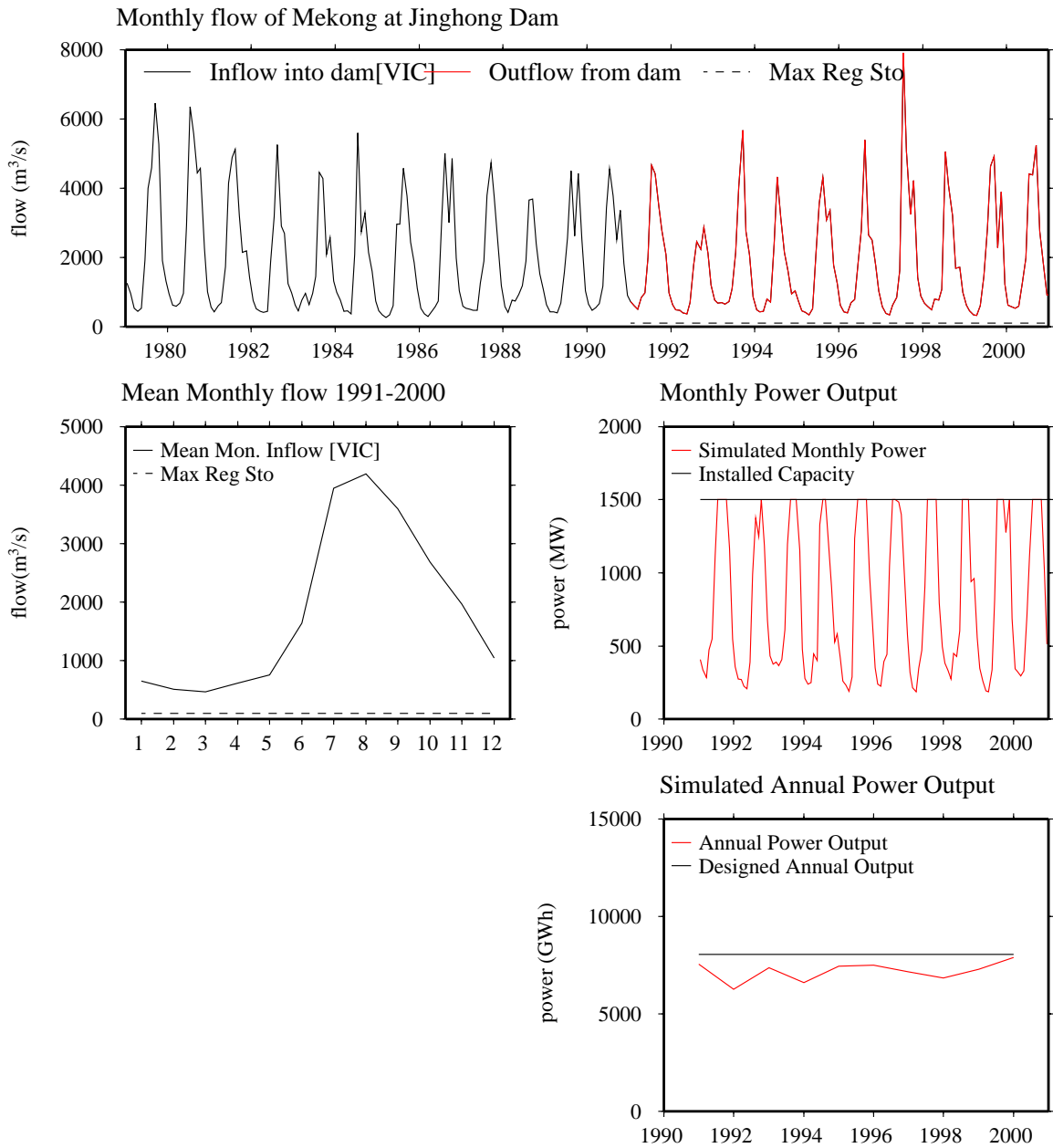


Figure 4.21 MWMM output for proposed Jinghong Dam [Dam 6 in Figure 4.15]

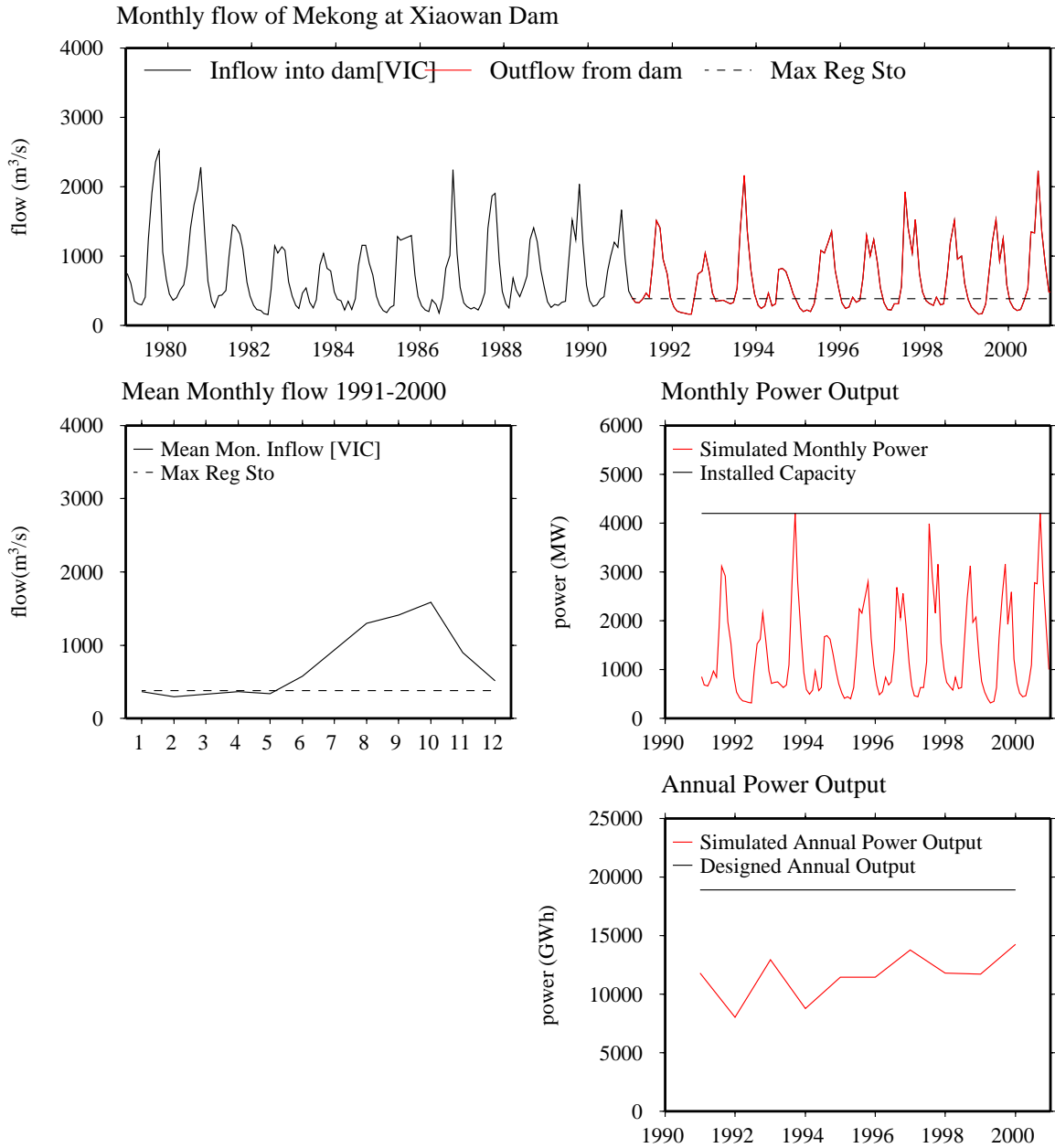


Figure 4.22 MWMM output for proposed Xiaowan Dam [Dam 7 in Figure 4.15]

#### ***4.6 Effects of flow regulation on streamflow***

All the dams on the main-stem of the Mekong in the MWMM are operated as run-of-the-river dams, and hence the effects of these dams on the monthly streamflow of main-stem Mekong are insignificant. The other three dams considered in the MWMM, namely Ubol Ratana dam on Chi River, Pak Mun dam on Mun River, and Nam Ngum dam on Nam Ngum River, are on tributaries of the main-stem Mekong. The Pak Mun dam is a run-of-the-river dam and hence does not affect the monthly discharge regimes of the Mun River. The Ubol Ratana and Nam Ngum dams have large storage reservoirs, but are located on tributaries whose mean annual contribution to the main-stem Mekong at Stung Treng is less than 2.5% (see Table 4.7) and whose mean monthly contribution to the main-stem Mekong at Stung Treng is less than 3.5%. Thus, all of the dams considered in the MWMM only affect the monthly streamflow of some of the tributaries and their effect on the monthly streamflow main-stem Mekong is quite small.

## Chapter 5: Vegetation Scenarios

### 5.0 Overview

A brief summary of the history of development in the Mekong River basin was provided in Chapter 2. In this chapter, the VIC hydrologic model and the Mekong water management model (MWMM), described in Chapters 3 and 4, are used to investigate the impacts that long-term changes in vegetation and flow regulation might have had on the basin hydrology.

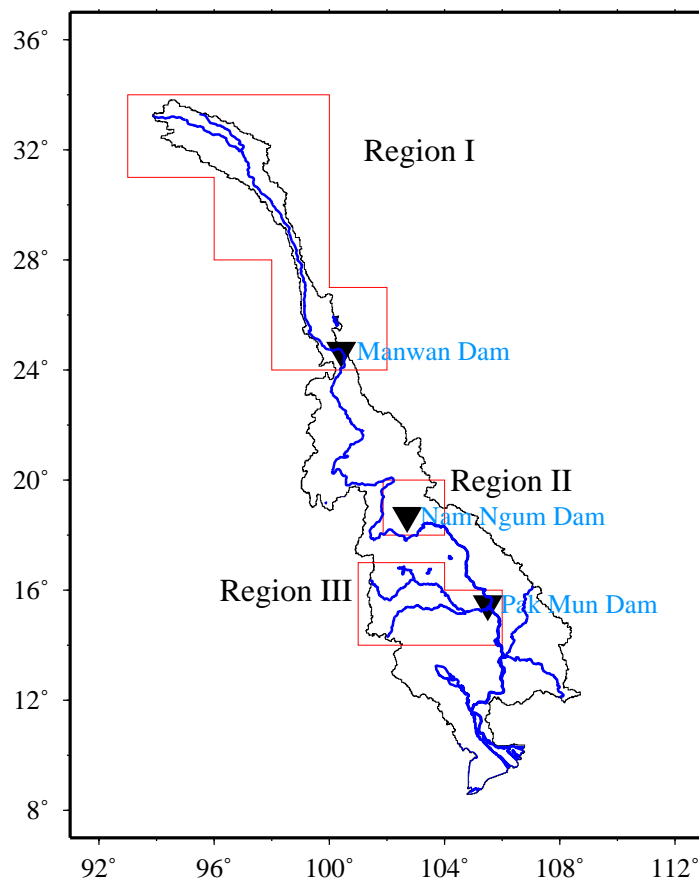


Figure 5.1 Three regions selected for the investigation of impacts due to land cover change

For purposes of this investigation, three regions within the Mekong basin (Figure 5.1) were evaluated using three land cover scenarios. Each of the three regions of Figure 5.1 form contributing drainage areas to one or more of the major dams represented in the MWMM (see Section 4.5). The three land cover scenarios are: the current land cover scenario, a historical land cover (HLC) scenario and a future land cover (FLC) scenario. The current land cover for the Mekong basin was described in Section 4.1.3. The HLC is intended to represent the land cover in its pristine form, prior to human development. Lack of information about the historical vegetation necessitated that assumptions be made to construct the HLC. FLC represents the land cover after conversion of all the existing forests and other vegetation to cropland. Thus the HLC and FLC are intended to represent end-point scenarios to allow investigation of streamflow sensitivity to maximum changes in vegetation cover. In Section 5.1 and Section 5.2 the construction of HLC and FLC are described.

Following development of the land cover scenarios, VIC model runs were made using all the land cover scenarios. The results of these simulations on streamflow are analyzed in Section 5.3. Subsequently the effects of land-use change on hydropower generation and irrigation are investigated using the MWMM, results of which are discussed in Section 5.4.

### ***5.1 Historical Land Cover***

The construction of HLC ideally would be based on recorded information about land cover. However, no such data were available, so assumptions were made to construct this scenario. Using the current land cover map (see Figure 4.2), each region in Figure 5.1 was identified with one historical vegetation class (see sub-sections 5.1.1-5.1.3). This historical vegetation class could be any predominant current vegetation class, other than cropland, that currently exists in the region. Only the cropland vegetation class was

assumed to be the result of anthropogenic changes in all the three regions. The other vegetation classes were assumed to be devoid of any human influence.

To obtain the HLC for a region, the fractional coverage of the historical vegetation class identified for that grid cell, was incremented by the fractional coverage of cropland in the grid cell – i.e., the cropland was replaced with the identified historical vegetation class. When the historical vegetation class identified for the region was not present in a model grid cell, the fractional coverage of cropland was completely replaced with an equal fractional coverage of the historical vegetation class. For such model cells, the rooting depths were changed accordingly, and monthly LAI values were assigned based on the monthly LAI plot for the current vegetation cover (Figure 4.3). The predominant historical and current vegetation classes, for each region in Figure 5.1, are described in the following sub-sections. The constructed HLC is shown in Figure 5.2.

#### 5.1.1 Region I

Region I consists of the drainage to the Manwan Dam in the Yunnan Province of China (Figure 5.1). Large-scale human development is not prevalent in this region due to the hilly terrain and narrow gorges. This region receives monsoon rainfall and the seasonal variation in rainfall is not as much as the seasonal variation in rainfall in other parts of the basin. Grasslands predominate in the upper portion of this region and evergreen needle-leaf forests and woodlands cover the lower portion (Figure 4.2). Land-use changes were assumed to have taken place only in the lower elevation areas of Region I. The HLC for this region was assumed to be woodland.

#### 5.1.2 Region II

Region II consists of the drainage to the Nam Ngum Dam in Northern Laos (Figure 5.1), which has hilly terrain and annual precipitation of more than 1000 mm (Section 2.1.2). Though shifting cultivation is practiced in Northern Laos, cropland is not a significant fraction of the current vegetation cover (Figure 4.2). Deciduous broad-leaf forests and woodland dominate the current vegetation cover of this region. The HLC for this region was assumed to be deciduous broad-leaf forest.

### 5.1.3 Region III

Region III consists of the drainage to the Pak Mun Dam in Northeastern Thailand (Figure 5.1). Though sandy and saline soils of this region make the land unsuitable for water-intensive crops, dry season irrigation is extensive (Section 2.3.3). Cropland and grasslands dominate the current vegetation cover of this region, where annual precipitation is 1000-1250 mm. Wooded grassland was the assumed HLC for this region.

## ***5.2 Future Land Cover***

The Future land cover (FLC) scenario corresponds to conversion of all the existing forests and other vegetation to cropland. The method of construction of FLC is the same for all of the three regions - all vegetation is reset to cropland, with a fractional coverage of 0.99. The rest of the region in each grid cell was assumed to be consisting of human settlements. Fixed monthly LAI of 0.2 for January, 0.1 for February and March, 0.3 for April, 0.4 for May, June, July and August, 0.6 for September, 0.8 for October and November, and 0.2 for December were assigned to each model grid cell.

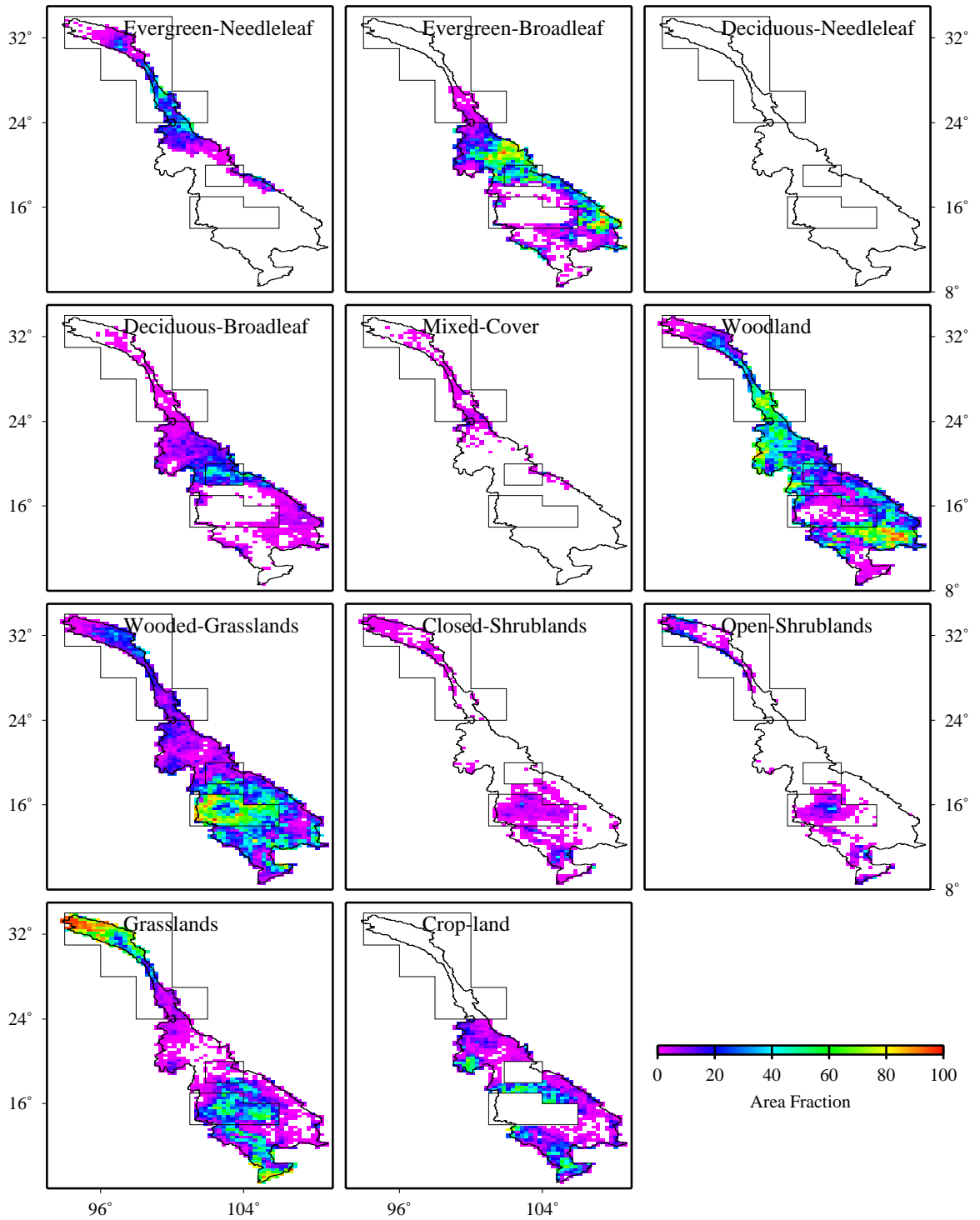


Figure 5.2 Constructed historical land cover

### 5.3 Effects of Land-use Change on Streamflow

The effects of land-use change in the three regions were studied using the HLC and FLC vegetation scenarios. The VIC model was run in water balance mode (see section 4.4), at a daily time step – for the period January 1979 through December 2000, using the HLC and the FLC, in place of current land cover data. The streamflow thus simulated at the outlet of each of the three regions was compared with the streamflow generated at these points using the current land cover data. The changes in streamflow, due to the prescribed changes in land cover, are attributed mainly to changes in monthly LAI, since the distribution of roots in different soil layers (Table 4.2) is approximately the same. The HLC for all three regions typically had higher monthly LAI, resulting in a net increase in evapotranspiration, thus producing less streamflow (see Tables 5.1 and 5.2). The FLC for all the three regions had lower monthly LAI, resulting in a net decrease in evapotranspiration, thus producing more streamflow.

Table 5.1 Mean monthly streamflow ( $\text{m}^3/\text{s}$ ) using the current land cover and percentage change in streamflow relative to current land cover conditions

	1	2	3	4	5	6	7	8	9	10	11	12
<b>Region I</b>												
Current	425	342	361	416	402	713	1312	1711	1879	1815	1072	607
HLC	-1.1%	-2.0%	-4.2%	-3.9%	-2.3%	-1.6%	-0.5%	-0.3%	-0.4%	-0.5%	-0.6%	-0.8%
FLC	8.3%	16.1%	37.8%	40.4%	26.4%	18.6%	16.4%	18.7%	15.8%	8.0%	3.7%	5.1%
<b>Region II</b>												
Current	19	11	16	67	301	536	541	681	751	293	76	22
HLC	2.4%	1.9%	1.2%	0.6%	-0.5%	-1.1%	-1.1%	-0.7%	-0.5%	-0.1%	1.3%	4.0%
FLC	12.3%	22.2%	35.9%	28.1%	26.3%	29.7%	31.1%	24.3%	17.6%	17.8%	23.4%	6.3%
<b>Region III</b>												
Current	254	124	91	118	316	665	956	1434	2447	2372	1271	476
HLC	-14.7%	-19.7%	-30.0%	-43.4%	-50.6%	-40.2%	-34.6%	-36.6%	-35.5%	-35.5%	-31.9%	-23.0%
FLC	20.9%	27.0%	27.2%	4.1%	-19.9%	4.6%	33.6%	46.0%	46.7%	44.8%	32.6%	19.6%

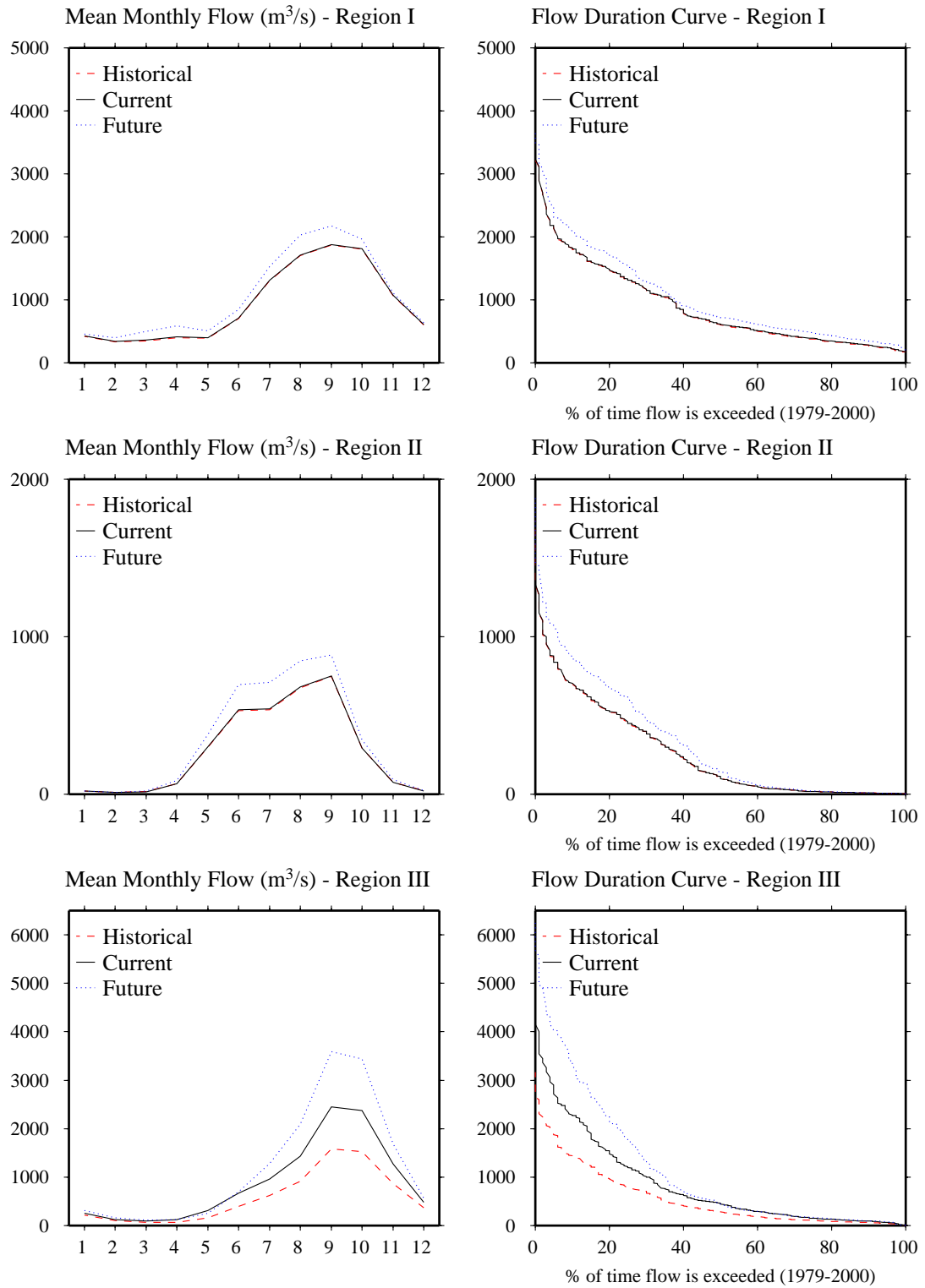


Figure 5.3 Mean monthly streamflow generated using HLC and FLC for all the three regions

Table 5.2 Mean annual streamflow ( $\text{m}^3/\text{s}$ ) using the current land cover and percentage change in streamflow relative to current land cover conditions

	Region I	Region II	Region III
Current	921	276	877
HLC	-0.9%	-0.6%	-34.7%
FLC	15.2%	24.3%	35.9%

The HLC for Region I and Region II does not differ significantly from the current land cover, and hence the monthly streamflow generated using the HLC (see Figure 5.3) is within 4% of the monthly streamflow generated using the current land cover (Table 5.1). The FLC for Regions I and II, represents a significant change in land cover, thus resulting in a 15% change in annual streamflow for Region I and 34% change in annual streamflow for Region II.

From Figure 4.2 it is evident that Region III has the greatest amount of cropland in the Mekong basin. The greatest changes in simulated monthly and annual streamflow occur in this region, as expected (Figure 5.3). The use of HLC results in a maximum decrease of 33% in monthly streamflow and 30% decrease in annual streamflow (Tables 5.1 and 5.2). Unlike Region I and Region II, the increase in annual streamflow in Region III, using FLC, is comparable to the decrease in annual streamflow due to the HLC.

### 5.3.1 100-year flood

A Gumbel probability distribution was fit to the annual maximum daily streamflow generated using the current land cover, HLC and FLC. The change in magnitude of the 100-year flood in the case of HLC and FLC is shown in Table 5.3. This change in the magnitude of the 100-year flood, in all the three regions, is less than the change in magnitude of the mean annual streamflow (see Table 5.2)

Table 5.3 Magnitude of the 100-year flood ( $m^3/s$ ) and percentage change relative to current land cover conditions

	Manwan (I)	Nam Ngum (II)	Pak Mun (III)
Current	8001	5071	9679
HLC	-0.3%	-0.2%	-33.2%
FLC	4.3%	8.5%	35.4%

#### ***5.4 Effects of Land-use Change on Hydropower Production and Irrigation***

The monthly streamflow generated using the HLC and FLC, at the outlet of the three regions in Figure 5.1, was used as input to the MWMM. The MWMM was run for the dams in the three regions, under the current operating procedures. The change in annual power output, due to the prescribed changes in land cover, for each of the three dams is summarized in Table 5.4. The change in annual power output is due to the changes in streamflow resulting from the use of HLC and FLC.

Table 5.4 Mean annual power output (GWh) and percentage change relative to current land cover conditions

	Manwan (I)	Nam Ngum (II)	Pak Mun (III)
Current	5683	908	499
HLC	-0.9%	-0.1%	-20.6%
FLC	10.1%	8.9%	9.9%

The mean annual water consumed by all forms of irrigation in Southeast Asia for the period 1980-1995 was approximately  $250 \text{ km}^3/\text{yr}$  (Shiklomanov, 2000), equivalent to  $11100 \text{ m}^3/\text{s}$ . The total irrigated area in Thailand accounts for 30% of the total irrigated area in Southeast Asia (FAOSTAT, 2001) and the total irrigated area in Northeastern Thailand (most of which is Region III) is 7% of the total irrigated area in Thailand (Mongkolsawat et al., 2000). Assuming that irrigation water use in Southeast Asia is roughly constant per unit irrigated area (regardless of the type of irrigation), the irrigation

consumption of Region III is 2.1% of the total irrigation consumption of Southeast Asia, which is equivalent to  $230 \text{ m}^3/\text{s}$ , which compares with an increase in mean annual streamflow of  $306 \text{ m}^3/\text{s}$  for current relative to historic land cover conditions

Irrigated area accounts for 3% of the total area of Northeastern Thailand and 6% of the agricultural area. In the future scenario (FLC), all the existing vegetation is replaced with cropland, i.e., the agricultural area in this scenario is 100% of the total area. Assuming that the proportion of irrigated land to the total agricultural land remains the same in the FLC scenario (6% of the total area), the irrigation consumption in this scenario would be  $460 \text{ m}^3/\text{s}$ , i.e. an additional consumption of  $230 \text{ m}^3/\text{s}$ . The increase in mean annual streamflow for Region III in the FLC scenario of  $306 \text{ m}^3/\text{s}$  (see Table 5.2) is of the same order of magnitude as the increase in irrigation consumption. Therefore, an increase in streamflow due to a change in land cover (from HLC to current land cover and current land cover to FLC) is offset by an increase in demand for irrigation water.

## Chapter 6: Results and Conclusions

The VIC model was implemented at a  $\frac{1}{4}$  degree resolution for the Mekong River basin, in water balance mode, at a daily time step, for the period January 1979 through December 2000. In parts of the Lower Mekong basin, where precipitation was inadequately represented due to scarce meteorological station density and hilly terrain, the precipitation data were scaled to obtain a reasonable agreement between simulated and observed runoff as described in Section 4.4.1. The VIC model was then calibrated so that simulated streamflow matched observed streamflow to a reasonable extent.

A water management model (MWMM), which simulates the effects of flow regulation by existing and planned major dams and reservoirs in the basin, was developed. The MWMM operates on a monthly time scale and is driven by streamflow data simulated by the VIC model. The VIC model and the MWMM were then used to evaluate changes in streamflow due to prescribed changes in land cover. An historical land cover scenario (HLC) and a future land cover scenario (FLC) were developed to analyze changes in monthly streamflow in three different regions of the basin. The HLC and FLC are intended to represent end-point scenarios to allow investigation of streamflow sensitivity to maximum changes in vegetation cover. The impacts of land cover change on regional hydropower and regional flooding was discussed.

The results of this study are as follows:

1. The VIC simulated mean annual streamflow is within 2% of the observed annual streamflow for most of the discharge measurement stations with streamflow record length exceeding five continuous years.
2. The MWMM simulates a minimum of 90% of the average annual observed (or designed) power output for 6 of the 7 dams considered in the MWMM. This

underestimation is attributed to lack of sufficient information about the operational policies of dams, lack of sufficient information on actual power generated by dams, and the errors associated with the streamflow data used to drive the MWMM. The overall effects of the existing dams and proposed large dams considered in the MWMM, on the monthly streamflow of main-stem Mekong, were found to be less than 3.5% on average.

3. The maximum predicted streamflow change for current relative to historic land cover conditions was an increase of 53 percent in mean annual streamflow for the Chi-Mun River, a tributary to the Lower Mekong Basin in which major conversions of forest to cropland (affecting an estimated 15% of the basin) have occurred over the last 50 years. For other regions, the changes were much smaller, ranging from 0.5% to 1%. For the Mekong near its mouth the predicted change in mean annual discharge was 2%. The increased streamflow for current land cover relative to historic land cover conditions is offset by an equal order of magnitude increase in demand for irrigation water.

## **LIST OF REFERENCES**

Abdulla, F. A., D. P. Lettenmaier, E. F. Wood, and J. A. Smith, 1996, Application of a Macroscale Hydrologic Model to Estimate the Water Balance of the Arkansas-Red River Basin, *J. Geophys. Res.*, 101(D3), pp. 744-749.

Amornsakchai, S., Annez, P., Vongvisessomjai, S., Choowaew, S., Thailand Development Research Institute (TDRI), Kunurat, P., Nippanon, J., Schouten, R., Sripapatprasite, P., Vaddhanaphuti, C., Vidthayanon, C., Wirojanagud, W., Watana, E., 2000, Pak Mun Dam, Mekong River Basin, Thailand, *A WCD Case Study prepared as an input to the World Commission on Dams*, Cape Town. [Available online at <http://www.dams.org/studies/th/>]

Bakker, K., 1999, The politics of hydropower: developing the Mekong, *Political Geography*, 18, pp. 209-232.

Batjes, N. H., 1995, A homogenized soil data file for global environmental research: A subset of FAO, ISRIC and NCRS profiles, *Rep. 95/10*, International Soil Reference and Information Center (ISRIC), Wageningen, Netherlands, 50 p. [Available from ISRIC, P.O. Box 535. 6700 AJ, Wageningen, Netherlands]

Berman, M. L., 1998, Opening the Lancang (Mekong) River in Yunnan: Problems and Prospects for Xishaungbanna, Dept of Asian Languages and Literatures, University of Massachusetts, Amherst. [Available online at <http://www.dbr.nu/data/pubs/thesis/Lancang.htm>]

Bo, U. S., and U. Z. Win, 2000, RPA report on Nam Mae Hkok Watershed, Eastern Shan State Myanmar - Watershed Profile, Poverty Reduction & Environmental Management in Remote Greater Mekong Subregion (GMS) Watersheds Project (Phase I), ADB Regional Technical Assistance 5771. [Available online at <http://www.mekonginfo.org>]

Bogardi, J. J., and L. Duckstein, 1992, Interactive Multiobjective Analysis embedding the decision maker's implicit preference function, *Water Resources Bulletin*, American Water Resources Association, 28 (1), pp. 75-88.

Boonpiraks, S., October 1992, Thai-Myanmar joint hydro schemes, *Water Power and Dam Construction*, pp. 40-41.

Carter, A. J., and R. J. Scholes, 1999, Generating a global database of soil properties, Environmentek CSIR, 10 p.

Chapman, E. C., and H. Daming, 2000, Downstream Implications of China's Dams on the Lancang Jiang (Upper Mekong) and their Potential Significance for the Greater Regional Cooperation Basin-Wide, International Mekong Research Network, Australian

- National University, Canberra. [Available online at <http://www.anu.edu.au/asianstudies/mekong/dams.html>]
- Chazee, L., 1994, Shifting cultivation systems in Laos: present system and their future, *Shifting Cultivation Systems and Rural Development in the Lao PDR*, Report of the Nabong Technical Meeting, Vientiane, pp 66-97. [Available from UNDP Resident Representative, P.O. Box 345, Vientiane, Lao P.D.R.]
- Cheong, G. and CPAWM, 1998, Resource Management in the Lao Mekong Basin, *Working Paper Series*, Asia Research Centre, Murdoch University. [Available online at <http://www.arc.murdoch.edu.au/arc/wpapers.html#mekong>]
- Cherkauer, K. A. and D. P. Lettenmaier 1999, Hydrologic Effects of Frozen Soils In The Mississippi River Basin, *J. Geophys. Res.*, 104 (D16), pp. 19599-19610.
- Chuhan Z., X. Yanjie, W. Guanglun, and J. Feng, 2000, Non-linear seismic response of arch dams with contraction joint opening and joint reinforcements, *Earthquake engineering and structural dynamics*, 29, pp. 1547-1566.
- Cosby, B.J., G. M. Hornberger, R. B. Clapp, and T.R. Ginn, 1984, A statistical exploration of the relationships of soil moisture characteristics to the physical properties of soils, *Water Resour. Res.*, 20, pp. 682-690.
- Dansie, J., March 1994, Laos hydro to power Thai economy, *International Water Power and Dam Construction*, pp 18-20.
- FAO, 1995, The digital soil map of the world, Version 3.5, United Nations Food and Agricultural Organization, CD-ROM. [Available from Food and Agricultural Organization of the United Nations, Viale delle Terme di Caracalla, 00100 Rome, Italy.]
- FAO Cambodia Online, 2000, Environment: Concepts and Issues, at <http://www.un.org/kh/fao/environment/>
- FAOSTAT, 2001, FAO on-line database at <http://apps.fao.org/>
- FIVAS (The Association for International Water and Forest Studies), 1996, The Mekong Region, *Power Conflicts*, at [http://www.solidaritetshuset.org/fivas/pub/power\\_c/index.htm](http://www.solidaritetshuset.org/fivas/pub/power_c/index.htm)
- Gartrell, A., 1997, Resource Management in the Cambodian Mekong Basin, *Working Paper Series*, Asia Research Centre, Murdoch University. [Available online at <http://www.arc.murdoch.edu.au/arc/wpapers.html#mekong>]

- Gerakis, A., 1999, A computer program for soil textural classification, *Soil Sci. Soc. Amer. J.*, 63, pp. 807-808.
- Hamlet A. F., and D.P. Lettenmaier, 1999, Effects of Climate Change on hydrology and water resources in the Columbia River Basin, *J. Amer. Water. Res. Assoc.*, American Water Resources Association, 35 (6), pp. 1597-1623.
- Hansen, M.C., R. S. Defries, J. R. G. Townsend, and R. Sohlberg, 2000, Global land cover classification at 1km spatial resolution using a classification tree approach, *Int. J. Remote Sensing*, 21, pp. 1331-1364.
- Hinton, P., 1998, Resource Management in the Yunnan Mekong Basin, *Working Paper Series*, Asia Research Centre, Murdoch University. [Available online at <http://wwwarc.murdoch.edu.au/arc/wpapers.html#mekong>]
- Hirsch, P. and Cheong, G., 1996, Natural Resource Management in the Mekong River Basin: Perspectives for Australian Development Cooperation, *Final overview report to AusAID*, University of Sydney.
- Huffman G.J., Adler R.F., Arkin P., Chang A., Ferraro R., Gruber A., Janowlak J., McNab A., Rudolf B., Schneider U., 1997, The Global Precipitation Climatology Project (GPCP) Combined Precipitation Dataset, 78 (1), *Bulletin of the American Meteorological Society*, pp. 5-20.
- Huffman G.J., Adler R.F., Rudolf B., Schneider U., Keehn P.R., 1995, Global Precipitation Estimates Based on a Technique for Combining Satellite-Based Estimates, Rain Gauge Analysis, and NWP Model Precipitation Information, *American Meteorological Society*, 8, pp. 1284 – 1295.
- ICCILMB (Interim Committee for Coordination of Investigation of the Lower Mekong Basin, 1992, Fisheries in the Lower Mekong Basin (Review of Fishery Sector in the Lower Mekong Basin), Mekong Secretariat, Bangkok, Thailand.
- ICOLD (International Commission on Large Dams) Online, 2000, A Brief Introduction To Dachaoshan Hydropower Project, <http://www.icold-cigb.org.cn/icold2000/st-a5-01.html>
- ICOLD (International Commission on Large Dams) Online, 2000, Manwan Hydropower Station, <http://www.icold-cigb.org.cn/icold2000/st-a5-03.html>
- Ikunaga. M., 1999, The Forest Issue in Cambodia – Current Situation and Problems: An Analysis Based on Field Research, *IDRI Occasional Paper No. 12*, FASID (Foundation for Advanced Studies on International Development), Tokyo, Japan.

International Rivers Network, 1999, *Power Struggle: The Impacts of Hydro-development in Laos*, Berkeley, California, 68 p.

Kalnay E., and Co-authors, 1996, The NCEP/NCAR 40-year reanalysis project, *Bull. Amer. Meteor. Soc.*, 77, pp. 437-471.

Lao Agricultural Census Office, 2000, *Lao Agricultural Census for 1998-99, Highlights*, Steering Committee for the Agricultural Census, Agricultural Census Office, Vientiane.

Leung, L. R., A. F. Hamlet, D. P. Lettenmaier, A. Kumar, 1999, Simulations of the ENSO hydroclimate signals in the Pacific Northwest Columbia River Basin, *Bull. Amer. Meteor. Soc.*, 80, pp. 2313-2329.

Liang, X., D. P. Lettenmaier, and E. F. Wood, 1996, One dimensional statistical dynamic representation of subgrid spatial variability of precipitation in the two-layer variable infiltration capacity model, *J. Geophys. Res.*, 101, pp. 21403-21422.

Liang, X., D. P. Lettenmaier, E.F. Wood, and S. J. Burges, 1994, A simple Hydrologically Based Model of Land Surface Water and energy Fluxes for General Circulation Models, *J. Geophys. Res.*, 99, pp. 14415-14428.

Liang, X., E. F. Wood, D. P. Lettenmaier, D. Lohmann, A. Boone, S. Chang, F. Chen, Y. Dai, et al., 1998, The project for Intercomparison of Land-Surface Parameterization Schemes (PILPS) Phase 2(c) Red-Arkansas River Basin experiment: 2. Spatial and temporal analysis of energy fluxes, *Global Planet. Change*, 19, pp. 137-159.

Lohmann, D., E. Raschke, B. Nijssen, and D. P. Lettenmaier, 1998, Regional scale hydrology: I. Formulation of the VIC-2L model coupled to a routing model, *Hydrol. Sci. J.*, 43, pp. 131-141.

Lohmann, D., R. Nolte-Holube, and E. Raschke, 1996, A large-scale horizontal routing model to be coupled to land surface parameterization schemes, *Tellus*, 48A, pp. 708-721.

McCormack G., 2001, Water Margins, Competing Paradigms in China, *Critical Asian Studies*, 33(1), pp. 5-30.

Miller, F., N. V. Thinh, D. T. M. Duc, 1999, Resource Management in the Vietnamese Mekong Basin, *Working Paper Series*, Asia Research Centre, Murdoch University. [Available online at <http://wwwarc.murdoch.edu.au/arc/wpapers.html#mekong>]

Mongkolsawat, C., P. Thirangoon, R. Suwanwerakamtor, N. Karladee, S. Paiboonsak, and P. Champathet, 2000, An Evaluation of Drought Risk Area in Northeast Thailand

using Remotely Sensed Data and GIS, ACRS 2000. [Available online at <http://www.gisdevelopment.net/aars/acrs/2000/ts5/env004pf.htm>]

MRC Annual Report, 2000, Mekong River Commission Secretariat, Phnom Penh, Cambodia.

MRC Annual Report, 1998, Mekong River Commission Secretariat, Phnom Penh, Cambodia.

MRC Annual Report, 1994, Mekong River Commission Secretariat, Phnom Penh, Cambodia.

Nijssen, B., D.P. Lettenmaier, X. Liang, S. W. Wetzel, and E. F. Wood, 1997, Streamflow Simulation for Continental-Scale River Basins, *Water Resour. Res.*, 33(2), pp. 711-724.

Nijssen, B., R. Schnur, and D. P. Lettenmaier, 2001a, Global retrospective estimation of soil moisture using the Variable Infiltration Capacity land surface model, 1980-1993, *J. Climate*, 14, pp. 1790-1808.

Nijssen, B., G. M. O'Donnell, D. P. Lettenmaier, D. Lohmann, and E. F. Wood, 2001b, Predicting the discharge of global rivers, *J. Climate*, 14, pp. 3307-3323.

North A. M., and H. Demaine, 2000, Study of Large Dams and Recommendations: Pilot Case Study – The Nam Ngum 1 Dam in Lao PDR, Project RETA 5828, *East /South-East Asia Regional Consultation*, World Commission on Dams, Cape Town. [Available online at <http://www.dams.org/docs/submissions/ins158.pdf>]

NTFP (The Non-Timber Forest Products Project), 2000, A study of the Downstream Impacts of the Yali Falls Dam in the Se San River Basin in Ratnakiri Province, Northeast Cambodia, The Fisheries Office. [Available online at [http://www.usyd.edu.au/su/geography/mekong/case\\_studies/yali\\_hydro/ratanakiri\\_report.pdf](http://www.usyd.edu.au/su/geography/mekong/case_studies/yali_hydro/ratanakiri_report.pdf)]

O'Donnell G., B. Nijssen, D. P. Lettenmaier, 1999, A simple algorithm for generating streamflow networks for grid-based macroscale hydrological models, *Hydrol. Proc.*, 13, pp. 1269-1275.

Pednekar, S., 1997, Resource Management in the Thai Mekong Basin, *Working Paper Series*, Asia Research Centre, Murdoch University. [Available online at <http://wwwarc.murdoch.edu.au/arc/wpapers.html#mekong>]

Pluss A. E., July 1986, Nam Ngum Project in Laos Completed, *Water Power and Dam Construction*, pp. 43–45.

Puustjarvi, E., 2000a, Review of Policies and institutions Related to Management of Upper Watershed Catchments – Yunnan, China, Poverty Reduction & Environmental Management in Remote Greater Mekong Subregion (GMS) Watersheds Project (Phase I), ADB Regional Technical Assistance 5771. [Available online at <http://www.mekonginfo.org>]

Puustjarvi, E., 2000b, Review of Policies and institutions Related to Management of Upper Watershed Catchments – Laos, Poverty Reduction & Environmental Management in Remote Greater Mekong Subregion (GMS) Watersheds Project (Phase I), ADB Regional Technical Assistance 5771. [Available online at <http://www.mekonginfo.org>]

Puustjarvi, E., 2000c, Review of Policies and institutions Related to Management of Upper Watershed Catchments – Vietnam, Poverty Reduction & Environmental Management in Remote Greater Mekong Subregion (GMS) Watersheds Project (Phase I), ADB Regional Technical Assistance 5771. [Available online at <http://www.mekonginfo.org>]

Rainboth, W. J., 1996, *Fishes of the Cambodian Mekong*, FAO species identification field guide for fishery purposes, Food and Agriculture Organization of the United Nations, Rome.

Rigg, J., 1995, In the fields there is dust, *Geography*, 80(1), pp. 23-32.

Shepard, D.S., 1984, Computer Mapping: the SYMAP Interpolation Algorithm, In: *Spatial Statistics and Models*, Gaile and Willmott, eds.

Shiklomanov, I. A., 2000, Appraisal and Assessment of World Water Resources, *Water International*, International Water Resources Association, 25 (1), pp. 11-32.

Son, D. K., 1998, Development of agricultural production systems in the Mekong Delta, Development of Farming systems in the Mekong Delta of Vietnam, JIRCAS, CTU & CLRRI, Ho Chi Minh City, Vietnam.

Storck, P., and D. P. Lettenmaier, 1999, Predicting the effect of a forest canopy on ground snow accumulation and ablation in maritime climates, *Proc. 67<sup>th</sup> Western Snow Conf.*, Fort Collins, CO, pp. 1-12.

Todini, E., 1996, The ARNO rainfall-runoff model, *J. Hydrology*, 175, pp. 339-382.

Wood A. W., Maurer E. P., Kumar A., Lettenmaier D. P., 2000, Long range experimental hydrologic forecasting for the eastern US during summer 2000, *J. Geophys. Res.* (In review)

Wood E. F., 1991, Land Surface-Atmospheric Interactions for Climate Modeling-- Observations, Models and Analysis, Ed., (Kluwer).

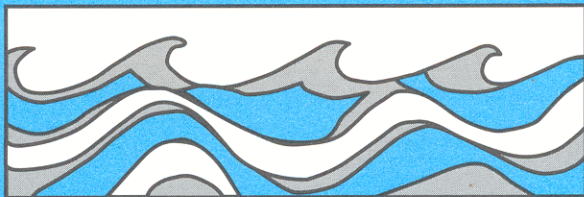
Xuemin, C., August 1991, A review of major schemes progressing in China, *Water Power and Dam construction*, pp. 47-51.

University of Washington  
Department of Civil and Environmental Engineering



# EFFECTS OF STREAMFLOW REGULATION AND LAND COVER CHANGE ON THE HYDROLOGY OF THE MEKONG RIVER BASIN

Gopalakrishna Goteti  
Dennis P. Lettenmaier



Water Resources Series  
Technical Report No. 169  
December 2001

Seattle, Washington  
98195